JYU DISSERTATIONS 530

Salla Mattola

Virus-host Interactions during Nuclear Egress of Parvoviruses

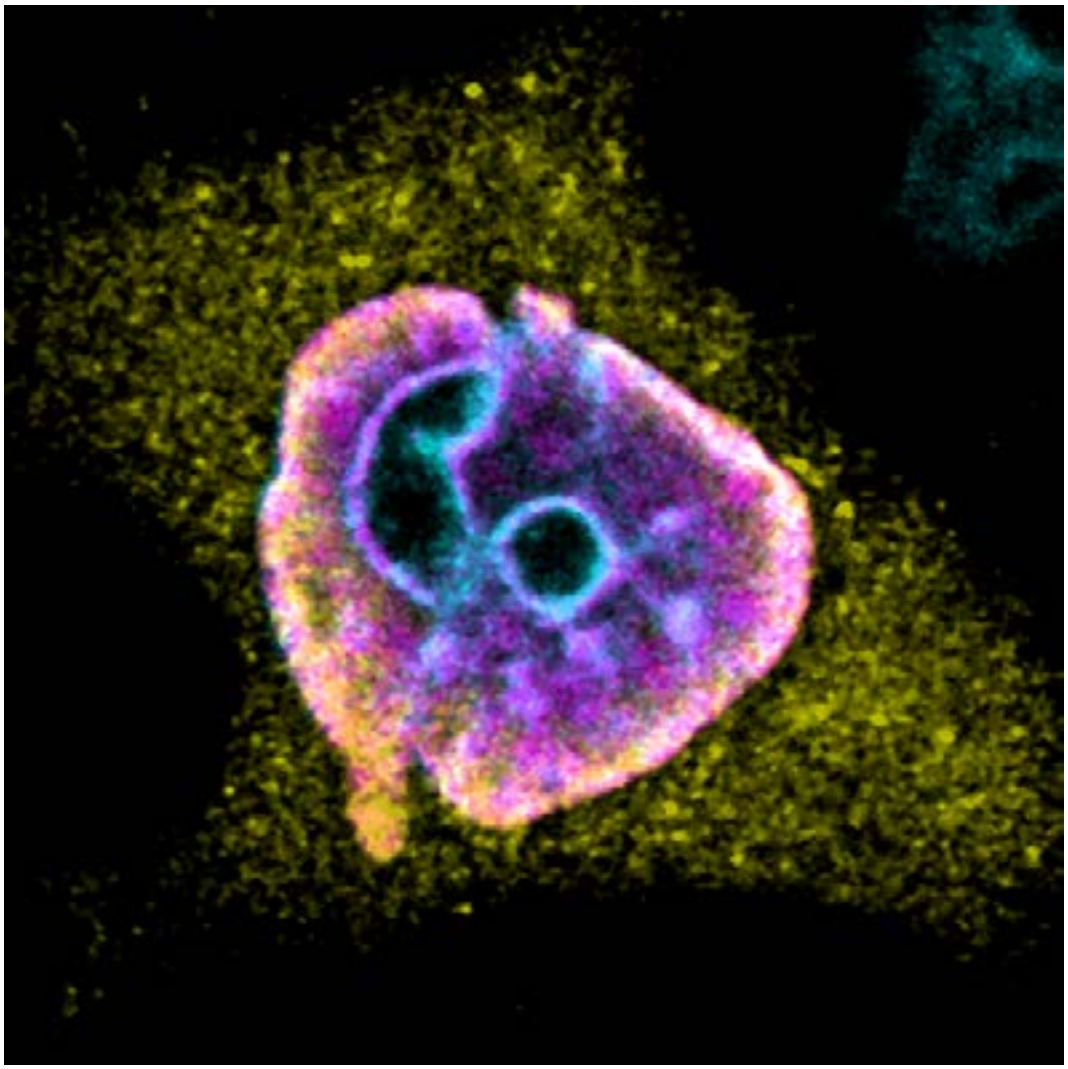

UNIVERSITY OF JYVÄSKYLÄ
FACULTY OF MATHEMATICS
AND SCIENCE

JYU DISSERTATIONS 530

Salla Mattola

Virus-host Interactions during Nuclear Egress of Parvoviruses

Esitetään Jyväskylän yliopiston matemaattis-luonnontieteellisen tiedekunnan suostumuksella
julkisesti tarkastettavaksi Ylistönrinteen auditoriossa YAA303
kesäkuun 3. päivänä 2022 kello 12.

Academic dissertation to be publicly discussed, by permission of
the Faculty of Mathematics and Science of the University of Jyväskylä,
in building Ylistönrinne, Auditorium YAA303, on June 3, 2022, at 12 o'clock.

JYVÄSKYLÄN YLIOPISTO
UNIVERSITY OF JYVÄSKYLÄ

JYVÄSKYLÄ 2022

Editors
Matti Jalasvuori
Department of Biological and Environmental Science, University of Jyväskylä
Päivi Vuorio
Open Science Centre, University of Jyväskylä

ISBN 978-951-39-9177-7 (PDF)
URN:ISBN:978-951-39-9177-7
ISSN 2489-9003

Permanent link to this publication: http://urn.fi/URN:ISBN:978-951-39-9177-7

ABSTRACT

Mattola, Salla M
Virus-host interactions during nuclear egress of parvoviruses
Jyväskylä: University of Jyväskylä, 2022, 80 p.
(JYU Dissertations
ISSN 2489-9003; 530)
ISBN 978-951-39-9177-7 (PDF)
Yhteenveto: Parvoviruksen vuorovaikutukset isäntäsolun tumassa
Diss.

Autonomic parvoviruses, small non-enveloped ssDNA viruses, encode only a limited number of proteins, which makes them highly dependent on the functions provided by the host cell. Besides two capsid proteins, VP1 and VP2, which form the capsid, autonomous parvoviruses encode two nonstructural proteins, NS1 and NS2. In this thesis, we used canine parvovirus as a model virus to study nuclear virus-host interactions and egress of progeny virus at late stages of infection. The NS1 of canine parvovirus has been identified to take part in multiple functions in infection, but the role of the smaller nonstructural protein NS2 has remained an enigma. In the first part of the study, we utilized proximity-dependent biotin identification (BioID), a powerful mass spectrometry-based tool capable of recognizing dynamic and transient interactions, to elucidate the role of NS2 in infection. The interactome linked NS2 to multiple proteins with possible relevance to the progression of infection. Notably, some gene ontology functions that were represented among the identified proteins were chromatin remodeling and DNA damage response, suggesting a regulatory involvement of NS2 in these processes. Moreover, the resolved BioID analysis revealed NS2 association with nucleolar proteins. In the second part of the study, we studied the nucleolar structure by deploying confocal imaging combined with human-in-the-loop (HITL) machine learning segmentation. Our findings show that nucleolar structure is changed during infection and intact NS2 has a role in these alterations. In the third part of the study, we showed that in addition to active CRM1-driven nuclear exit, the nuclear egress of capsids is facilitated by G2/M transition- and apoptosis-induced increase in the nuclear envelope permeability.

Keywords: Apoptosis; BioID; canine parvovirus; chromatin; CRM1; DNA damage response; G2/M transition; NS2

Salla Mattola, University of Jyväskylä, Department of Biological and Environmental Science, P.O. Box 35, FI-40014 University of Jyväskylä, Finland

TIIVISTELMÄ

Mattola, Salla M
Parvoviruksen vuorovaikutukset isäntäsolun tumassa
Jyväskylä: Jyväskylän yliopisto, 2022, 80 s.
(JYU Dissertations
ISSN 2489-9003; 530)
ISBN 978-951-39-9177-7 (PDF)
Yhteenveto: Parvoviruksen vuorovaikutukset isäntäsolun tumassa
Diss.

Parvovirukset ovat pieniä viruksia, jotka ovat vaipattomia, sisältävät yksijuosteista DNA:ta ja ovat isäntäsolun toiminnoista hyvin riippuvaisia. Tässä tutkimuksessa paneuduttiin koiran parvoviruksen ei-rakenteellisen proteiinin vuorovaikutuksiin isäntäsolun proteiinien kanssa käyttäen hyödyksi massaspektrometriaan pohjautuvaa BioID-menetelmää. NS2:n havaittiin vuorovaikuttavan erityisesti kromatiinin muokkaamiseen sekä DNA-vauriovasteeseen liittyvien proteiinien kanssa. Havaintojen tueksi NS2:n mutaation vaikutuksia edellä mainittuihin prosesseihin tarkasteltiin mm. konfokaalimikroskopiaan ja koneoppimiseen pohjautuvien mikroskopia-analyysien keinoin. NS2:n mutaatiolla havaittiin olevan vaikutusta myös tumajyvästen rakenteeseen, mahdollisesti BioID:ssä havaittujen vuorovaikutusten kautta. NS2:n roolin lisäksi tutkimuksessa tarkasteltiin mekanismeja, joilla syntyneet viruskapsidit kulkeutuvat ulos tumasta. Havaittiin että viruskapsidien kuljetus tumasta ulos oli yhteydessä tuman sykliini B1:n määrän huomattavaan kasvuun. Sykliini B1:n määrä tumassa kasvaa tiedettävästi solusyklin G2/M siirtymän ja aikaisen apoptoosin yhteydessä. Mitoosia ja apoptoosia estävien kemikaalien läsnä ollessa kapsidien kuljetus ulos tumasta estyi. Lisäksi tumakalvon läpäisevyyden havaittiin muuttuvan infektiossa fluoresenssin häviämiseen pohjautuneessa koeasetelmassa. Fluoresenssin häviäminen palautui inhibiittorien läsnä ollessa lähes lähtötasolleen. Kokonaisuudessaan tämä väitöskirjatyö tarjoaa uutta tutkimustietoa parvoviruksen ja isännän vuorovaikutuksista sekä mahdollisista mekanismeista, joilla kapsidit kulkeutuvat ulos tumasta.

Avainsanat: Apoptoosi; DNA-vauriovaste; G2/M siirtymä; Koiran parvovirus; kromatiini; massaspektrometria; NS2.

Salla Mattola, Jyväskylän yliopisto, Bio- ja ympäristötieteiden laitos PL 35, 40014 Jyväskylän yliopisto

Author's address *Salla Mattola*
Department of Biological and Environmental Science
P.O. Box 35
FI-40014 University of Jyväskylä
Finland
salla.m.mattola@jyu.fi

Supervisors Docent Maija Vihinen-Ranta
Department of Biological and Environmental Science
P.O. Box 35
FI-40014 University of Jyväskylä
Finland
Maija.vihinen-ranta@jyu.fi

Docent Elina Mäntylä
BioMediTech, Faculty of Medicine and Health Technology
Tampere University
Arvo D219, Arvo Ylpön katu 34
33520 Tampere
Finland
elina.mantyla@tuni.fi

Reviewers Professor emeritus Veijo Hukkanen
Virology, Institute of Biomedicine Infections and Immunity,
Medisiina D 7th floor University of Turku
Kiinamyllynkatu 10 D
FIN-20520 Turku, Finland
veijo.hukkanen@utu.fi

Docent Sami Oikarinen
BioMediTech, Faculty of Medicine and Health Technology
Tampere University
Arvo F316, Arvo Ylpön katu 34
33520 Tampere
Finland
Sami.oikarinen@tuni.fi

Opponent Professor Jose M Almendral
Centro de Biología Molecular "Severo Ochoa" (CSIC-UAM)
Universidad Autónoma de Madrid
28049 Cantoblanco, Madrid, Spain
jmalmendral@cbm.csic.es

CONTENTS

LIST OF ORIGINAL PUBLICATIONS

The thesis is based on the following original papers, which will be referred to in the text by their Roman numerals (I–III):

I Mattola S*, Salokas K*, Aho V, Mäntylä E, Salminen S, Hakanen S, Niskanen EA, Svirskaite J, Ihalainen TO, Airenne K, Kaikkonen-Määttä M, Parrish CR, Varjosalo M, Vihinen-Ranta M, 2022. Parvovirus nonstructural protein 2 interacts with chromatin-regulating cellular proteins. PLoS Pathog. 2022 Apr 8;18(4):e1010353.

II Mattola S, Leclerc S, Hakanen S, Aho V, Parrish CR and Vihinen-Ranta M., Parvovirus infection alters the nucleolar structure. Manuscript.

III Mattola S*, Mäntylä E*, Aho V, Salminen S, Oittinen M, Salokas K, Järvensivu J, Hakanen S, Ihalainen TO, Viiri K, and Vihinen-Ranta M., 2022. G2/M transition and apoptosis facilitate the nuclear egress of parvoviral capsids. Manuscript in revision in Journal of Virology.

Responsibilities of the author in the thesis articles:

Articles I &III The author took part in planning the experimental work and performed most of the experiments. In addition, the author took part in analyzing the microscopy data and interpreting the results. Most of the figures in the article were produced by the author. The author contributed to the writing of the article together with the co-authors.

Article II The author conceptualized the study and planned the experimental work. In addition, the author did the majority of the experimental work and participated in the analyses. The author contributed to the writing of the article together with the co-authors.

ABBREVIATIONS

AAV	Adeno-associated virus
APC	Anaphase promoting complex
ATM	Ataxia telangiectasia mutated
ATR	Ataxia telangiectasia and Rad3 related
BioID	Proximity-dependent biotin identification
Cdk1	Cyclin-dependent kinase
CPV	Canine parvovirus
CRM1	Chromosomal region maintenance 1
DDR	DNA damage response
DFC	Dense fibrillar center
DSB	Double-stranded DNA break
ER	Endoplasmic reticulum
FACT	Facilitates chromatin transactions -complex
FC/DFC	Fibrillar center/dense fibrillar center interface
FC	Fibrillar center
FPLV	Feline panleukopenia virus
GC	Granular center
GO	Gene ontology
HeLa	Cervical carcinoma cells
hpi	Hours post infection
HSV-1	Herpes simplex virus 1
ki-67	Proliferation marker ki-67
LAD	Lamin-associated domains
LMB	Leptomycin B
MDC1	Mediator of DNA damage checkpoint protein 1
MVM	Minute virus of mice
NE	Nuclear envelope
NES	Nuclear export signal
NLFK	Norden laboratory feline kidney cells
NLS	Nuclear localization signal
NOR	Nucleolar organization region
NoRC	Nucleolar chromatin remodeling complex
NPC	Nuclear pore complex
NR	Nucleolar rim
NS1	Nonstructural protein 1
NS2	Nonstructural protein 2
ONM	Outer nuclear membrane
PLA	Proximity ligation assay
PTM	Posttranslational modification
RPA	Replication protein A
SMARCA	SWI/SNF-related matrix-associated actin-dependent regulator of chromatin subfamily A member 5
SSRP1	Structure Specific Recognition Protein

TAD	Topologically associated domains
VP	Viral structural protein
VP1	Viral structural protein 1
VP2	Viral structural protein 2
VP3	Viral structural protein 3

1 INTRODUCTION

The cell is the most fundamental structural part of living organisms, capable of self-reproduction via cell division. One of the primary functions of the cell is to carry out the central dogma of life by copying genetic information stored in the cell nucleus, transcribing this information in the form of an mRNA molecule, and translating the mRNA into an amino acid chain that folds into a protein. The specific structure of a protein resides in the composition and order of the amino acid chain -resulting in a 3D structure that serves a function needed by the cell. Environmental factors can cause DNA damage, and maintaining the integrity of the genetic code is crucial. Cells can sense and repair the damaged DNA via cross-functional signaling pathways and feedback systems.

Viruses are incapable of fulfilling the central dogma by themselves. Therefore, they depend on binding to a suitable host cell, evading the host´s defense systems, and finally harnessing the cellular functions for their reproduction. The properties of a virus can be summarized by the properties of its structural parts, genome, and nonstructural and structural proteins. To fully understand how a virus reaches its reproductional capacity, we need to understand what functions a single viral protein bears and how the protein interacts with the host cell. The pathogenic prospects of the virus lie in the disruption caused by viral reproduction to the functions of the cell. Therefore, besides being exciting research subjects, viruses can serve as valuable tools to use for basic research of the biology of the cells.

DNA viruses and autonomous parvoviruses, including canine parvovirus (CPV), replicate, assemble, and package the progeny virions in the cell nucleus, utilizing the pre-existing nuclear processes of DNA replication, gene transcription, and material exchange systems. The reproduction of autonomous parvoviruses is highly cell cycle dependent. Viral DNA is replicated during the synthesis phase of the cell cycle when cellular DNA replication occurs. Besides replication, the transcription of viral genes and viral capsid assembly of autonomous parvoviruses are cell cycle-dependent (Wolter *et al.* 1980, Gil-Ranedo *et al.* 2015). Some autonomous parvoviruses specifically target and kill cancer cells which makes them promising agents of oncolytic viral therapy.

Moreover, the newly found human autonomous parvoviruses bufavirus (identified in 2012), tusavirus (identified in 2014) and cutavirus (identified in 2016) provide a connection to human diseases, adding to the significance of autonomous parvovirus research (Väisänen *et al.* 2017).

CPV is a simple virus with only four proteins. The functions of one of them, the nonstructural protein NS2, have remained unknown. In this work, we used BioID, a powerful proximity-based method previously used to identify the interactomes of many cellular proteins and a few viral proteins, to resolve the interactome of the NS2 with cellular proteins. Furthermore, the high incidence of nucleolar associations of the NS2 led us to elucidate the infection-induced changes on the structure of the nucleolus. Besides enlightening the role of NS2, the thesis will provide a new aspect to the viral life cycle of the CPV, and to the dependence of progeny virus nuclear egress on G2/M transition and apoptosis.

2 REVIEW OF THE LITERATURE

The host cell exploitation by DNA viruses leads to multiple changes in the structure and functions of the nucleus. The expanding replication centers, which act as hubs for viral replication, modify the surrounding chromatin structure and interact with host structures (Charman and Weitzman 2020). CPV infection additionally alters the nuclear envelope (NE) and nuclear lamina (Ihalainen *et al*. 2009, Mäntylä *et al*. 2015, 2016). For this reason, to understand the processes leading to progeny virus production, we must first understand the functions of the eukaryotic cell nucleus.

2.1 Chromatin organization and function

The nucleus provides many functions that are crucial for the existence of the cell. Highly sophisticated chromatin organization and nuclear architecture have evolved to serve these tasks. The nucleus consists of several spatial and functional compartments such as chromatin domains and protein-containing structures including nuclear speckles, paraspeckles, Cajal bodies, and PML nuclear bodies.

The organization of the nuclear genetic material has a complicated structure with multiple nested layers. The DNA in eukaryotic cells is arranged in chromosomes, which are spatially located in chromosome territories (Cremer and Cremer 2010). The telomere regions of specific acrocentric chromosomes form the nucleolus, implying that there is at least some spatial organization at the chromosome level (Henderson *et al.* 1972). Within the chromosomes, specific regions of the chromosome are replicated at different phases during the S phase of the cell cycle (O'Keefe *et al.* 1992).

The term chromatin includes the genetic material DNA and nucleosomes formed from histone proteins that bind the DNA. This kind of structure enables the loosening and tightening of the fiber for functional purposes. Nucleosomes are formed from four main histone proteins: H2A, H2B, H3, and H4. These

histones form heterodimers that bind together and form an octamer, the nucleosome (Luger *et al.* 1997). DNA wraps around the nucleosome, and the fifth histone protein, linker histone H1, stabilizes the structure. Nucleosomes control the packing efficacy of the chromatin via posttranslational modifications (PTMs) in the tail regions of the histones. Acetylation and methylation were the first PTMs found, and they are, therefore, the most studied histone modifications (Allfrey *et al*. 1964). Histone PTMs are regulatory elements involved in modulation of genomic architecture, replication, transcription, DNA repair, and recombination. Besides acetylation and methylation, over 20 other PTMs have been identified in specific sites of the histone tails. The proteins that maintain and regulate the PTMs can be categorized into three groups: writers (adding PTMs), readers (recognizing PTMs) and erasers (removing PTMs) (Millán-Zambrano *et al*. 2022). For example, the well-known histone acetyltransferase acts as a writer by adding acetyl groups, and histone deacetylase acts as an eraser by removing acetyl groups (Bannister and Kouzarides 2011). Histone PTMs can be related to a specific metabolic state (Dai *et al*. 2020). The trimethylated state of H3 lysine 4 has been strongly associated with active transcription, possibly through H3K4me3-TAF3 interaction leading to the recruitment of transcription factor II D (Lauberth *et al.* 2013). Histone phosphorylation at the H3S10 site is specific for chromatin condensation in mitosis, starting from the pericentromeric area and spreading to the whole chromosome (Hendzel *et al.* 1997). Phosphorylation of H3S10 is required to initiate mitotic chromatin condensation but is also disposable for the maintenance of condensation (van Hooser *et al.* 1998). Moreover, the dynamics of different chromatin regions vary. The binding of the H1 linker histone to the chromatin is more dynamic in euchromatin regions than in densely packed heterochromatin (Misteli 2000). The stable nature of heterochromatin is maintained by the heterochromatin protein 1 (HP1) (Cheutin *et al.* 2003). Besides writers, erasers and readers, chromatin structure and organization are regulated through several complexes, affecting the spacing between nucleosomes, nucleosome composition, and transcription. Nucleolar remodeling complex (NoRC) participates in gene silencing by recruiting histone deacetylases and DNA methyltransferase (Santoro *et al.* 2002). Histone chaperone complexes affect chromatin by regulating nucleosome assembly. Facilitates chromatin transcription (FACT) complex can bind both H2A-H2B and H3-H4 dimers (Burgess and Zhang 2013).

Chromosomes are specifically organized in the nucleus. When parts of the nucleus are irradiated by a laser, randomly arranged chromosomes would show DNA damage at random positions of the genome. However, laser irradiation induces random DNA damage only to specific chromosomes (Cremer *et al.* 1982, Longo and Roukos 2021). This means that the chromosomes are not intermixed but instead form chromosome territories. The spatial and temporal organization of the genome is essential for replication, transcription, and DNA damage repair. Genome is organized in two distinct compartments, loosely packed open euchromatin and densely packed compact heterochromatin. Euchromatin contains regions that have high gene density and heterochromatin regions that have low gene density. This division is believed to facilitate gene expression in

the gene-rich areas of euchromatin. However, euchromatin does not equal transcriptional activity, even though the easy access facilitates the process (Gilbert *et al.* 2004). Moreover, the gene-rich and gene-poor regions occupy areas differing in volume (Croft *et al.* 1999). Besides chromatin areas, the nucleus has regions devoid of chromatin called interchromatin regions. Whereas chromatin-containing regions contain very little RNA, the interchromatin space is filled with RNA and proteins. Therefore, the interchromatin area is thought to be a region where transcription, RNA processing, and transport occur. The interchromatin space forms a network that is believed to be connected to the nuclear pores. (Cremer *et al.* 2000, Visser *et al.* 2000, Markaki *et al.* 2010). The simple division between interchromatin and chromatin regions might be an oversimplified model since the chromosome territories of interphase nuclei are mobile and translocate, forming areas where chromosome territories intermingle with each other (Branco and Pombo 2006). Active genes can be translocated to sites containing the necessary machinery needed for transcription. These sites are sometimes referred to as transcription factories (Osborne *et al.* 2004). Active transcription occurs in transcription factories containing active RNA polymerases (Iborra *et al.* 1996).

The development of high throughput methods such as high-throughput chromosome conformation capture, has enabled to resolve the chromatin-chromatin associations and the nuclear architecture of the whole genome (Rao *et al.* 2014, Kempfer and Pombo 2020). Based on the analysis, chromatin was found to form loops that associate with regions referred to as topologically associated domains (TADs). In addition to TAD-type domain, chromatin associated with nuclear lamina forms a different type of domain: lamin associated domain (LAD). TAD- and LAD-containing regions give rise to the division of the genome into two separate compartments, compartment A and compartment B. Compartment A is composed of chromatin containing TADs, whereas compartment B is composed of LAD-containing regions. Whereas TADs are transcriptionally active regions, LADs occupying the nuclear periphery close to the nuclear lamina and surroundings of the nucleolus are transcriptionally inactive, containing condensed chromatin. The genome organization to TAD and LAD regions has a unique role in replication timing. TAD regions containing open chromatin are replicated early on, whereas the highly condensed LAD regions are replicated later (Pope *et al.* 2014). Furthermore, TAD region boundaries have been associated with DNA topoisomerase complexes (Rasim Barutcu *et al.* 2017).

Proteins of DNA viruses interact with chromatin-organizing proteins and complexes, thereby affecting the nuclear chromatin organization. Dense chromatin areas have been shown to restrict the movement of larger viruses such as Herpes simplex virus 1 (HSV-1) (Myllys *et al.* 2016, Aho *et al.* 2019, 2021). The translocation of HSV-1 progeny capsids to the nuclear envelope is facilitated towards the end of infection by the infection-induced chromatin reorganization. Measured diffusion coefficients for HSV capsids are lower in chromatin-containing regions than in chromatin-lacking regions (Aho *et al.* 2021). CPV infection induces drastic chromatin organization at the late stages of infection. The chromatin of an infected cell is marginalized to the nuclear envelope and to

the close vicinity of chromatin-depleted structures, shown in these studies to be nucleoli (Ihalainen *et al.* 2009). The expansion and fusing of autonomous parvovirus replication centers, also known as autonomous parvovirus-associated replication (APAR) bodies, result in changed chromatin organization in infected cells (Cziepluch *et al.* 2000, Ihalainen *et al.* 2009). One proposition is that the molecular crowing of the expanding replication areas leads to chromatin marginalization via depletion attraction. The formed chromatin-excluded regions are found to be of homogenic nature with rapid molecular dynamics despite the nuclear overcrowding. Viral capsid dynamics of CPV are altered by the changing nuclear architecture of infected cells (Ihalainen *et al.* 2009).

2.2 Nucleolus

The cell nucleus harbors multiple nuclear bodies that are essential for various aspects of nuclear function. These bodies are rich in proteins and, in some cases, RNAs (Mao *et al.* 2011). The most recognizable of these structures is the nucleolus. As a nonmembranous organelle, the diffusion of proteins and other molecules is not obstructed by a rigid barrier. Despite of this, the nucleolus contains a large number of nucleolus-specific proteins forming a specific nuclear compartment. The proteomic study identified 1,318 nucleolar proteins (Stenström *et al.* 2020). Many of these proteins are mobile and they shuttle between the nucleolus and other organelles, one of the most prominent targets being the mitochondria. (Daniely and Borowiec 2000, Kim *et al.* 2005, Jia *et al.* 2017, Stenström *et al.* 2020). Due to its nonmembranous structure, the nucleolus is an organelle that provides a unique nucleoplasm-nucleolus interface for studies of nuclear interactions (Lafontaine *et al.* 2021). Liquid-liquid phase separation model provides needed stability to the structure, still enabling the free diffusion of proteins, substrates, and products in and out of the structure (Falahati *et al.* 2016). The most studied function of the nucleolus is ribosome biogenesis. Lately, more nucleolar functions, such as stress responses, have emerged (Latonen 2019). In addition to crucial roles in the biological processes of the cell, the nucleolus has a significant role in the progression of many diseases such as cancer, neurodegeneration, and ribosomopathies (Correll *et al.* 2019).

Nucleoli are formed around nucleolar organization regions (NORs). NORs found in the acrocentric regions of chromosomes 13, 14, 15, 21, and 22 encode ribosomal RNA. The nucleolus is surrounded by dense heterochromatin, where chromatin regions subsequent to the NOR regions are silenced (McStay 2016). One way to simplify the organization of the nucleoli in the cell nucleus is to think of the nucleoli as lipid droplets in a liquid. The nucleolus goes through organizational changes due to the condensation and decondensation of the chromosomes, causing the lipid droplets to gather and disperse. Recently, members of the heterochromatin protein 1 (HP1) family have been associated with liquid-liquid phase separation (LLPS), and H3K9me seems to be required for the maintenance of the liquid-liquid phase (Larson *et al.* 2017, Strom *et al.* 2017,

Qin *et al.* 2021). The size and shape of the nucleoli change throughout the cell cycle (Hernandez-Verdun 2011, Caragine *et al.* 2019) and are determined by the liquid properties of the nucleoli (Brangwynne *et al.* 2011). The maintenance of nucleolus-nucleoplasm interphase is dependent on ATP-related processes including transcriptional and epigenetic changes of chromatin (Caragine *et al.* 2019, López *et al.* 2020). The dependence of the nucleolar integrity on chromatin is consistent with the liquid-liquid interface model. However, existing theories cannot explain the variation in nucleolar volume (Caragine *et al.* 2019). The nucleolus can be divided into specific subcompartments which take care of different tasks. The granular center (GC) in the central area of the nucleolus encloses the fibrillar centers (FC). FCs consist of ribosomal DNA (rDNA) and is lined with the dense fibrillar center (DFC) The fourth nucleolar subcompartment is the newly established nuclolar rim (NR) located around the GC (Fig. 1). The organizational model of the NR is highly dependent on cell cycle, with a high number of proteins localizing to the chromosomal periphery during mitosis. One of the identified rim proteins is the proliferation marker ki-67 (Stenström *et al.* 2020).

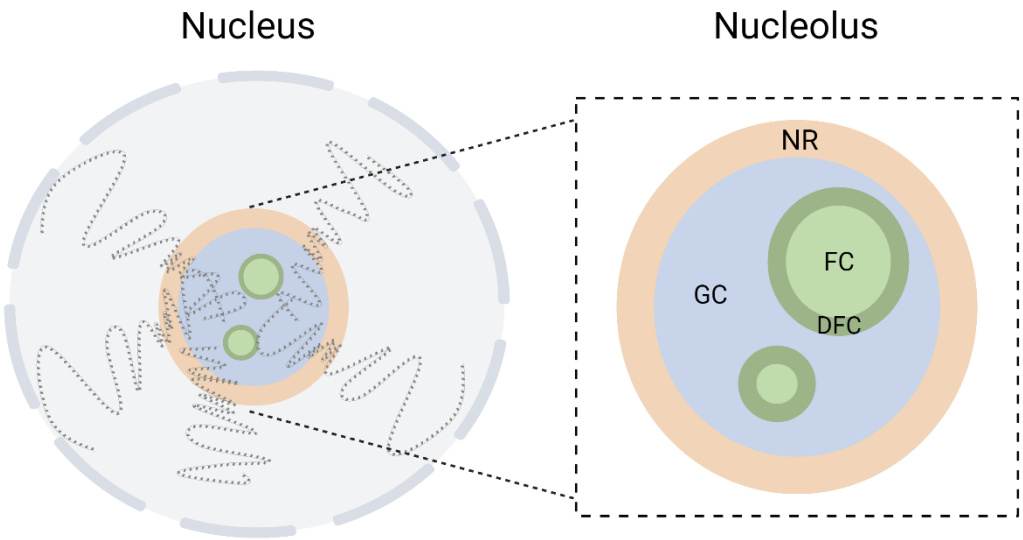

FIGURE 1 Localization and structure of the nucleolus. Nucleoli are formed from the chromosomal territories of five metacentric chromosomes, chr 13, chr 14, chr 15, chr 21, and chr 22, depicted in the overview of the nucleus (left). The figure on the right shows the positioning of the nucleolar substructures including the granular center (GC), fibrillar center (FC), dense fibrillar center (DFC), and nucleolar rim (NR). Figure reproduced from study II. Image created with BioRender.

Protein synthesis of the cell requires functional ribosomes. Ribosome biogenesis is a complex series of events which are mainly carried out in the nucleolus. The condensed biomolecular structure of the nucleolus is essential for ribosome production. Ribosome biogenesis starts with rDNA transcription residing in the FC. Transcription of rDNA requires its specific polymerase, RNA polymerase I. Actual active transcription occurs in the fibrillar and dense fibrillar centers (FC/DFC) interface. The pre-assembly of ribosomes and preceding modification of pre-rRNAs take place in the GC (Falahati *et al.* 2016, Correll *et al.* 2019). In humans, the transcription of 47S pre-rRNAs is accompanied by formation of DFCs (Yao *et al.* 2019). The pre-assembled ribosomes move from the nucleolus to the nucleoplasm and finally to the cytoplasm, where the final ribosome assembly and quality control take place. The whole process is controlled by over 200 assembly factors (Peña *et al.* 2017).

2.3 Nuclear envelope and nuclear pore complexes

The nuclear envelope (NE) is a phospholipid bilayer membrane structure that surrounds the nuclear genome and controls the nuclear translocation of material such as ions, proteins and nucleic acids (Hetzer 2010). The NE is formed from the inner nuclear membrane (INM) and outer nuclear membrane (ONM), and a single-membrane structure called the endoplasmic reticulum (ER) extends from the ONM. Moreover, the ER shares similar properties with the ONM. Because ONM and ER are continuous, the perinuclear space (PNS) located between the nuclear membranes and ER lumen are connected (Stewart *et al.* 2007). The translocation of molecules across the NE is mediated by nuclear pore complexes (NPCs). Smaller nonpolar molecules such as water, sugars, and ions can move through the pores passively, while active transport is needed for larger molecules (Wente and Rout 2010).

NPC consists of approximately 30 proteins referred to as nucleoporins (Cronshaw *et al.* 2002). Two of these proteins, Pom121, and gp210, are integral membrane proteins that bind the structure to the membrane (Suntharalingam and Wente 2003). The NPCs are symmetrically arranged, following an eightfold symmetry (D'Angelo and Hetzer 2008). Molecules smaller than 60 kDa can pass freely through the 9 nm wide portal (Ohno *et al.* 1998, Beck *et al.* 2007). However, the NPC has been reported to accommodate the transport of macromolecules as wide as 39 nm (Panté and Kann 2002). The transport through NPCs is regulated via nuclear localization signals (NLS). Proteins containing this short specific amino acid sequence are targeted to the nucleus. Similarly, the export of proteins out of the nucleus occurs via recognition of nuclear export signals (NES) (Lange *et al.* 2007, Terry *et al.* 2007). Karyopherin protein family (Kaps) includes many proteins capable of recognizing both NLS (importins) and NES signals (exportins). The active transport utilizes Ran-GTPase during transport. The most distinguished importins are importins α and β, and exportin chromosome region maintenance 1 (CRM1) will be viewed more thoroughly in this thesis regarding

parvovirus infection. NPCs fluctuate during the cell cycle, influencing further the nuclear import and export of molecules (Antonin *et al.* 2008).

The nuclear lamina, constructed from intermediate filaments lamins, is essential for stability and structure of the nucleus. Monomeric lamins form dimers by intertwining their rod regions. A and B type lamins form the meshwork via interaction between the head and tail regions (Aebi *et al.* 1986, Goldman *et al.* 2002). Besides its structural function, A-type lamins have essential roles in regulation of transcription (Lund *et al.*). The lamina is attached to the inner nuclear membrane through membrane-bound proteins, including emerin and lamin B type receptors and other membrane proteins capable of sensing mechanic stress (Lammerding *et al.* 2005, Nikolakaki *et al.* 2017). Besides attaching to the NE via membrane proteins, the nuclear lamina binds chromatin and helps to maintain chromatin integrity (Ulianov *et al.* 2019). During cell division and apoptosis, nuclear lamina is degraded via phosphorylation. Cell cycle-related changes also include the disruption of nuclear pore complexes. For example, Nup98 is hyperphosphorylated by Cdk1 and Nek kinases during the early prophase, leading to the disruption of NPC in prometaphase (Laurell *et al.* 2011, Linder *et al.* 2017). During the cell cycle, NPCs go through changes in distribution and density. During the G1-S phase, NPCs are excluded from parts of the NE. Interestingly these areas are rich in Lamin A and emerin but devoid of Lamin B (Maeshima *et al.* 2006, Imamoto and Funakoshi 2012). Notably, Mäntylä *et al*. 2015 showed that during CPV infection NPCs accumulate to the apical side of the cell simultaneously with lamin B1 reorganization to the apical side and a decrease in the total amount of lamin A/C. Phosphorylation of lamins is a cell cycle-dependent event involving Cdk1-mediated phosphorylation. Notably, Lamin A and B have different disassembly and assembly pathways. B-type lamins accumulate in regions with nuclear pore complexes, whereas A-type lamins accumulate in the regions without NPCs (Mäntylä *et al.* 2015).

2.4 Parvoviruses and canine parvovirus

Members of the family parvoviridae are small noneveloped viruses, possessing a linear ssDNA genome of 4-6 kb in size and a nonenveloped capsid. The pathogenicity of parvoviruses ranges from subclinical to lethal. Parvoviruses infect a large variety of species. The family has traditionally been divided into two subfamilies, viruses capable of infecting vertebrates (*Parvovirinae*) and invertebrates (*Densovirinae*). However, the recently found chapparvoviruses infect vertebrates but are genetically closer to *Densoviridae*. Therefore, the family *Parvoviridae* has been revised and rearranged to include a new subfamily *Hamaparvovirinae* (Pénzes *et al.* 2020). Members of the genus *Dependoparvovirus* require a co-infection with a helper virus (e.g. HSV-1 or Adenovirus). Members of the genus protoparvovirus encapsidate predominantly negative-strand ssDNA (Cotmore *et al.* 2019). The members of the family are considered to have monosense genomes. However, recently a new frameshifted gene has been

identified for adeno-associated virus (AAV) (genus *Dependovirus*) (Ogden *et al.* 2019, Elmore *et al.* 2021, Galibert *et al.* 2021, Hull *et al.* 2022). Parvoviruses have been mainly studied for their intrinsic attributes that make them good candidates for oncolytic clinical therapy and to be utilized as viral vectors (Marchini *et al.* 2015).

Exceptionally for a DNA virus, parvoviruses have a high evolutionary rate comparable to RNA viruses, e.g. 0.7-7.1 x 10^{-3} sequence changes per site per year in canine parvovirus (CPV) and feline panleukopenia viruses (FPLV). It has been proposed that the ssDNA template and the replication mechanism might be prone to error, and that the proof-reading mechanism might not be involved or at place in infected cells. This high evolutionary rate has been linked to the evolutionary emergence of CPV from FPLV. (Shackelton *et al.* 2005).

Canine parvovirus (CPV) belongs to the family *Parvoviridiae*, the subfamily *Parvovirinae*, and the genus *Protoparvoviruses*. CPV emerged in the late 1970s from a feline parvovirus spreading globally partly due to the stable structure of the capsid and due to human behavior (Reed *et al.* 1988, Truyen *et al.* 1995, Shackelton *et al.* 2005). The only working vaccine against parvoviruses has been developed against CPV (Carmichael *et al.* 1983). CPV is a small virus with a linear ssDNA genome of 5.3 kb in length. The genome encodes two structural proteins, VP1 and VP2, and two nonstructural proteins, NS1 and NS2, transcripted from two genes through alternative splicing (Reed *et al.* 1988).

2.4.1 Viral structural proteins and capsids

Many smaller viruses have adopted a de novo mechanism called "overprinting". Due to critical nucleotide substitutions, an alternative reading frame emerges from the original gene. This results in two overlapping genes: one pre-existing ancestral gene, and a new gene coding a novel protein that shares the functions of the preceding gene (Pavesi 2021). Since parvoviruses consist of two genes, both encoding more than one viral protein, it is feasible that parvoviral transcripts have emerged through this mechanism.

Capsid structures have been determined in atomic or near-atomic resolution for a range of parvoviruses, including human bocavirus, human parvovirus B19, Aleutian mink disease parvovirus, AAV type 2, and canine parvovirus (Tsao *et al.* 1991, Xie and Chapman 1996, McKenna *et al.* 1999, Kaufmann *et al.* 2004, Gurda *et al.* 2010, Cotmore and Tattersall 2014).

Icosahedral parvoviral capsids, ~18-25 nm in diameter, consist of three viral structural proteins, VPs 1, 2, and 3 (Tsao *et al.* 1991). All VP proteins are transcripts of the same gene, and the C-terminal ends of all the proteins are identical (Reed *et al.* 1988). The largest parvovirus minute virus of mice (MVM) capsid protein is the 83 kDa-sized VP1. The other two, VP2 and the cleaved VP3, are reasonably similar in size (67 kDa and 65 kDa, respectively) (Tattersall *et al.* 1977). During DNA encapsidation, the N-terminal ends of VP2 are externalized to the outside of the capsid (Tsao *et al.* 1991, Agbandje-McKenna *et al.* 1998, Kontou *et al.* 2005). The externalization results in proteolytic cleavage of the VP2 N-terminus, forming an N-terminally shortened VP3 (Maroto *et al.* 2004). One

CPV capsid consists of 60 structural proteins, the major protein being the VP2 (~ 90 % of the capsid) and the minor one VP1 (~ 10 % of the capsid), forming an icosahedral T=1 structure (Tsao *et al.* 1991, Suikkanen *et al.* 2003b). A closer examination of the complex capsid structure reveals the surface landscape of the virus; pore-like structures at the fivefold axis, spikes at the threefold axis, and a valley-like structure at the twofold axis (Tsao *et al.* 1991, Callaway *et al.* 2017). The major capsid protein VP2 forms eight-stranded antiparallel β barrels (Agbandje and Chapman 2006). The N-terminus of the CPV VP1 capsid protein is a requisite for infection but not for assembly (Vihinen-Ranta *et al.* 2000). MVM oligomers are transported to the nucleus via a structured nuclear localization motif (Lombardo *et al.* 2000). The dominating nuclear localization motif of the oligomers prevails over the NLS of VP1 (Riolobos *et al.* 2006).

2.4.2 Nonstructural proteins of parvoviruses

The small genome of parvoviruses is efficiently packed, transcribing two nonstructural proteins in addition to the two or three structural proteins. Contrary to the structural proteins, the nonstructural proteins have an identical N-terminus of 78 amino acids (Wang *et al*. 1998). For CPV, the functions of the nonstructural protein 1 (NS1) have been characterized, but the role of the second nonstructural protein (NS2) has remained an enigma (Wang *et al.* 1998, Niskanen *et al.* 2010, 2013).

2.4.2.1 NS1

Parvoviral NS1 has an important role in the replication and promotion of viral transcription. NS1 can bind to multiple sites of the viral genome (Nüesch *et al.* 1995, Cotmore *et al.* 2007, Niskanen *et al.* 2013). MVM NS1 causes site-specific nicking of the single-strand viral genome required for replication initiation. The nickase activity of NS1 can also induce unspecified nicking of the host genome, resulting in the accumulation of DNA damage (Nüesch *et al.* 1995, op de Beeck and Caillet-Fauquet 1997). The CPV NS1 protein (76.7 kDa) is a multifunctional phosphoprotein (Fig. 2). NS1 of CPV and MVM bind the transcription activation region of the viral promoter in a process requiring ATP (Christensen *et al.* 1995, Niskanen *et al.* 2013). Parvoviral NS1 has also helicase activity. To initiate the replication, cooperation with replication protein A (RPA) is required (Christensen *et al.* 1997, Christensen and Tattersall 2002). ATPase activity is required for the functionality of CPV NS1 (Niskanen *et al.* 2010).

MVM NS1 interacts with the catalytic subunit of casein kinase II, CKIIalpha, interfering with host cell signaling, which is believed to lead to cytotoxicity and viral capsid phosphorylation (Nüesch and Rommelaere 2006). Besides the functions tended by the N-terminal end of the protein, the C-terminal phosphorylation of the protein might impact the replication efficiency and pathogenicity of the virus (Miao *et al.* 2022). Moreover, the phosphorylation status of cellular proteins is changed in the presence of MVM NS1 (Anouja *et al.*

1997). Generally, parvovirus NS1 protein expression is known to induce cell cycle arrest and apoptosis (Moffatt *et al.* 1998, Morita *et al.* 2003, Hsu *et al.* 2004, Poole *et al.* 2004, Hristov *et al.* 2010, Mincberg *et al.* 2011, Saxena *et al.* 2013).

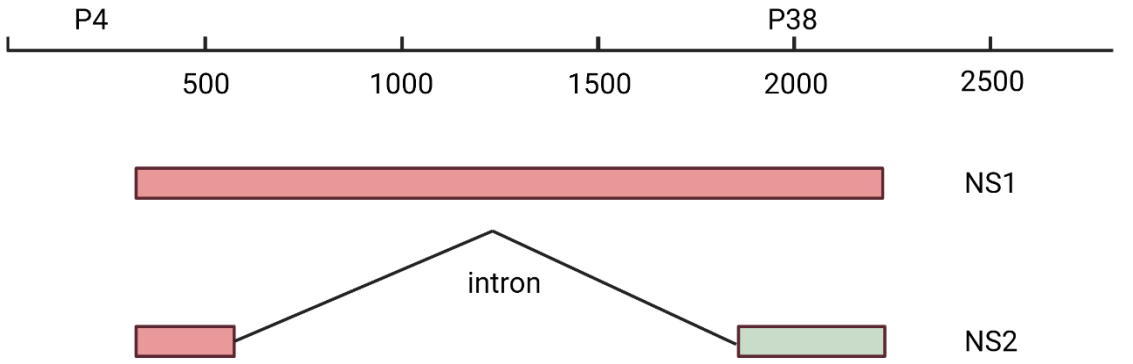

FIGURE 2 Schematic model of CPV NS1 and NS2 expressed from the same gene with differing exons. Linear ssDNA genome with promoter regions P4 and P38 is shown. NS1 and NS2 transcribed from the nonstructural protein open reading frame controlled by the P4 promoter are presented. NS2 is alternatively spliced from the same region as NS1. Red regions of are similar whereas green region is in different reading frame. Image modified from Wang *et al.* 1998. Image created with Biorender.

2.4.2.2 NS2

The knowledge of protoparvovirus NS2 function is largely based on studies of MVM. The requirement of MVM NS2 for productive infection varies by the host. Specifically, NS2 is dispensable in infection of immortalized human cell lines while being essentially required for infection and progeny virus production of murine cells (Naeger *et al.* 1990, Cater *et al.* 1992). The replication of MVM depends on the nuclear accumulation of NS2 (Choi *et al.* 2005), and deletion of NS2 results in ineffective replication center formation (Ruiz *et al.* 2011). MVM NS2 has also been shown to control the capsid assembly and viral genome translation (Cotmore *et al.* 1997). Knowledge of MVM NS2 interaction with cellular proteins has remained limited. However, MVM NS2 is known to interact with survival motor neuron protein (Smn) and some members of the 14-3-3 regulatory protein family (Brockhaus *et al.* 1996, Young *et al.* 2002). In addition, MVM NS2 interaction with CRM1 mediates the nuclear exit of progeny virus (Bodendorf *et al.* 1999, Ohshima *et al.* 1999, Miller and Pintel 2002). The role of CPV NS2 has remained largely unknown. The sole existing study on CPV NS2 determined the effect of NS2 deletion on viral replication and pathogenesis in both cell culture and in dogs (Wang *et al.* 1998).

2.4.3 Parvoviral lifecycle

Evolutionally related FPLV and CPV bind to the transferrin receptor on the host cell surface during the initial step of infection (Parker *et al.* 2001, reviewed in Ros *et al.* 2017). The other protoparvoviruses, MVM, porcine parvovirus (PPV) and rat parvovirus H-1 PV, utilize sialic acid receptor for their entry (Ros *et al.* 2017). Following receptor binding, capsids are internalized via the clathrin-mediated endocytic pathway (Parker *et al.* 2001, Ros *et al.* 2017). Initially, capsids enter early endosomes, then recycling endosomes, and finally vesicles characterized as late endosomes and lysosomes (Suikkanen *et al.* 2002). The acidic microenvironment of these endolysosomal vesicles is required to set off the conformational changes of capsids required for endosomal escape (Ros *et al.* 2017). The acidic environment triggers the exposure of phospholipase A2 activity of the N-terminal VP1, allowing release of capsids from endosomes (Zádori *et al.* 2001, Suikkanen *et al.* 2003b). Once in the cytoplasm, capsids are translocated towards the nucleus by dynein motor protein along microtubules (Suikkanen *et al.* 2002, 2003a). The NLS located in the VP1 N-terminus is required for nuclear import of CPV capsids (Vihinen-Ranta *et al.* 2002), and capsids recruit importin β to enter through the NPCs (Mäntylä *et al.* 2020).

Replication of ssDNA viruses depends on multiple cellular factors available during the host's DNA synthesis in the cell cycle S-phase. Parvoviruses are able to replicate only during S-phase. Initiation of the virus replication has been shown to rely on cyclin A and Cdk2 activities (Bashir *et al.* 2001). The timing and nuclear localization of capsid disassembly has remained unknown. However, it has been suggested that the exposure of the genome after disassembly would lead to the activation of DNA damage responses and prevention of the cell cycle progression towards mitosis. This enhances infection by providing extended time for viral replication (Cotmore and Tattersall 2014). In vitro studies have suggested that capsids release their genomes in 3' to 5' orientation from intact capsids (Cotmore *et al.* 2010). Both transcription and replication occur concurrently, requiring the viral genome to be conversed to replicative form dsDNA (Wolter *et al.* 1980, Cotmore and Tattersall 2014). NS1 has an essential role in both processes (Nüesch *et al.* 1995, Christensen *et al.* 1997, Christensen and Tattersall 2002, Niskanen *et al.* 2013). The ssDNA parvoviral genome has inverted terminal repeats at each end. The dsDNA is synthesized via linear adaptation of the rolling hairpin synthesis model (Cotmore and Tattersall 2014). Following the synthesis, the dsDNA strands are displaced and newly formed strands act as templates for replication. Parvoviral replication is initially dependent on cyclin A, cyclin A-dependent kinase, and subsequently on DNA polymerase δ, proliferating cell nuclear antigen and replication protein A (Christensen *et al.* 1997, Bashir *et al.* 2001, Christensen and Tattersall 2002). The formation of replication fork starts from the 3' prime end of viral dsDNA. The left-hand inverted terminal repeat acts as a primer for the synthesis of the positive-sense strand (Christensen *et al.* 1997, Cotmore and Tattersall 2014). At this stage, transcription is started, and the produced NS1 is required to bind the replication origin site at the 5' end of the genome (Cotmore *et al.* 2000). Together with high-

mobility group proteins, NS1 binds and nicks the right-end origin site (Cotmore and Tattersall 1998). Proliferating cell nuclear antigen is needed to protect the ssDNA formed at this state (Christensen and Tattersall 2002). The replication continues with the help of NS1, which acts as a helicase to open the double-stranded genome in a 3' to 5' direction by covalently linking to the 5' end of the viral genome (Nüesch *et al.* 1995, Christensen and Tattersall 2002). After the whole linear genome has been replicated, NS1 induces a nick at the left-end origin site together with the parvovirus initiation factor, activating the NS1 endonuclease activity (Cotmore and Tattersall 1998). Viral genome transcription is temporally regulated, first the promoter P4 is activated for production of NS1 and NS2 mRNA, and then promoter P38 for VP1 and VP2 mRNA (Clemens and Pintel 1988, Tullis *et al.* 1994). Both of the Y-shaped left hairpin axial "ears" are needed for transcription (Li *et al.* 2013). NS1 contributes to transcription initiation by ATP-dependent binding to transactivation region of the P38 protomer (Christensen *et al.* 1995).

The assembly of parvovirus progeny viruses depends on nuclear import of viral structural proteins VP1 and VP2. In MVM infection, the nuclear import of VPs, and thus the assembly of progeny capsids, is dictated by the progression of the cell cycle. Nuclear import of VPs occurs during the S phase followed by the assembly of progeny capsids, independently of viral replication. The cytoplasmic VPs are imported into the nucleus as phosphorylated trimers. The trimers are formed from either two VP2 and one VP1 or three VP2 proteins, with five times higher phosphorylation of the VP1s. Phosphorylation of assembled full capsids is reduced (Gil-Ranedo *et al.* 2015). In addition, the N-terminal domain of VP2, hidden in the assembled empty capsids, is exposed in the DNA-containing capsids (Gil-Ranedo *et al.* 2018). Parvoviruses differ in their capability to encapsidate viral genomes. Some parvoviruses, such as CPV and MVM, pack minus-sense ssDNA genomes exclusively, whereas others, such as human parvovirus B19, can pack both positive and negative strands (Cotmore and Tattersall 2005).

After assembly, progeny capsids must escape the nucleus. Previous studies have revealed that the nuclear egress of MVM capsids is mediated by CRM1 (Eichwald *et al.* 2002, Miller and Pintel 2002, Maroto *et al.* 2004, Engelsma *et al.* 2008). The NES needed for CRM1-mediated export is localized in the VP2 N-terminus (Maroto *et al.* 2004), which is only exposed in capsids that contain viral DNA (Hernando *et al.* 2000). The nuclear egress of full MVM capsids is also enhanced by phosphorylation of capsid surface, specifically the N-terminus of VP2 (Wolfisberg *et al.* 2016). Moreover, the necessary subsequent release of the capsids out of the cell has been suggested to involve activation of cell death (Nykky *et al.* 2010).

2.4.4 Dependence of the parvoviral lifecycle on DNA damage response and cell cycle regulation

Cell cycle functions include replication of cellular genome, mitosis and formation of two daughter cells. In the course of cell division the cell goes through many

changes that affect especially the structure of the nucleus. Cell cycle can be divided into four phases: G1 phase when the cell grows, S phase when DNA replication takes place, G2 phase when the cell prepares for mitosis, and M phase when the cell divides by mitosis. During the interphase (G1 to G2) the cell doubles its size and genome. The progression of the cell cycle is controlled by cyclins and cyclin-dependent kinases (Cdks) (Masui and Markert 1971, Evans *et al.* 1983, Jackson 2008, Wang *et al.* 2014). Different cyclins and Cdks are expressed during different phases of the interphase. Cdk1 controls the progression of the cell cycle from the S phase to G2 with A-type cyclins, and from G2 to M phase together with B-type cyclins (cyclin B1, B2 and B3) (Masui and Markert 1971, Malumbres 2014). The activity of these complexes can be inhibited via various Cdk inhibitors belonging to the Cip/Kip (p21, p27 and p57) and Ink4 (p15, p16, p18 and p19) families (Karimian *et al.* 2016).

The activation of Cdk1 initiates the degradation of cyclin B1, a process that will lead to the mitosis. During prophase that initiates mitosis chromosomes get condensed, NE becomes disintegrated, and mitotic spindles form. In metaphase cells the chromosomes align at the centre of the spindle preparing for the separation of sister chromatids to the opposite sides of the dividing cells in anaphase (Burke and Ellenberg 2002, Park *et al.* 2018, Crncec and Hochegger 2019, Pavin and Tolić 2021). Finally, after nuclear envelope reformation and chromatin decondensation in telophase, the cell goes through cytokinesis forming two daughter cells. Mitotic exit in anaphase is controlled by anaphase-promoting complex (APC) together with cdc20 activation. First, APC degrades cyclin B1 by inactivating the Cdk1-cyclin B complex (Park *et al.* 2018, Crncec and Hochegger 2019). Chromosomal condensation during mitosis is mediated by different effectors: cohensins which keep the sister chromatids together from G2 to anaphase, and condensins which induce tight packaging of chromosomes during pro- and metaphases (Brooker and Berkowitz 2014, Skibbens 2019).

Damage of cellular DNA activates a specific DNA damage response (DDR) pathway. Recognition of DNA damage recruits proteins responsible for DNA damage repair to the site of the damage. Activation of DDR leads to cell cycle arrest until the damage has been repaired, or in the case of excess DNA damage to the activation of pre-apoptic signals. Fate of the cell is determined by the extent of the damage and the effectiveness of the DNA damage repair machinery. Activation of the signaling routes depends on the quality of the damage. Ataxia telangiectasia and Rad3-related (ATR) kinase activation is linked to replication fork stalling. Activation of ataxia telangiectasia mutated (ATM) kinase is linked to a double-stranded DNA break (DSB). DNA-dependent protein kinase DNA-PK kinase together with its catalytic subunits Ku70 and Ku80 have been associated with non-homologous end joining repair, a form of DSB (Shiotani and Zou 2011, Blackford and Jackson 2017). Initiation of the DDR response with the kinases leads to the phosphorylation of the histone variant H2AX and to the activation of the repair cascade (Kinner *et al.* 2008).

In virus infections, DDR can have reciprocal functions by either promoting the infection and viral reproduction or benefiting host response to the infection. Proteins involved in the DDR response are known to share some functions with

the innate immunity response (Lilley *et al.* 2007, Jackson and Bartek 2009, Trigg and Ferguson 2015). Autonomous parvoviruses as well as AAV have been shown to induce DNA damage response in host cells leading to cell cycle stalling. As autonomous parvoviruses are incapable of forcing the cell to enter the S phase, which is needed for effective replication, they must wait for the cell to enter it to start the infection. After entering the S phase, parvoviruses are able to control the cell cycle progression to advance virus production by stalling cell cycle progression to S phase and later to G2/M checkpoints. These regulation processes are likely induced by DNA damage response (Fig. 3) (Chen *et al.* 2010, Luo *et al.* 2011a). AAV infection in the presence of helper adenovirus infection has been shown to cause activation of the DNA damage response pathway, distinct from the effect caused by AAV or adenovirus alone. Infection causes autophosphorylation of the ATM- and DNA-dependent protein kinase catalytic subunits. Full activation of the pathway requires replication of the AAV genome (Schwartz *et al.* 2009). Replication-related proteins of AAV, so called Rep proteins, interact with the Mre11 part of the MRN complex, which is an important initiator of the ATM response (Smith-Moore *et al.* 2018). The DNA damage caused by AAV has been reported to mimic stalled replication forks (Jurvansuu *et al.* 2005).

MVM NS1 causes nicks in the host DNA, resulting in cell cycle arrest (op de Beeck and Caillet-Fauquet 1997). Additionally, MVM infection causes accumulation of phosphorylated proteins of the ATM signalling route to the replication start sites together with the viral replication protein NS1. Chemical hindering of the ATM route with ATM inhibitors results in restricted MVM replication and enhances the virus-induced cell cycle arrest. Interestingly, viral replication was found to be a requisite for the ATM signalling pathway activation, as expression of the viral proteins by themselves and viral protein-deficient mutant infection did not have an effect on the DDR response (Adeyemi *et al.* 2010). During viral replication, emerging viral DNA is bound to RPA, a known activator of ATR, yet this does not lead to the full activation of ATR response since activation of Chk1 is not reached during MVM infection (Adeyemi *et al*. 2014, Majumder *et al*. 2017). MVM has been shown to introduce a prominent premitotic block that is independent of p21 and ATR/Chk1 signalling routes (Adeyemi *et al*. 2014).

In addition to ATM inhibition, ATM-deficient cell line as well as Mre11 knockdown cells have been used to study the effect of DDR on minute virus of canines infection. Blocking ATM activation results in inefficient replication and virus production as well as reduction of cell death, whereas knocking down Mre11 manifests as reduction of viral replication. The reduction of viral replication was displayed by a decrease in NS1 expression. DDR activation in infection was also p53 dependent. Infectious viral clones with removed terminal repeat regions did not activate any of the studied DDR routes, leading to the conclusion that replication of the viral genome is a requisite for DDR (Luo *et al.* 2011b). Expression of human parvovirus B19 (B19V) viral proteins was not capable of triggering DNA damage response. Surprisingly UV-inactivated B19 did not lead to DDR, whereas UV-inactivated AAV was capable of triggering

DDR in a process that mimicked the stalled replication fork. (Jurvansuu *et al.* 2005, Lou *et al.* 2012). For B19 cell cycle arrest during the infection was reported to be caused by viral NS1 protein, in a p53-independent manner, irrelevant to the DNA damage response (Lou *et al.* 2012). In comparison to MVM, the activation of ATM, ATR, and the DNA-dependent protein kinase catalytic subunit has been found to be required for effective human Bocavirus 1 infection (Deng *et al.* 2017).

The association of MVM viral genomes with host chromatin has been demonstrated by using a novel high-throughput Viral Chromosome Conformation Capture assay. Proceeding infection leads to the emergence of new DNA damage sites, and viral genomes were seen to associate with these sites. Moreover, introduction of externally induced DNA damage to a specific genomic locus with laser irradiation or with CRISPR-Cas9 resulted in viral genome association with these regions. V3C-seq also revealed that viral genomes associated not only with DNA damage but also with TADs. (Majumder *et al.* 2018).

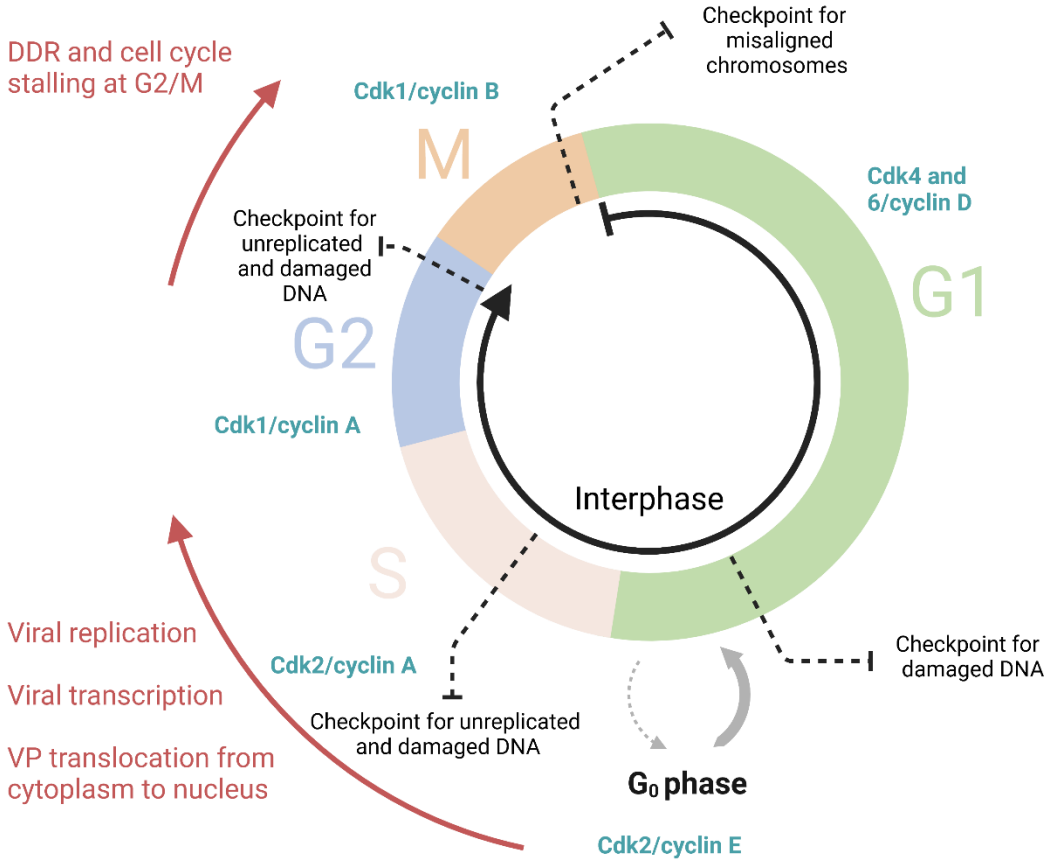

FIGURE 3 Schematic overview of the cell cycle and cell cycle checkpoints coupled with the parvoviral lifecycle. Checkpoints controlling the progression of the cell cycle, the principal proteins and complexes effecting the progression (in green) and the events of the viral lifecycle (in red) are shown. Image created with BioRender.

2.4.5 Parvoviruses and apoptosis induction

Apoptosis takes part in many different processes in an organism, and it is especially vital for the development of the individual. Apoptotic cell death enables development steps by eliminating unneeded cells or tissues in the embryo (Kerr *et al.* 1972, Hengartner 2000). Apoptosis provides a defense mechanism against DNA damage, which is generally activated in virus-infected cells (Elmore 2007, Lilley *et al.* 2007). Apoptosis can also result from the accumulation of unfolded or misfolded proteins in the endoplasmic reticulum (ER) (Hetz *et al.* 2020). Hallmarks of apoptosis include shrinkage of the cells, condensation and fragmentation of chromosomal DNA, NE blebbing, nuclear fragmentation into apoptotic bodies, and the removal of the apoptotic cells by phagocytosis (Saraste and Pulkki 2000, Hengartner 2000).

DNA damage can lead to cell cycle arrest and apoptosis. The central mediator of this process is the tumor suppressor gene p53. The early initiators of DNA damage, ATM and CHK phosphorylate p53, result in the activation of proapoptotic signals (Norbury and Zhivotovsky 2004). Apoptosis is initiated via proapoptotic signals such as regulating protein bcl-2. Further activation of apoptosis via caspase cascades occurs when the apoptosome complex is formed from apoptosis protease–activating factor 1 molecules after cytochrome c is released from the mitochondria. This leads to the activation of the initiator caspase, caspase-9 (Yuan and Akey 2013). The primary apoptotic mediators, caspase proteases, are capable of cleaving proteins. Caspases can be classified as initiators and effectors. The initiation of apoptosis happens through a cascade of caspase activation. Inactive caspases are activated by proteolytic cleavage to their active form (Hengartner 2000). After the initial activation of caspase-9, effector caspases such as caspase-3 are activated (Jänicke *et al.* 1998).

Caspase activation leads to the activation of DNases, including caspase activated DNase (CAD) and DNase II (Hengartner 2000, Samejima and Earnshaw 2005). Other target proteins for caspases include nuclear lamins. The cleaving of lamins results in nuclear lamina breakdown and facilitation of nuclear fragmentation (Rao *et al.* 1996). Besides activation of apoptosis, many external signals that promote survival can be activated, leading to inhibition of apoptosis. PI 3-kinase induces the promotion of cell survival. The phosphorylation cascade leads to the activation of Akt protein serine/threonine kinase, further amplifying the signal via other mediators. Besides the external survival signals, external death signals can influence the outcome for the cell. These tumor necrosis factors bind TNF receptors, resulting in caspase activation and apoptosis promotion (Elmore 2007). Cell death signaling and how the fate of the cell is determined are complicated processes, with a myriad of signaling molecules taking part in the decision. In recent years different kinds of cell death types have been identified. Apoptotic cell death can be divided into mitotic cell death and anoikis, whereas necrosis can be methuosis, necroptosis, NETosis, pyronecrosis, and pyroptosis. Besides the apoptotic and necrotic pathways entosis, ferroptosis, lysosome-dependent cell death, and parthanatos pathways can be identified as their own

types (Nirmala and Lopus 2020). The specifics of virus-induced cell death in terms of these newly formed subcategories of cell death require further studies.

Many viruses modulate the apoptotic pathways of their hosts. Induction of apoptosis usually leads to the pathogenesis of the virus, whereas premature cell death through apoptosis can hinder the production of infectious viruses (Shen and Shenk 1995). Viruses belonging to the family parvoviridae are known to induce cell death through apoptosis, generally involving the NS1 (Chen and Qiu 2010). Human parvovirus B19 NS1 protein can induce apoptosis in erythroid cells via pathways involving caspase-3 (Moffatt *et al.* 1998). Expression of B19 NS1 in CS-7 cells led to apoptosis dependent on p53, similarly to caspase-3 and caspase-9 but not caspase-8 and in addition to an increase of proapoptotic Blc-2 members Bax and Bak (Hsu *et al.* 2004). In hepatocytes, the induction of apoptosis involved similarly caspase-3 and caspase-9 but not caspase-8 (Poole *et al.* 2004). Both MVM infection and MVM NS1 expression induce apoptosis in rat fibroblast cells in p53-independent manner (Mincberg *et al.* 2011). Interestingly, Aleutian mink disease virus (AMDV) capsid protein expression leads to the activation of apoptosis, with the characteristic of high caspase-10 involvement and in vitro cleavage of the capsid by caspase-7 (Cheng *et al.* 2010). Autonomous parvovirus H1 has been shown to induce apoptosis in a variety of cell lines, however, the disruption of the cell membrane indicated involvement of necrosis (Rayet *et al.* 1998, Ran *et al.* 1999). Expression of parvovirus H1 NS1 leads to activation of caspase-3 and caspase-9 and cell lysis (Hristov *et al.* 2010). The induction of apoptosis by H1 is specific to human hepatoma cells over human primary hepatocytes (Moehler *et al.* 2001). The MVC infection has been linked to Bax translocation to the mitochondrial membrane, leading to activation of caspases 6, 8, and 9, followed by caspases 3/7, 10, and 12 (Chen *et al.* 2010). Furthermore, CPV is known to induce apoptosis, with time-dependent caspase-9, caspase 3/7, and caspase 8 activation. Moreover, similarly to H1 infection, cell membrane integrity was lost in CPV-infected cells, indicating a secondary necrosis event after apoptosis induction (Nykky *et al.* 2010). CPV variant CPV-2a has been found to induce apoptosis through the involvement of both intrinsic and extrinsic pathways involving caspases 2, 8, 9, and 12, including the involvement of p53 (Doley *et al.* 2014). A study focusing on CPV NS1 expression and apoptosis showed that NS1 induces apoptosis in p53-independent manner (Saxena *et al.* 2013). It seems clear that apoptosis is activated in parvovirus-infected cells, with some host cell and virus type-specific differences. How proapoptotic and survival-promoting signals are regulated during parvovirus infection has been less studied. However, MVM NS2 is known to interact with a known survival-promoting proteins survival motor neuron protein (Smn) and some members of the 14-3-3 protein family (Brockhaus *et al.* 1996, Young *et al.* 2002). Whether these interactions promote or inhibit apoptosis is not known.

3 AIMS OF THE STUDY

NS2 is one of the two nonstructural proteins of CPV. Current knowledge on functions of autonomous parvovirus NS2 is based on studies with MVM. The role of NS2 in CPV infection has remained largely unknown. Besides other known functions, MVM NS2 participates in the nuclear egress of the capsids together with CRM1. The nuclear exit of CPV progeny viruses has not yet been studied extensively. Altogether, this thesis aims to elucidate the role of NS2 and the mechanisms of viral progeny capsid nuclear egress.

Listed below are the specific aims of each of the studies included in this thesis:

I) To identify proteins associated with CPV NS2 and to clarify the role of NS2 in infected cells.

II) To elucidate infection-induced alterations of nucleolar structure and role of NS2 in the process

III) To illuminate how G2/M transition and apoptosis participate in progeny virus egress.

4 MATERIALS AND METHODS

This chapter summarizes the materials and methods used in the original articles of this thesis. Key experiments are explained in more detail. In addition, materials, reagents, equipment, and techniques have been categorized into subtables (Tables 1, 2, 3, 4, 5 and 6). More detailed descriptions of used materials and methods can be found in the original publications and manuscripts.

4.1 BioID (I, II)

BioID was performed in the study I and the data were revisited in the study II. Here, a stable Flip-in TREX 293 cell line expressing HA-BirA*-NS2 fusion protein was created. Stable protein expression of the fusion protein was induced with 2 ug/ml tetracycline at 4 hpi, simultaneously with the induction samples were supplemented with 50 mM biotin. At 24 hpi, biological duplicates of both infected and noninfected cells were collected, together with negative controls supplemented with tetracycline. Samples were purified with affinity columns, processed, and analyzed as described in Liu *et al*. 2018. The data was further analyzed and filtered (Bayesian FDR of 0.05 as cut-off). Controls to filter out unspecific nuclear pore component biotinylation induced by most cargo proteins and other control runs were performed with different GPF-BirA* constructs. Overview of the process is explained in Fig. 5.

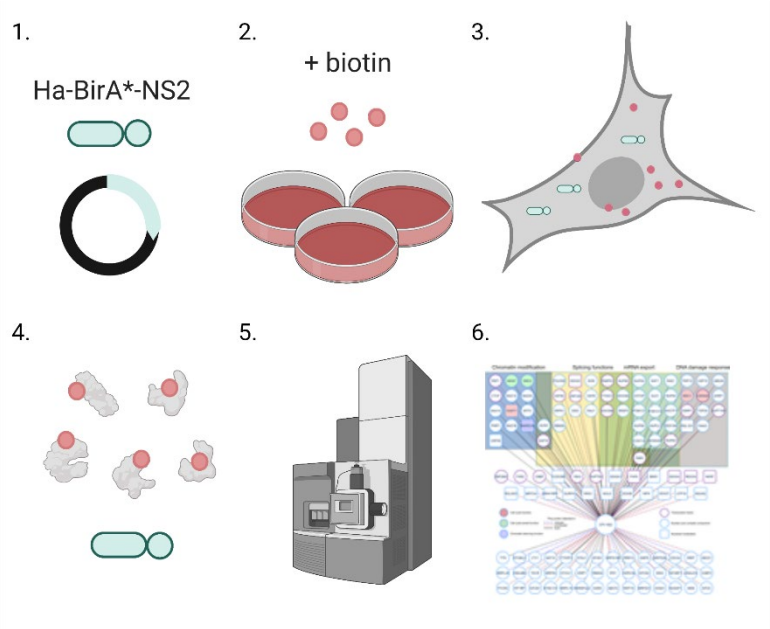

FIGURE 4 Overview of the BioID analysis of NS2 associated proteins. BioID was used to identify the interactome for CPV NS2. (1) First, tetracycline-inducible Flp-In T-REx 293 cells were transfected with HA-BirA*-NS2 fusion protein, and a stable cell line was established. (2) Biotin was added to the culture media, and tetracycline was used to initiate the fusion protein expression. Infected samples were inoculated with CPV. (3) During incubation, biotin ligase activity of HA-BirA*-NS2 fusion protein induced proximity-dependent biotinylation of associated proteins. (4) Cells were lysed, purified with affinity columns, digested, and desalted (5) Biotinylated proteins were recognized with mass spectroscopy (6) Interactome of NS2-associated cellular proteins in noninfected, and infected cells were created. The image was reproduced with modifications from (Mattola *et al.* 2021) and created with BioRender.com.

4.2 Proximity ligation assay (I)

Proximity ligation assay (PLA) was used to recognize protein targets localized close together with specific antibodies in fixed samples. Recognized antigens were within 40 nm apart (Söderberg *et al.* 2006). Quantitation of NS2 specific interactions was done by calculating the number of PLA foci and comparing them with negative (PLA signal formation impossible) and positive controls (PLA signal formation certain). The principle of the method is explained in Fig. 5.

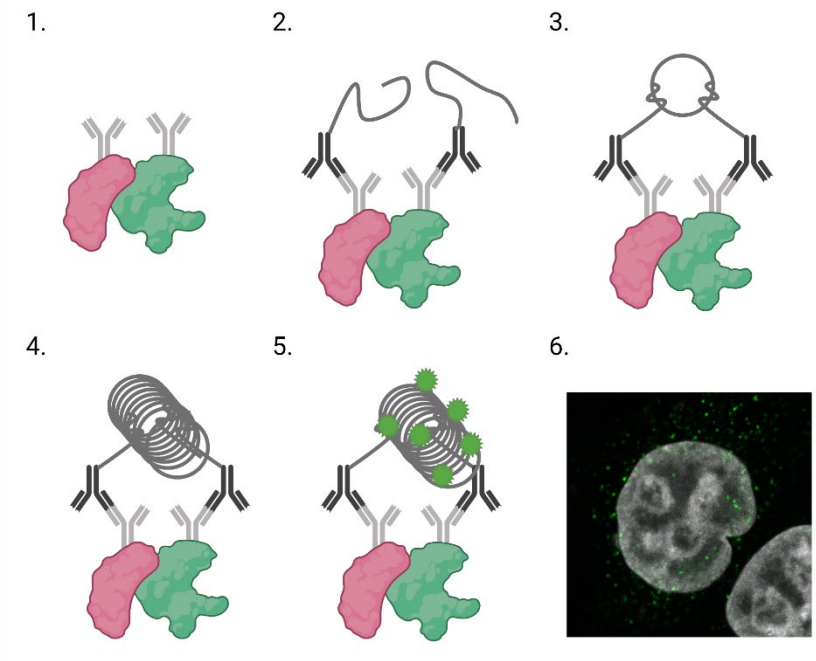

FIGURE 5 Workflow of PLA analysis. Workflow of PLA used in the study I to verify the close proximity of NS2 protein in infected cells and NS2-EGFP in transfected cells with specific host protein targets identified with BioID. Proteins are illustrated in red and dark green. (1) Primary mouse antibodies and rabbit antibodies (in grey) against viral NS2 or EGFP of NS2-EGFP expressing cells and host-associated proteins of interest, SWI/SNF-related matrix-associated actin-dependent regulator of chromatin subfamily A member 5 (SMARCA5), histone variant macro-H2A.1, structure-specific recognition protein (SSRP1) and Mediator of DNA damage checkpoint protein 1 (MDC1), were used to recognize the studied proteins. (2) PLA oligonucleotide probes bound to secondary antibodies were used to recognize the primary antibodies and their antigens. (3) The close proximity, an indication of interaction between the studied proteins, led to (4) amplification of the probes. (5) The amplificated DNA of the probe (circular grey structure) enables the attachment of fluorescent probes (bright green). (6) Confocal microscopy image shows the intracellular distribution of the PLA signals (green). The image was reproduced with modifications from Mattola *et al*. 2021 and created with BioRender.com.

4.3 NS2 mutants (I, II)

The NS2 specific splice site mutants used in studies I and II have been previously characterized in Wang *et al*. 1998. These mutants were based on similar MVM NS2 splice mutants that led to inefficient replication of MVM in murine cells, the natural host of MVM (Naeger *et al.* 1990, 1993, Cater and Pintel 1992). Five single-point mutants focusing on either NS2 donor or acceptor splices site were created in the CPV infectious clone (p265). All the point mutations were designed to

terminate the NS2-specific exon without effect to the NS1. Therefore, NS2 cannot be detected in cells transfected with the mutants with NS2 C-terminal antibody. In this thesis, we focused on two mutants, one with a point mutation on the donor splice site of the gene and another with a point mutation on the acceptor splice site of the alternative splice site, leading to the inactivation of splice donor and acceptor, respectively. In the original publication, the mutants are referred to as G533A and A2033T according to the mutation site (Wang *et al.*1998). Here, these mutants are referred to as donor and acceptor mutants.

4.4 Machine learning based segmentations (II)

Nucleolus segmentations in study II were based on nucleolin labeling. The segmentations were performed with a human in the loop (HITL) machine learning algorithm. HITL-based image analysis methods have generally been applied for biomedical image analysis (Patel *et al.* 2019, Bobes-Bascarán *et al.* 2021). Here, human validation was used to train a python programming language-based algorithm to predict the segmentation of the nucleoli (labeled with nucleolin) in 3D images in noninfected, infected, or mutant transfected cells. A U-shaped algorithm of a deep neural network (DDN) was utilized. In brief, manually segmented nucleoli of a few cells were used to predict the segmentations for all the planes of the 3D image stack within the sample. Human corrections to the prediction were introduced, and the DNN was retrained. Additional images were inserted into the analysis in every iteration. DNN was used to segment the nucleoli when the DNN had reached DNN loss function. (II, Fig. S1). The segmented nucleoli were used for further analyses of the size of the nucleoli and the average number of nucleoli in each cell nucleus.

TABLE 1. Cell lines, viruses, mutant infectious clones, and plasmids used in the studies.

Cells, viruses and plasmids	Source	Published	Study
Cell lines			
Flp-In T-REx 293	Invitrogen, Life Technologies, USA		I, II
NLFK	CR. Parrish, Cornell University, Ithaca, NY		I, II, III
Hela	ATCC		I
NLFK-EGFP		Ihalainen et al. 2009	III
Viruses and mutants			
CPV	Produced from p265	Suikkanen et al 2002	I, II, III
p265	CR. Parrish, Cornell University, Ithaca, NY		I, II
G533A	CR. Parrish, Cornell University, Ithaca, NY	Wang et al. 1998	I, II
A2033T	CR. Parrish, Cornell University, Ithaca, NY	Wang et al. 1999	I, II
Plasmids			
NS2-EGFP		original publication	I
HA-BirA*-NS2		Liu et al. 2018	I, II
Importin-α-GFP	E. Gratton, UC Irvine, CA		III
GFP-BirA* constructs		Liu et al. 2018	I

TABLE 2. Antibodies and microscopy sample preparation reagents used in the studies.

Antibodies and microscopy sample preparation	Antigen/cat nro	Source	Published	Study
Primary antibodies				
NS1	NS1 protein	Gift C. Astell, Canada	Yeung et al. 1991	I, II, III
NS2	mAb peptide against NS2 C-term.	Parrish lab, USA	Wang et al. 1998	I
A3B10	mAb against intact capsids	Parrish lab, USA	Weichert et al. 1998	II, III
VP2	rAb agaist VP2	Parrish lab, USA	Weichert et al. 1998	III
anti-HA-tag	rAb, ab9110,	Abcam, UK		I
anti-GFP	9F9.F9, ab1218	Abcam, UK		I
SMARCA5	rAb, ab183730	Abcam, UK		I
SSRP1	rAb, ab137034	Abcam, UK		I
MDC1	rAb, PA5-82270	Thermo Fisher Scientific, USA		I
γ-H2AX	rAb, ab2893	Abcam, UK		I,III
macro-H2A.1	rAb, ab183041	Abcam, UK		I
H3K9me3	rAb, ab8898	Abcam, UK		I
H3K27ac	rAb, ab4729	Abcam, UK		I,III
Ki-67	rAb anti-MKI-67, ab15580	Abcam, UK		II
Nucleolin	rAb, ab22758	Abcam, UK		I,II
CRM1	rAb, ab24189	Abcam, UK		III
Cyclin B1	rAB ab2949	Abcam, UK		III
Cyclin B1 Alexa Fluor® 555	rMAb, ab214381	Abcam, UK		III
γ-H2A.X (pS139) Alexa Fluor® 647	rMAb, ab195189	Abcam, UK		I, III
Lamin B1	rAb, ab16048	Abcam, UK		III
Importin β	mMAb, KPNB1, ab2811	Abcam, UK		III
Ran	rAb, ab53774	Abcam, UK		III
Fluorescent secondary antibodies				
Goat anti-mouse Alexa Fluor® 488	A32723	Thermo Fisher Scientific, USA		I,II,III
Goat anti-mouse Alexa Fluor® 555	A21127	Thermo Fisher Scientific, USA		I
Goat anti-mouse Alexa Fluor® 546	A11030	Thermo Fisher Scientific, USA		I,II,III
Goat anti-mouse Alexa Fluor® 633	A21050	Thermo Fisher Scientific, USA		III
Goat anti-mouse Alexa Fluor® 647	A21236	Thermo Fisher Scientific, USA		I,II,III
Goat anti-rabbit Alexa Fluor® 488	A32731	Thermo Fisher Scientific, USA		I,II,III
Goat anti-rabbit Alexa Fluor® 555	A21424	Thermo Fisher Scientific, USA		I
Goat anti-rabbit Alexa Fluor® 546	A11035	Thermo Fisher Scientific, USA		I,II,III
Goat anti-rabbit Alexa Fluor® 633	A21071	Thermo Fisher Scientific, USA		III
Goat anti-rabbit Alexa Fluor® 647	A21245	Thermo Fisher Scientific, USA		I,II,III
Microscopy sample embedding				
ProLong™ Diamond anti-fade media with DAPI	15205739	Molecular Probes™		I,II,III
ProLong™ Glass antifade mountant with NucBlue™	P36983	Thermo Fisher Scientific, USA		I,III

TABLE 3. Reagents used in the studies.

Reagents	Source	Study
Tranfections		
Lipofectamine 3000 transfection reagent	Thermo Fisher Scientific, USA	I, II, III
JetOptimus transfection reagent	Polyplus transfection, France	I, II
TransIT 2020 transfection reagent	Mirus Bio LLC, USA	III
BioID		
tetracycline	Merck KGaA, Germany	I
Biotin	Merck KGaA, Germany	I
Inhibitors		
LMB	Abcam, UK	III
Cdk1 inhibitor RO-3306	SelleckChem, Germany	III
Cas 3 inhibito Z-DEVD-FMK	Bio-Techne, USA	III
Kits		
Duolink In Situ Orange Mouse/Rabbit kit	Merck KGaA, Germany	I
Other		
Hoechst 33342	Thermo Fisher Scientific, USA	III
DNaseI	Promega, USA	I
TRIZOL	Gibco, Thermo Fisher Scientific, USA	I
SYBR Green	Applied Biosystems, USA	I
TaqMan Ribosomal RNA Control Reagents	Applied Biosystems, USA	I

TABLE 4. Primers used in RT-qPCR.

Target gene	Primer name	Primer sequence (5'-3')	Position	Study
NS1	RT-NS1-5	AAATGTACTTTGCGGGACTTGG	1126-1147	I
	RT-NS1-3	CACCTCCTGGTTGTGCCATC	1211-1231	I
NS2	RT-NS2-5	CTCGCCAAAAAGTTGCAAAGAC	520-530 and 2003-2013	I
	RT-NS2-3	TGCAAGGTCCACTACGTCCG	2075-2094	I

TABLE 5. List of confocal microscopes and other equipment used in the studies.

Equipment	Source	Study
Microscopes		
PLA	Olympus FluoView FV1000, Japan	I
	Nikon A1R, Japan	I
Confocal imaging	Olympus FluoView FV1000, Japan	I,III
	Nikon A1R, Japan	I,II,III
	Leica TCS SP8 FALCON, Germany	I,II,III
FLIP	Nikon A1R, Japan	III
Mass spectrometry		
Q-Exactive mass spectrometer	Thermo Fisher Scientific, USA	I
RT-qPRC		
ABI PRISM 7700 Sequence Detection System	Applied Biosystems	I

TABLE 6. Summary of data and microscopy image analysis tools used in the studies.

Data analysis	Software/method	Reference	Study
Advanced image analysis			
General image processing	ImageJ		I,II,III
Nuclei segmentation	ImageJ / Otsu method	Otsu et al. 1979	I,II,III
Distribution and intensity analyses	ImageJ		I,II,III
PLA quantification	Python		I
Quantification of replication centers	Python		I
Pearson correlation	ImageJ		II
FLIP	ImageJ		III
machine learning based nucleoli segmentation	HITL algorithm, Python	unpublished	II
Proteomics tools			
Mass spectroscopy data analyses	SAINTexpress	Teo et al. 2014	I
Filtering of the BioID data	CRAPome	Mellacheruvu et al. 2013	I
Context-based estimation of NS2 localization.	MS-microscopy online tool	Liu et al. 2018	I
GO biological process annotation of interactors	PANTHER	http://www.pantherdb.org	I,II
ChIPseq analyses			
ChIP-seq	described in Mäntylä et al 2016		III
ChIP-qPCR	described in Mäntylä et al 2016		III
GO biological process term enrichement analyses	GO Enrichment Analysis	http://geneontology.org/	III

5 RESULTS

5.1 NS2 associates with chromatin-modifying proteins

5.1.1 CPV NS2 interactome is different in noninfected and infected cells (I)

In the study I, the nuclear interactome of CPV NS2 was determined with BioID. The proteomic network consisted of 122 unique high-confident NS2-associated proteins including 44 proteins in noninfected cells, 17 proteins in infected cells, and 61 proteins seen in both.

The interactome-based MS microscopy analysis was used to clarify the context of the nuclear localization of HA-BirA*-tagged NS2. A reference molecular context map was used to determine the localization of BirA* fusion protein. The method assumes that there is an association with the spectral count and temporal association with the bait and prey proteins (Liu *et al.* 2018). Here, NS2 was found to localize mainly to the nucleolus, NE, and chromatin. Remarkably a shift in the association to these nuclear components was observed in infection (Fig. 6). In noninfected cells, the NE localization was preferred, whereas in infection the interactome changed towards chromatin.

Moreover, redistribution of NS2 was also observed in confocal microscopy in NS2-EGFP expressing cells. Similar to the NS2, NS2-EGFP localized to the nuclear envelope and specific foci located around and inside the nucleoli. Consistent with NS2-EGFP and HA-BirA*-tagged NS2, immunolabeled NS2 localized to the cytoplasm, nucleus, or the nucleolus, in infection progression specific manner. (I, Figs 1B, 1C and 1D).

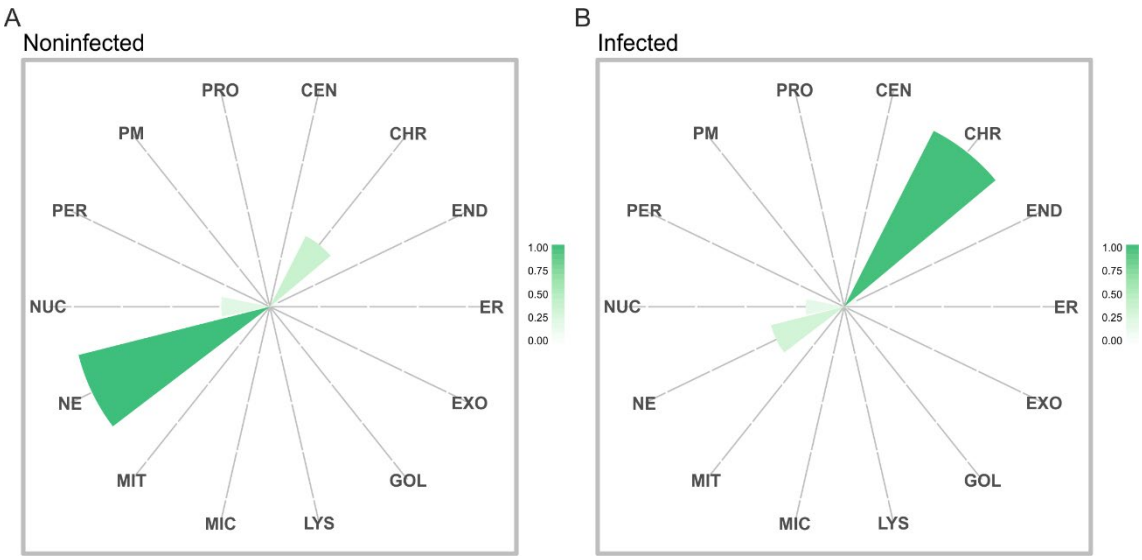

FIGURE 6 Localization on HA-BirA* tagged NS2 in (A) noninfected and (B) infected samples. Localizations were assessed based on the interaction of the bait with specific prey proteins. The color assigned to each localization is based on the annotation frequency (light green: 0–0.25, green: 0.25–0.5, dark green: 0.5–1). The score represents the similarity of the interactions with bait and prey proteins. Mass spectrometry microscopy-based association of the protein of interest to nucleolus (NUC), peroxisomes (PER), plasma membrane (PM), proteasome (PRO), centrosome (CEN), chromatin (CHR), endosome (END), endoplasmic reticulum (ER), exosome (EXO), Golgi (GOL), lysosome (LYS), mitochondria (MIC), microtubule (MIT) and nuclear envelope (NE) is shown. The markers used for nucleoli (NUC), and nuclear envelope (NE) were rRNA 2′-O-methyltransferase fibrillarin, histone H3.1, and prelamin-A/C, respectively. Figure reproduced from study I (Fig. 3).

5.1.2 NS2 is associated with host proteins related to DNA damage and chromatin organization (I)

Gene ontology analyses of NS2-associated proteins showed enrichment of hit proteins related to chromatin organization (GO:0006325), DNA damage response (GO:0006974), mRNA splicing (GO:0008380), and nuclear export of mRNA (GO:0006406) both in noninfected and infected cells (I, Table S2 and Fig. 2B). The study I focused on NS2 association with chromatin remodeling and organization and DNA damage responses (Table 5). PLA-based interaction analysis showed a significant increase in interactions between NS2 and selected NS2-associated proteins in infected cells in comparison to noninfected cells (I, Figs 5 and 6).

Finally, to elucidate the role of NS2 in chromatin remodeling, the intensities and distributions of DAPI-labeled DNA and specific epigenetic markers were analyzed in HeLa cells transfected with wt infectious clone, the replication-deficient NS2 splice donor mutant, or the splice acceptor mutant (Wang *et al.* 1998). The used markers were H3K27ac for active euchromatin (I, Fig. 7) and H3K9me3 for heterochromatin (I, Fig. S6). Additionally, to address the role of

NS2 in DNA damage, the intensity and distribution of γ-H2AX and MDC1 were analyzed in the presence of wt NS2 and NS2 mutants in HeLa cells (I, Fig. 8). Studies revealed that transfection with the NS2 splice donor mutant led to changes in chromatin organization and distribution. The amount of euchromatin marked by H3K27ac was significantly increased in the splice donor mutant transfected cells compared to wt transfected cells. In contrast, the amount of H3K27ac was significantly decreased in wt transfected cells in comparison to nontransfected cells. The amount of H3K9me3 was significantly increased with respect to nontransfected cells in wt transfected cells but not in in the splice donor mutant transfected cells. Distributions of both analyzed markers in the splice acceptor mutation transfected cells were similar to the wt. Analysis of γ-H2AX intensity, a prominent marker for DNA damage, revealed significantly lower intensities of γ-H2AX in the splice donor mutant transfected cells. Mutation to the splice acceptor site did not lead to significant changes in γ-H2AX distribution or intensity in comparison to the wt. Interestingly, the intensity and distribution of the NS2-associated DNA damage mediator protein MDC1 were different in both mutants in comparison to wt transfected cells.

TABLE 5 NS2-associated proteins linked to chromatin remodeling and DNA damage response. Represented list of high-confidence (BFDR ≤0.05) interactor proteins involved in chromatin modification (blue, 34 proteins in total) and DNA damage response (gray, 14 proteins in total).

Prey	PreyGene	Noninfected average spectral count	Infected average spectral count	Noninfected BFD	Infected BFDR
P46013	MKI67	76.5	78.5	0.04	0.02
O60264	SMARCA5	27.5	20.5	0	0.04
Q14676	MDC1	22.5	24.5	0.02	0.01
O76021	RSL1D1	21.5	0	0	0
Q9UIG0	BAZ1B	19	14.5	0	0.01
P11388	TOP2A	17	10.5	0	0
Q9Y5B9	SUPT16H	11	6	0	0
O95347	SMC2	9	6.5	0	0.03
Q9NRL2	BAZ1A	9.5	7	0.01	0.03
Q9UIF9	BAZ2A	7.5	7.5	0	0
P49711	CTCF	6	0	0.02	0
Q08945	SSRP1	6.5	4	0	0
O75367	H2AFY	6.5	7	0	0
P41227	NAA10	4	3	0	0.01
Q96T23	RSF1	3	0	0.01	0
O00422	SAP18	4.5	4	0.01	0.01
Q14694	USP10	4	0	0.02	0
Q8N726	CDKN2A	2.5	0	0.04	0
Q06787	FMR1	4	4	0	0
Q13610	PWP1	2.5	3	0.03	0.03
P61088	UBE2N	3	4	0.01	0.01
Q9P275	USP36	2.5	3	0.04	0.02
Q96T88	UHRF1	0	2.5	0	0.01
Q9Y483	MTF2	0	2	0	0.01
Q14669	TRIP12	0	2.5	0	0.01

5.1.3 Replication center formation is affected in the presence of NS2 donor mutant

Besides the changes in chromatin organization and DNA damage, the NS2 donor mutant transfection affected establishment of the viral replication centers (I, Fig. 9). The progression of the infection led to the fusion of the replication foci at 24 hours post transfection in both wt and NS2 splice acceptor mutant transfected cells. However, in the splice donor mutant transfected cells the size of replication centers was smaller and their number was increased.

5.2 Nucleolar structure is altered during CPV infection

5.2.1 The size and structure of nucleoli is altered in infection (I, II)

CPV NS2 BioID, in study I, revealed a subpopulation of NS2 interactions to be located in the nucleolus. In study II, we revisited the BioID data focusing on NS2-associated nucleolar proteins and the association and localization of those proteins in nucleolar subcompartments of the nucleolar proteome as described in (Stenström *et al.* 2020) (the human protein atlas project).

NS2-associated proteins were identified in all nucleolar subcompartments, the granular and fibrillar centers, and the nucleolar rim in both noninfected and infected cells. The identified nucleolar proteins have roles in various biological processes (Fig. 7). Interestingly, the associated proteins specific to fibrillar centers in noninfected cells were not shared with other subcompartments (II, Fig. 4 and Supplementary Fig. S2 and Table S1).

To elucidate the effect of infection on nucleolar structure, the nucleoli were labeled with nucleolin antibody. First, the nucleolin label was segmented using a machine learning-based method (II, supplementary Fig. S1). Then, the number and size of nucleoli at 8, 12, and 24 hpi were analyzed. These analyses revealed a significant decrease in the size of the nucleoli in late infection and only a slight change in the number of nucleoli at 24 hpi. Moreover, a highly significant decrease in nucleolar nucleolin to nuclear nucleolin ratio at 24 hpi was detected implying increased shuttling of nucleolin out of the nucleoli in late infection. Interestingly this change was coupled with a significant decrease in the amount of nucleolar DNA at 24 hpi (II, Figs 1 and 2).

The high number of nucleolar associations indicated a possible role for NS2 in nucleolar structure alterations. To clarify this, the number and size of the nucleoli were analysed in the presence and absence of full-length NS2 with the previously established NS2 mutants. The wild-type infection increased the number of nucleoli, but the mutants did not. On the contrary, the size of the nucleoli decreased in wt transfected cells in comparison to nontransfected and the NS2 splice donor mutant transfected cells. Moreover, the average nucleolar DNA content was significantly higher in wt and mutant transfected cells compared to nontransfected cells, and the DNA distribution of donor mutant

transfection varied from that of wt and acceptor mutant transfected cells (II, Figs 6 and 7).

Finally, the average orientation angle of the nucleoli was examined. Here, the angle between the major nuclear axis and the major axes of the nucleoli were determined. Surprisingly, the NS2 splice donor mutation affected the nucleolar angles. (II, Fig. 8).

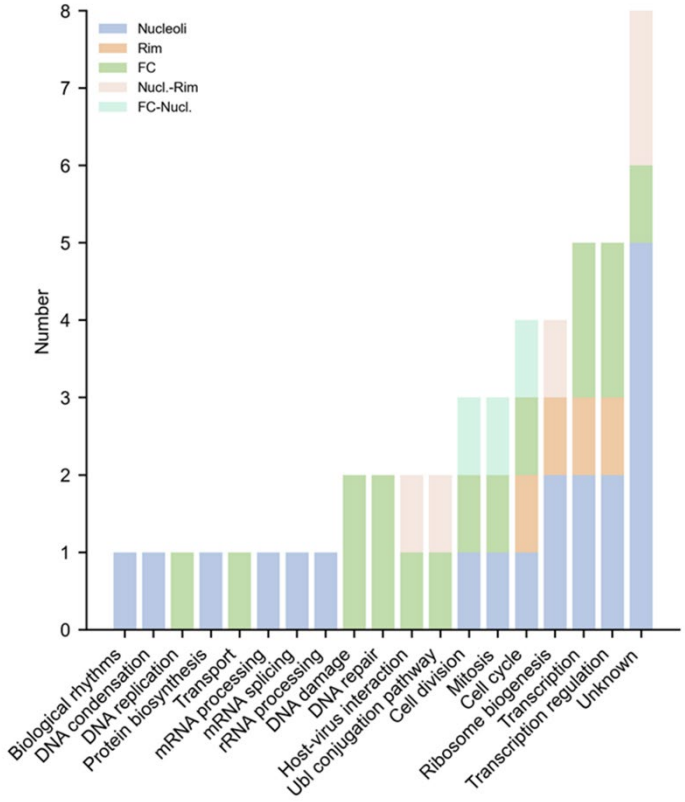

FIGURE 7 Enriched gene ontology biological processes of NS2-associated nucleolar proteins and the corresponding nucleolar localization.

5.2.2 Association between nucleolar rim protein and chromatin changes in infection (I, II)

The nucleolar rim protein ki-67 is the strongest hit protein with the highest spectral count identified by BioID analysis (I, supplementary Table S1). To further analyze the actual involvement of ki-67 in the chromatin reorganization and nucleolar structure changes, labeled ki-67 was analyzed for its intensity, distribution, and correlation with chromatin in noninfected and CPV-infected NLFK cells at 24 hpi (II, Fig. 5).

The total intensity of DNA and ki-67 significantly increased in infected cells. The distribution of DNA followed the distribution of ki-67 in infected cells. Interestingly, the Pearson correlation coefficient of ki-67 with DNA was negative in noninfected cells corresponding to a weak negative correlation, but the

correlation of ki-67 with DNA in infected cells was positive. The change in correlation was found to be highly significant. Altogether, this showed that DNA associates differently with ki-67 in noninfected and infected cells.

5.3 Progeny virus egress is enhanced by G2/M activation and apoptosis (III)

5.3.1 Inhibition of cell cycle progression and early apoptosis influence capsid egress

The prevailing view is that parvovirus capsids exit the nucleus by utilizing CRM1-mediated export in an active process that requires NS2. Study III further inspected the processes leading to the nuclear egress of progeny capsids in CPV infection. The results suggested that CRM1 inhibition with leptomycin B (LMB) could not fully inhibit the nuclear egress of capsids either at 24 hpi or 30 hpi in NLFK cells (III, Fig. 1 and Supplementary Fig. S1). Furthermore, it was shown that viral replication-initiated DNA damage response leads to the accumulation of cyclin B1 into the nucleus (III, Figs 3 and 4). The relation of cyclin B1 accumulation to capsid distribution changes was observed. As the infection proceeded, the cyclin B1 accumulation was significantly increased at the start of viral capsid egress (III, Fig. 5). This led us to conclude that the nuclear egress of progeny virus capsids is most likely affected by G2/M transition- or apoptosis-related nuclear cyclin B1 accumulation (Fig. 8) (Hagting *et al.* 1999, Yang *et al.* 2001, Porter and Donoghue 2003, Porter *et al.* 2003, Miyazaki and Arai 2007). Corroborating with the early apoptosis theory, nucleus-to-cytoplasmic ratios of known apoptosis markers Importin α, importin β, and Ran represented a distribution ratio related to apoptosis activation in infected cells (III, Fig. 7 and Supplementary Fig. S5). As a further proof, the effect of Cdk1 and caspase-3 inhibition on progeny capsid egress was examined (III, Figs 6 and 8). Capsid release to the cytoplasm in late infection was visibly decreased when G2/M transition and pro-apoptotic caspase-3 were inhibited.

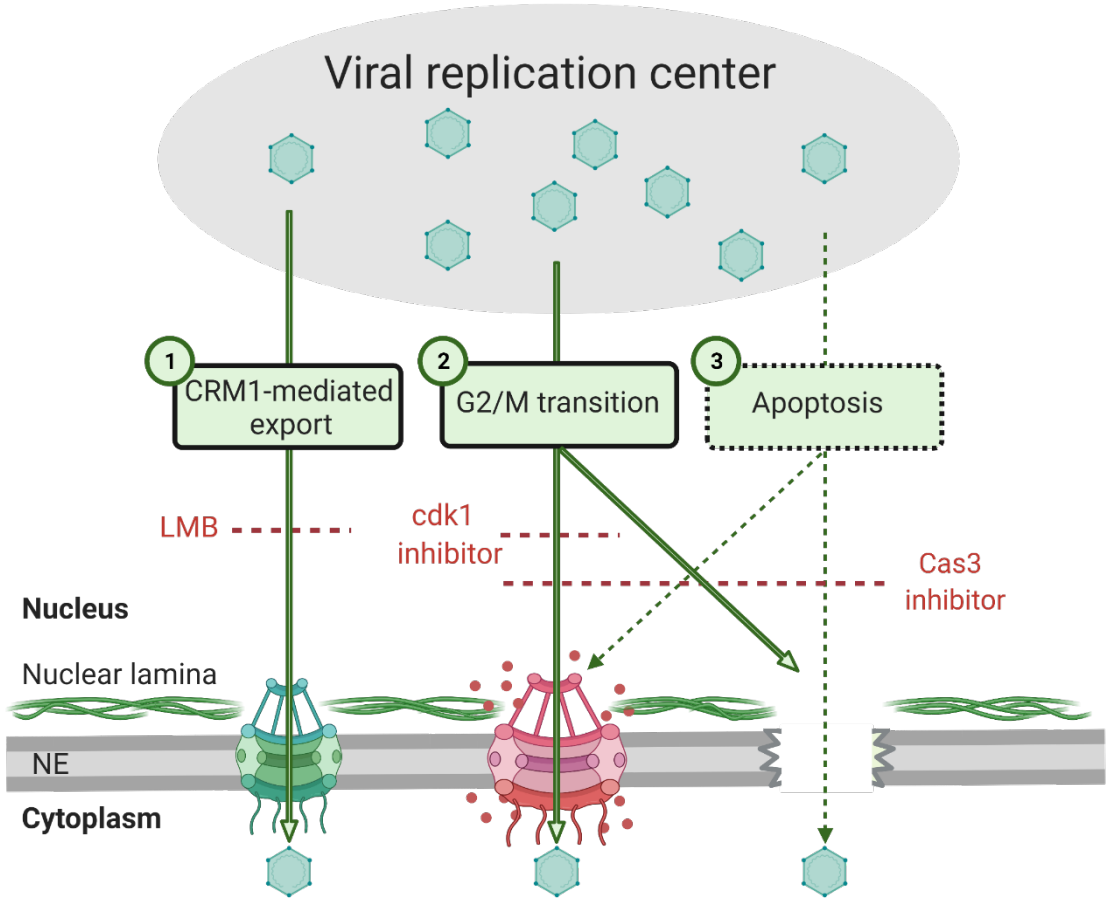

FIGURE 8 Schematic model depicting the implementations of the inhibitors to the cell cycle (Leptomycin B, caspase-3 and Cdk1) and the observed cellular counterparts used in study III, Figure reproduced from study III.

5.3.2 The altered permeability of the nuclear envelope in infection is linked to G2/M transition and early apoptosis (III)

A possible explanation for the G2/M- and apoptosis-related increase in progeny capsid egress is the infection-induced change in the NE integrity. The NE permeability was studied using fluorescent loss in photobleaching experiments in EGFP-expressing NLFK cells. (III, Fig. 2). Alongside infection, the effect of Cdk1 and caspase-3 inhibition on NE permeability was examined. An apparent change in the integrity of the NE was seen, and the change was reversible to some extent with the inhibitors, indicating an involvement of both G2/M transition and early apoptosis in NE permeability (III, Supplementary Fig. S2).

5.3.3 Infection leads to epigenetic activation of host genes involved in mitosis and apoptosis (III)

Next, to investigate the regulation of mitosis- and apoptosis-related genes, the H3K27 acetylation profiles of noninfected and infected cells were compared. An increase in total H3K27 acetylation, which is required for transcriptional activation, was detected in infected cells in comparison to noninfected cells (III, Fig. 9) (Heintzman *et al.* 2007, Wang *et al.* 2008). In addition, changes in the enrichment of genes in GO biological processes categories with acetylation gain and acetylation loss were reported. GO categories significantly enriched with acetylation gain were cell cycle process (GO:0022402), cell cycle (GO:0007049), and cellular response to DNA damage stimulus (GO:0006974). In contrast, significantly enriched categories with H2K27ac loss were regulation of programmed cell death (GO:0043067), regulation of apoptotic process (GO:0042981), and regulation of programmed cell death (GO:0043067) (III, Fig. 9 and Supplementary Table S1) (Fig. 9).

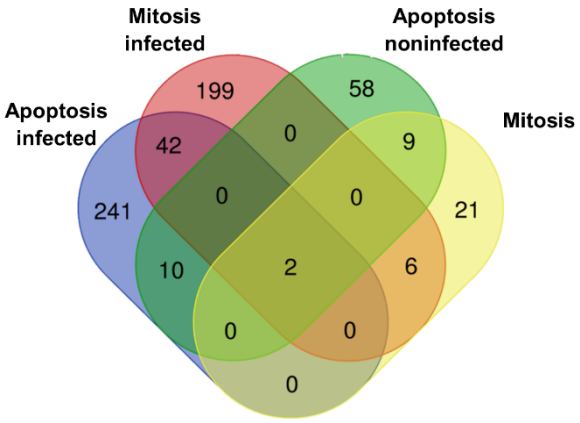

FIGURE 9 Virus-induced change in the regulation of mitosis and apoptosis. Genes associated with high amounts of H3K27ac in noninfected and infected cells. Apoptosis-related genes were pooled from GO categories: apoptotic process (GO:0043066), positive regulation of apoptotic process (GO:0043065), apoptotic process (GO:0006915), and apoptosis (GO:0042981). Mitosis-related genes were pooled form GO categories: regulation of mitotic cell cycle (GO:0007346), mitotic cell cycle (GO:0000278), mitotic cell cycle process (GO:1903047), and regulation of mitotic cell cycle phase transition (GO:1901990). Figure adapted from study III.

6 DISCUSSION

6.1 The role of NS2 in chromatin remodeling and DNA damage (I)

CPV infection alters the nuclear chromatin architecture (Ihalainen *et al*., 2009). In addition, parvoviruses induce a DNA damage response that facilitates viral replication (Adeyemi *et al.* 2010, Luo *et al.* 2011b). CPV NS1 has many functional properties required by the infection: site-specific DNA binding, ATPase, nickase, and helicase activity (Niskanen *et al.* 2010, 2013). The functions of the second nonstructural protein NS2 have remained poorly understood. However, studies on MVM NS2 suggest that the small nonstructural protein is required for effective replication, growth, and fusion of the replication centers and for capsid assembly (Cotmore *et al.* 1997, Choi *et al.* 2005, Ruiz *et al.* 2011). Based on the theory of de novo synthesis resulting in viral overlapping alternative transcription, it is expected that CPV NS2 might share some functions with the other parvoviral nonstructural protein NS1 (Pavesi 2021).

Our study provides a link between NS2 and multiple complexes involved in chromatin modeling and DNA damage responses (Mattola *et al.* 2022). The proteins of chromatin remodeling complexes including ISWI family complexes NoRC, WSTF-ISWI chromatin remodeling complex (WICH), ATP-dependent chromatin-remodeling factor complex (ACF) and remodeling and spacing factor complex (RSF) were represented in the BioID results. One of the NS2-associated proteins is SNF2H SMARCA5, a general subunit of the ISWI family complexes. SMARCA5 function is known to support the replication and immediate early gene expression of HSV-1 (Taylor and Knipe 2004, Bryant *et al.* 2011). The role of ISWI family complexes involved in CPV infection may be to maintain similar functions through NS2 involvement.

NS2 was associated with proteins of NoRC, a member of the ISWI family complexes, which regulates ribosomal gene transcription (Németh *et al.* 2004,

Strohner *et al.* 2004). The interactor of NS2 is a zinc finger domain protein 2A, BAZ2A, which is localized with the RNA polymerase transcription factor UBF and SMARCA5 (Strohner *et al.* 2001). Notably, the hit with the highest spectral counts, ki-67, involved in the organization of heterochromatin at the nucleolar rim, interacts with BAZ2A. The association of NS2 with NoRC is potentially important for progression of infection since nucleolar production of ribosomes is essential for translation of viral proteins. However, in viral infection NoRC might also have a role in modulation of immune response, which is undefined regarding CPV infection (Bianco and Mohr 2019).

The other ISWI complexes, WICH, ACF, and RSF, have also been associated with DNA viruses. Adenoviral E4orf4 associates with ACF targeting protein phosphatase 2A (PP2A) to the complex, inhibiting its function. Inhibition of the ACF is suggested to promote the function of WICH, an ACF homolog. Regulation of the complexes through E4orf4 results in a switch balancing the chromatin remodeling and cell death (Brestovitsky *et al.* 2011). In addition, WICH has been associated with RNA polymerase I (pol I) and rDNA transcription regulation (Percipalle *et al.* 2006). RSF is known to interact with ATM, and even though this interaction does not directly affect DNA damage signalling, RSF complex involvement is needed to facilitate DSB repair through modulation of chromatin, making it accessible for proteins required for the repair (Pessina and Lowndes 2014).

CPV NS2 is also associated with proteins involved in DNA damage response. These proteins include histone variant macro-H2A.1 and SSRP1. Macro-H2A.1 has been associated with promoting transcription suppression (Costanzi and Pehrson 1998). SSRP1 is a subunit of the facilitates chromatin transcription (FACT) complex. FACT complex functions during DNA replication, transcription, and repair by modulating nucleosome assembly and disassembly (Orphanides *et al.* 1998, Reinberg and Sims 2006, Bondarenko *et al.* 2015). Moreover, the FACT complex acts as a suppressor of replication stress by removing γ-H2AX histones from nucleosomes and replacing them with another histone variant, macro-H2A.1 (Kim *et al.* 2019). Notably, both γ-H2AX and macro-H2A.1 are mainly excluded from the replication area in CPV-infected cells (I, Supplementary Fig. S3).

An important CPV NS2-associated protein, MDC1, mediates recruitment of DDR factor ATM to DNA damage sites and interacts with both ATM and γ-H2AX (Lou *et al.* 2006). In MVM infection, replication centers are formed adjacent to γ-H2AX foci. As the infection proceeds, viral replication spreads to new sites of DNA damage (Majumder *et al.* 2018). Moreover, MDC1 has been shown to associate with the established replication centers of MVM. Similar to what was seen in our study, the infection with MVM NS2-null virus led to the establishment of replication centers, but the maturation of the replication centers was inefficient (Ruiz *et al.* 2011). In the same study, NS2 involvement in the recruitment of DDR-signaling proteins was studied. Even though the γ- H2AX phosphorylation was diminished in the NS2-null infection, NS2 was not involved in the recruitment of DDR factors. Nevertheless, the association of NS2 with MDC1 in our studies, together with the modulated recruitment of MDC1 with

both mutants, indicate involvement of NS2 in the ATM response to infection. Since the role of MVM NS2 has been suggested to be host cell-dependent, induced DNA damage responses might vary between the hosts (Naeger *et al.* 1990, Cater and Pintel 1992). Generally, the host range of autonomous parvoviruses is quite vast. For example, CPV evolved from the Feline panleukopenia virus (FPV) only recently, and the CPV variant CPV-2a used in the thesis has restored its ability to infect cat and dog cell lines. It would be intriguing to see whether the chromatin remodeling and DNA damage responses induced in infection differ between the cell lines compared to the human cell lines used in this study.

The association of NS2 with factors maintaining chromatin organization most likely assist the formation of viral replication area. Chromatin organization and development of replication centers have also a potential effect on intranuclear diffusion of viral capsids (Ihalainen *et al.* 2009, Aho *et al.* 2021). Altogether, our findings suggest that NS2-mediated chromatin changes might influence essential events of infection, maturation of viral replication centers, and intranuclear transport of progeny capsid during their nuclear egress.

6.2 Parvovirus-induced changes of nucleolar structure (II)

The large nuclear organelle nucleolus has an essential role in many critical functions of the cell. Its principal function is to maintain ribosome biogenesis by regulating rRNA transcription, processing, and assembly (Raška *et al.* 2006, Dubois and Boisvert 2016). It is known that environmental stress and the transcriptional status of the nucleolus-associated chromatin affect the nucleolar structure (McKeown and Shaw 2009, Boulon *et al.* 2010).

Several viruses utilize nucleolar proteins and nucleolar functions for their benefit. As a result, the nucleolar structure can undergo drastic changes in viral infection (Matthews 2001, Lee *et al.* 2003, Lymberopoulos and Pearson 2007, Callé *et al.* 2008, Salvetti and Greco 2014). Notably, progeny capsids of dependoparvovirus AAV are assembled in the nucleolus (Wistuba *et al.* 1997, Johnson *et al.* 2005). Furthermore, AAV transcribes an assembly-activating protein (AAP), which is capable of stabilizing the capsid structure and promoting viral structural protein interactions (Maurer *et al.* 2018). Interestingly, expression of AAP is not a requisite for productive infection with AAV serotypes 4,5 and 11 (Earley *et al.* 2017). Moreover, AAV2 capsids interact with nucleolar protein nucleolin both in vivo and in vitro, suggesting a role for nucleolin in capsid assembly (Qiu and Brown 1999). Similar associations with nucleolus have not been observed with other parvoviruses (Cotmore and Tattersall 2014). Furthermore, the distribution of nucleolin, the shuttling protein of the nucleolus, is known to change in virus infection. Nucleolin shuttling is extremely sensitive to environmental changes, steering the nucleolin to relocate to the nucleoplasm, cytoplasm and cell membrane (Daniely and Borowiec 2000, Kim *et al.* 2005, Jia *et al.* 2017). Nucleolin is relocated to the cytoplasm in poliovirus and adenovirus

infections. In HSV-1 and influenza infections, nucleolin facilitates virus binding to the cell membrane (Waggoner and Sarnow 1998, Matthews 2001, Greco *et al.* 2012, Chan *et al.* 2016, Kumar *et al.* 2016). In HSV-1 infection, nucleolin dispersion is mediated by the UL24 protein (Lymberopoulos and Pearson 2007). In addition, in cytomegalovirus infection, the localization of the replication protein UL84 is mediated by nucleolin (Bender *et al.* 2014).

Our studies indicated that the size and number of nucleoli change in late CPV infection. The nucleolar structure might be affected by the chromatin organization complexes described in detail in the first study (Mattola *et al.* 2022). For example, the WICH complex regulates rDNA transcription via Pol I association, facilitating the transcription (Percipalle *et al.* 2006). Association of CPV NS2 with NoRC complex (Mattola *et al.* 2022) could potentially be involved in nucleolar functions during parvovirus infection. The dynamics of the nucleoli depend on processes that consume ATP. In ATP-depleted cells the organization of the nucleolus was disrupted (Caragine *et al.* 2019). Since the functions of NoRC are ATP dependent, the role of ATP depletion in structural changes of nucleoli (Strohner *et al.* 2001) might be an intriguing aspect for future studies.

CPV infection leads to dispersal of nucleolin from the nucleoli. It has been described earlier that redistribution of nucleolin out of the nucleoli is triggered by cellular stress (Daniely and Borowiec 2000, Jia *et al.* 2017) and it can be also induced by virus infection, e.g. with HSV-1 (Lymberopoulos and Pearson 2007, Callé *et al.* 2008, Greco *et al.* 2012). Cellular stress proteins including heat-shock proteins are synthesized in cells exposed to stress, and they act during eradication of cellular stress (Hendrick and Hartl 1993, Carra *et al.* 2017). The heat-shock protein 70 (HSP70, HSPA1B) was among the highest spectral counts of CPV NS2-associated proteins. This finding supports a model where CPV infection-induced redistribution of nucleolin is caused by a virus-induced heat shock response. This is consistent with the previously published studies showing that oncolytic parvovirus H1 infection causes the release of heat shock protein HSP72 (Moehler *et al.* 2003). Moreover, our findings of small nucleolin-containing foci in infected cells are consistent with increased shuttling of nucleolin out from the nucleoli. It is possible that nucleoplasmic nucleolin might form aggregates that are not actual nucleoli. However, the function of these small foci remains to be disclosed. The formation of nucleolin foci has been linked to DNA damage response (DDR), where nucleolin is known to interact with DDR factor γ-H2AX and accumulate at the sites of DNA damage (Kobayashi *et al.* 2012). Nucleolin interaction with replication stress-related factors replication protein A (RPA)32 and proliferating cell nuclear antigen (PCNA) support the possibility of nucleolin involvement in replication stress-related processes (Kawamura *et al.* 2019).

Our interaction findings showing a high number of NS2 associations with nucleolar proteins suggest that nucleolus may play an important role in CPV infection. The heterochromatin-organizing protein ki-67 is among the top hits of CPV NS2-associated proteins. The expression and the functions of ki-67 are highly cell cycle dependent, with emphasis on chromosome integrity in mitosis (Gerdes *et al.* 1984, Cuylen *et al.* 2016). Due to its low association with resting cells, ki-67 has been used as a marker for cell proliferation. Moreover, it has been

proposed that the effect of ki-67 on the nucleolar organization is dependent on interactions with the small GTPase Ran and cyclin B1 (Schmidt *et al.* 2003). We showed that the association of host chromatin with ki-67 increases in late infection.

Association of chromatin with ki-67 as well as nucleolar functions fluctuate during the cell cycle. Ribosome production is at its highest during the G2 phase and diminishes during the prophase to be started again after mitosis. The size and number or nucleoli change during cell cycle progression (Hernandez-Verdun 2011, Caragine *et al.* 2019). In this thesis, we link the changes in late infection leading up to the nuclear egress of progeny viruses to G2/M transition and provide a link between NS2 and cell cycle-associated factors mediating, directly or indirectly, cell cycle changes. Therefore, we propose that the changes seen in the number and size of the nucleoli might be also related to cell cycle progression or cell cycle arrest caused by the infection.

The dynamics of the nucleoli are dependent on processes that consume ATP. In ATP depleted cells the organization of the nucleolus was seen to be disrupted (Caragine *et al.* 2019). Interestingly the correct function of NS1 is ATP dependent (Niskanen *et al.* 2010). Together these suggest that active replication during the viral infection could take part in the disruption of the nucleoli in infection. The structural changes seen in the nucleoli might also be due to the replication of the virus depleting the nucleus from ATP, which is required to preserve the nucleolar structure.

The structure of the nucleolus might be affected by the chromatin organization complexes described in detail in the first study. For example, the WICH complex regulates rDNA transcription via Pol I association, facilitating the transcription (Percipalle *et al.* 2006). The involvement of UBF with the NoRC complex in the nucleolus serves as a potential target to study nucleolar function during parvovirus infection due to the association of NS2 with its counterparts. Since the functions of NoRC are ATP dependent, its role in ATP depletion of the seen structural changes to the nucleoli might be an intriguing aspect for future studies (Strohner *et al.* 2001).

6.3 Progeny virus nuclear egress (III)

While parvovirus infection induces lysis of the host cell, it has been proposed that progeny viruses escape actively from the nucleus prior to the destruction of the host cell (Eichwald *et al.* 2002, Miller and Pintel 2002, Maroto *et al.* 2004, Engelsma *et al.* 2008, Chen and Qiu 2010, Wolfisberg *et al.* 2016). In the third study of the thesis, we proposed a new mechanism for nuclear egress of autonomous parvoviruses. We demonstrated that the egress of viral capsids is facilitated by G2/M transition and early apoptosis-induced changes, which lead to increased permeability of the nuclear envelope.

MVM progeny capsids exit the nucleus via CRM1-mediated pre-lysis exit strategy (Eichwald *et al.* 2002, Miller and Pintel 2002, Maroto *et al.* 2004, Engelsma

et al. 2008). The exposed N-terminal end of MVM VP2 has an essential role during the exit – it presents a nuclear export signal (NES) to the CRM1. Moreover, high phosphorylation of the N-terminal end of VP2 is needed for effective nuclear export (Maroto *et al.* 2004). The VP2 N-terminus on the capsid surface was found only in capsids with encapsidated DNA, implying that the CRM1-mediated egress mechanism is highly selective for infectious particles (Hernando *et al.* 2000). LMB inhibition of the CRM1-mediated export resulted in inhibition of progeny capsid nuclear egress in MVM and CPV infection (III Fig. 1.), (Maroto *et al.* 2004). More recently, another mechanism for prelytic egress of MVM capsids was proposed, suggesting that the nuclear egress of capsids depends on capsid surface phosphorylation and exposure of VP2 N-terminus (Wolfisberg *et al.* 2016).

Our results show that in CPV infection CRM1 inhibition with LBM alone is not enough to entirely block progeny capsid egress suggesting that alternative routes of exit are used (III). Replication of parvoviruses induces DNA damage in the host cell leading to cell cycle arrest at S and G2/M stages. Besides, DNA damage-related cell cycle arrest leads to activation of apoptosis (Chen *et al.* 2010, Adeyemi and Pintel 2014). The accumulation of cyclin B1 to the nucleus is a phenomenon known to be associated with the cyclin B1- Cdk1 complex translocation prior to the G2/M transition (Porter and Donoghue 2003). The accumulation of cyclin B1 to the nucleus starts in the G2 phase of the cell cycle, culminating prior to mitosis (Dulić *et al.* 1998, Rhind and Russell 2012). Here, we proposed that the accumulation of cyclin B1 in infected cells indicated nuclear egress of capsids at the G2/M. The finding was supported by impaired progeny capsid egress in the presence of Cdk1 inhibition, and by a reduction in the virus-induced NE permeability increase.

MVM studies showed that cyclin B1 transcription was inhibited and pre-mitotic block was released in infection (Adeyemi and Pintel 2014, Fuller *et al.* 2017). Since CPV-infection did not seem to implement cyclin B1 depletion, but rather the opposite, it seems possible that a similar block on cyclin B1-Cdk1 is either released in late infection or that the cyclin B1-mediated block is not in place.

Besides inducing cell cycle arrest, extensive DNA damage can lead to the programmed death of the cell, apoptosis (Enoch and Norbury 1995). CPV infection leads to apoptosis at the late stage of infection (Nykky *et al.* 2010). The Nucleocytoplasmic redistribution of importins α and β and Ran described in our studies for CPV infection is considered to be a hallmark of apoptosis (Ferrando-May 2005, Wilde and Zheng 2009). Besides other cellular factors, the nuclear localization of cyclin B1 is also linked to the decision process of the cell, leading to apoptosis as a response to DNA damage (Porter *et al.* 2003). In this work, we inhibited the progression of apoptosis with a specific inhibitor of an early apoptotic caspase, caspase-3. Like Cdk1 treatment, caspase-3 inhibition alone, although reducing progeny capsid translocation from nucleus to cytoplasm, was not enough to fully block progeny capsid egress or restore the NE permeability barrier in infection.

Involvement of G2/M transition and apoptosis in capsid egress were supported by the virus-induced activation of host genome regions regulating apoptosis- and mitosis-related gene expression. However, whether the mechanisms elucidated in this study are specific to capsids containing ssDNA, and therefore of importance to the active propagation of the virus infection, remains to be examined.

In addition, NS2 has been identified as one of the key actors for CRM1-mediated nuclear egress for MVM. In this thesis study, we studied the dependence of CPV egress on CRM1, but we did not look into the role of NS2 in the CRM1- mediated mechanism of egress. Due to the cell cycle dependence of CRM1-mediated export and the association of NS2 cell cycle with regulatory elements and the variability of its subnuclear localization during infection, it is possible to argue that NS2 might regulate the nuclear egress of progeny capsids by altering its subnuclear compartmentalization and hence its availability for CRM1 mediated export.

7 CONCLUDING REMARKS AND FUTURE PROSPECTS

In this thesis, previously unknown functions of CPV NS2 protein, including critical functions in chromatin remodeling and DNA damage response, were discovered. CPV infection also induced changes in the structure of nucleoli as infection proceeded Furthermore, alternative mechanisms of nuclear egress of virus progeny capsids, including cell cycle dependence and activation of early apoptosis, were observed.

Besides interaction with proteins involved in chromatin organization and DNA damage response, CPV NS2 is associated with proteins that take part in splicing and nuclear export of mRNA. The role of NS2 in mRNA processing and transport was left outside of the scope of this thesis, but these aspects of the NS2-related functions are intriguing. Especially since all the parvovirus gene products must go through splicing, the possible NS2-mediated self-regulation might help further to explain viral RNA processing. Furthermore, aside from the proteins investigated in the original articles included in the thesis, the CPV NS2 interactome includes many interesting targets related to gene transcription, such as topologically associated domains and nuclear speckles, as well as proteins maintaining chromosomal condensation during the cell cycle G2/M phase. Understanding the mechanisms of these associations might be fascinating not only for autonomous parvovirus research but also for DNA virus research in general.

CPV-induced structural changes of nucleolus described in article II indicate changes in its functional properties. To study further the role of NS2 in the function of the nucleolus, other subnucleolar structures and nucleolar factors such as fibrillarin need to be examined.

The microscopy image analysis of subcellular structures in virus research and in cell biology in general is hampered by segmentation of the structures of interest. The human in the loop machine learning segmentation, used here in the second substudy, could provide an alternative method to time-consuming manual segmentation methods.

This thesis presents novel mechanisms of autonomous parvovirus egress enhanced by G2/M transition and early apoptosis-induced changes in the NE permeability. We showed that CPV nuclear egress was not fully diminished in the presence of CRM1, Cdk1 or caspase-3 inhibition. This suggests that CRM1-mediated active transport might not be the only mediator of the nuclear to cytoplasmic translocation of capsids. Considering that autonomous parvovirus packaging is highly inefficient, with only approximately 10 percent of assembled capsids being full, it remains to be examined whether the active and passive transport routes are specific for only full or empty capsids. Further studies of mechanisms involved in G2/M transition and apoptosis-mediated egress of CPV capsids would benefit understanding progeny virus exit more extensively.

The connection between CRM1-mediated export and cell cycle might also explain why capsid egress is coupled with increase in nuclear cyclin B1. However, it does not explain why CRM1 inhibition is not enough to block nuclear egress of capsids. Studies indicate that leptomycin B-induced inhibition of CRM1 pathway influences the cell cycle progression by arresting it to G1 or G2 phase. CRM1 itself is known to function cell cycle dependently. CRM1 protein levels are maintained at stable levels during mammalian cell cycle, yet the expression of CRM1 on mRNA level is known to increase from early G1 and to peak at G2/M (Kudo *et al.* 1997). Our study proved that cell cycle progression has a role in capsid egress. However, further studies are needed to determine how all exit pathways work together and how viral proteins are involved in these processes.

Moreover, BioID studies revealed that CPV NS2 is associated with NPC-forming proteins. This might indicate that NS2 has a regulatory effect on nucleoporin formation or transportation of molecules in and out of the nucleus. Interestingly, both Rae1 and Nup98 were among the high confidence hits, both linked to the anaphase-promoting complex inhibition (I, table S1)(Antonin *et al.* 2008)). Together with the findings of G2/M transition-mediated capsid egress these results might indicate a more complex role for NS2, likely as a modulator of cell cycle progression in infection. Determining the relations between cell cycle control, progeny virus egress and NS2 subnuclear availability requires further studies.

Taken together, autonomous parvoviruses, with a minimal number of viral proteins, are excellent model viruses to study the effects of viral infection on the host cells. Moreover, the host tropism range of parvoviruses could be used to analyze host range specific changes in the role of NS2. All in all, this thesis serves as a promising platform to study further the mechanisms of nuclear events of parvovirus infection and the potential role of NS2 in manipulation of cellular processes during infection.

Acknowledgements

This study was carried out at the University of Jyväskylä, at the Department of Biological and Environmental Science.

First and foremost, I would like to acknowledge my supervisor Adjunct Professor Maija Vihinen-Ranta. Maija, thank you for making all my efforts feel appreciated and valued and creating an environment where new ideas have always been welcome. I truly value your supervision and all that I have learned from you.

Secondly, I would like to thank docent Elina Mäntylä for her excellent supervision and guidance throughout the duration of my studies.

I would like to also express my gratitude to all of my co-workers, Vesa Aho, Satu Hakanen, Sami Salminen, Visa Ruokolainen, Alka Gupta, Simon Leclerc and Laura Miettinen. Working with all of you has been a pleasure and a privilege. Especially, I would like to thank Vesa Aho and Satu Hakanen for their valued comments on the thesis.

The thesis follow-up group Teemu Ihalainen, Keijo Viiri and Matti Jalasvuori are thanked for their support and guidance.

I would like to acknowledge all our collaborators Kari Salokas, Julija Svirskaite, Markku Varjosalo, Mikko Oittinen, Keijo Viiri, Teemu Ihalainen, Einari Niskanen, Minna Kaikkonen-Määttä, Kari Airenne, Jani Järvensivu and Colin R Parrish for their contribution.

Especially, I am grateful to Kari Salokas for analyzes of the BioID data, Mikko Oittinen for ChIP-seq analyses, and Colin R Parrish for providing the mutants used in the studies. In addition, Alli Liukkonen and Wendy Weichert are thanked for their excellent technical support.

I am thankful to the reviewers, Professor emeritus Veijo Hukkanen and docent Sami Oikarinen, for their valuable comments on the thesis and Professor Jose M Almendral for agreeing to act as my opponent in my thesis dissertation.

Lastly, I would like to thank my family for all their support.

The work was funded by the doctoral programme in biological and environmental science and the Jane and Aatos Erkko Foundation.

YHTEENVETO (RÉSUMÉ IN FINNISH)

Parvoviruksen vuorovaikutukset isäntäsolun tumassa

Solun elämään kuuluu solun perimän kopiointi ja muokkaaminen siten, että se voidaan muuttaa proteiineiksi. Virukset ovat kykenemättömiä kopioimaan omaa perimäänsä täysin itsenäisesti, joten ne joutuvat hyödyntämään isännän toimintoja kyetäkseen lisääntymään. Virusten vuorovaikutus isäntäsolun kanssa tapahtuu virusgenomin ja proteiinien avulla. Ymmärtääksemme viruksen ja solun vuorovaikutusta tulee meidän ymmärtää kuinka viruksen eri proteiinit vuorovaikuttavat solun kanssa. Tässä väitöskirjassa vuorovaikutusta selvitetään käyttämällä malliviruksena koiran parvovirusta.

Koiran parvovirus kuuluu autonomisten parvovirusten ryhmään. Parvovirukset ovat pieniä patogeenejä, joiden perimä on pakattuna yksijuosteiseen DNA-molekyyliin. Koiran parvoviruksen, kuten DNA-virusten yleensä, elinkierron vaiheet tapahtuvat pääasiallisesti solun tumassa. Virus muodostaa infektion aikana tumaan replikaatioalueita, joissa sijaitsevat viruksen proteiinit ja genomi sekä useat viruksen tarvitsemat isäntäsolun proteiinit. Parvovirukset tuottavat kahdesta geenistään neljää proteiinia hyödyntäen vaihtoehtoista silmikointia. Tuotetuista proteiineista kaksi muodostaa viruskapsidin ja kaksi ei-rakenteellista proteiinia tukee viruksen lisääntymiskierron eri toimintoja. Autonomisten parvovirusten toisen ei-rakenteellisen proteiinin NS1:n merkitys infektiolle tunnetaan hyvin. Sen tiedetään tunnistavan ja sitoutuvan määrättyyn kohtaan DNA sekvenssistä, aiheuttaen DNA:han pieniä katkoksia. Lisäksi NS1 kykenee pilkkomaan ATP:tä sekä toimimaan DNA:ta avaavana helikaasina tukien toiminnallaan viruksen replikaatiota. Toisen ei-rakenteellisen proteiinin, NS2:en, toiminnasta ei tiedetä paljoa. Tämänhetkinen tutkimustieto pohjautuu pitkälti hiiren parvoviruksen NS2:en tutkimuksiin.

Tässä väitöskirjatyössä pyrittiin proteomiikan keinoin löytämään koiran parvoviruksen NS2:n vuorovaikutuksia isäntäsolun proteiinien kanssa. Tekniikkana käytettiin biotiiniligaasi-identifikaatiota (BioID). Vuorovaikuttavien proteiinien määrittämiseksi koiran parvoviruksen NS2 fuusioitiin biotiiniligaasiproteiinin kanssa. Fuusioproteiinia ilmentävissä soluissa ligaasi liittää pienen biotiinimolekyylin kaikkiin fuusioproteiinin läheisyyteen tuleviin solun proteiineihin. NS2-proteiinin vuorovaikutukset voitiin näin määrittää massaspektrometriaa hyödyntäen sekä ei-infektoiduissa että infektoiduissa soluissa. Menetelmänä BioID on herkkä, mahdollistaen myös heikkojen ja hetkellisten vuorovaikutusten havainnoinnin. BioID:tä hyödyntämällä tutkimuksessa kyettiin myös määrittämään proteiinin toimintaympäristö massaspektrometriamikroskopiaa ja proteiinikartastoa hyödyntämällä.

NS2:en havaittiin vuorovaikuttavan yhteensä 122 proteiinin kanssa. Nämä proteiinit osallistuvat erityisesti kromatiinin muokkaukseen ja

organisointiin, DNA vauriovasteeseen, sekä lähetti-RNA:n tuottoon ja tumasta uloskuljetukseen. Edellä mainittuja havaintoja tukivat NS2:n vaihtoehtoisen silmikoinnin alueen mutaation aiheuttamat muutokset kromatiinin jakaumassa (ja määrässä) sekä infektiolle tyypillisen vauriovasteen ilmenemisessä. NS2:n mutaatio esti myös virusinfektion tehokkaalle etenemiselle välttämättömien replikaatioalueiden muodostumisen.

BioID-tutkimuksemme osoitti myös, että NS2 vuorovaikuttaa tumajyväsen proteiinien kanssa. Seuraavaksi selvitimme NS2:en roolia tumajyväsen rakenteen säätelijänä hyödyntäen koneoppimista konfokaalimikroskopiakuvien analyysissä. Tarkastelua varten tumajyväset tunnistettiin niiden sisältämän nukleoliiniproteiinin avulla, ja niiden lukumäärä ja keskimääräinen tilavuus määritettiin. Saadut tulokset osoittivat, että tumajyvästen tilavuus pienenee merkittävästi myöhäisessä infektiossa. Jos merkittävä osuus NS2:sta poistettiin mutaation avulla, tumajyvästen pienenemistä ei havaittu.

NS2-vuorovaikutusten lisäksi väitöskirjassa tarkasteltiin solun toiminnan muutoksia, jotka tapahtuivat samanaikaisesti, kun infektiossa tuotetut viruskapsidit kuljetettiin ulos tumasta. Aiemmin MVM-viruksella saadut tulokset näyttivät viruskapsidien tumasta uloskulkeutumisen tapahtuvan aktiivisesti tumahuokosten kautta. Tässä työssä havaittiin kapsidien siirtymän tumasta sytoplasmaan liittyvän tumansisäisen sykliini B1:n määrän voimakkaaseen kasvuun. Vastaavan tumansisäisen sykliini B1:n kasvun tiedetään liittyvän kahteen solun kokonaisvaltaiseen muutokseen: solusyklin G2/M siirtymään ja solukuoleman aktivoitumiseen. Molemmat mainitut reitit lisäävät tumakalvon läpäisevyyttä, mikä mahdollistaa viruskapsidien pääsyn ulos tumasta.

NS2 proteiinilla näyttää olevan tuman kromatiinia ja tumajyvästä muokkaavia ominaisuuksia, mikä viittaa sen aikaisemmin tunnettua laajempaan rooliin viruksen replikaatiossa. Lisäksi solusyklin muutosten ja apoptoosin aktivoitumisen havaittiin olevan yhteydessä kapsidien uloskuljetukseen.

REFERENCES

Adeyemi R.O., Fuller M.S. & Pintel D.J. Efficient Parvovirus Replication Requires CRL4 Cdt2-Targeted Depletion of p21 to Prevent Its Inhibitory Interaction with PCNA.

Adeyemi R.O., Landry S., Davis M.E., Weitzman M.D. & Pintel D.J. 2010. Parvovirus minute virus of mice induces a DNA damage response that facilitates viral replication. *PLoS Pathogens* 6: 1–11.

Adeyemi R.O. & Pintel D.J. 2014. Parvovirus-induced depletion of cyclin B1 prevents mitotic entry of infected cells. *PLoS pathogens* 10.

Aebi U., Cohn J., Buhle L. & Gerace L. 1986. The nuclear lamina is a meshwork of intermediate-type filaments. *Nature* 323: 560–564.

Agbandje M. & Chapman M.S. 2006. *Correlating structure with function in the viral capsid. Parvoviruses* Correlating structure with function in the viral capsid. Kerr J. C.S.F., B.M.E., L.R.M.& P.C.R. (ed.).

Agbandje-McKenna M., Llamas-Saiz A.L., Wang F., Tattersall P. & Rossmann M.G. 1998. Functional implications of the structure of the murine parvovirus, minute virus of mice. *Structure (London, England : 1993)* 6: 1369–1381.

Aho V., Mäntylä E., Ekman A., Hakanen S., Mattola S., Chen J.H., Weinhardt V., Ruokolainen V., Sodeik B., Larabell C. & Vihinen-Ranta M. 2019. Quantitative microscopy reveals stepwise alteration of chromatin structure during herpesvirus infection. *Viruses* 11: 1–15.

Aho V., Salminen S., Mattola S., Gupta A., Flomm F., Sodeik B., Bosse J.B. & Vihinen-Ranta M. 2021. Infection-induced chromatin modifications facilitate translocation of herpes simplex virus capsids to the inner nuclear membrane. *PLoS Pathogens* 17: 1–20.

Allfrey V.G., Faulkner R. & Mirsky A.E. 1964. acetylation and methylation of histones and their possible role in the regulation of RNA synthesis. *Proceedings of the National Academy of Sciences of the United States of America* 51: 786–794.

Anouja F., Wattiez R., Mousset S. & Caillet-Fauquet P. 1997. The cytotoxicity of the parvovirus minute virus of mice nonstructural protein NS1 is related to changes in the synthesis and phosphorylation of cell proteins. *Journal of Virology* 71: 4671–4678.

Antonin W., Ellenberg J. & Dultz E. 2008. Nuclear pore complex assembly through the cell cycle: regulation and membrane organization. *FEBS letters* 582: 2004–2016.

Bannister A.J. & Kouzarides T. 2011. Regulation of chromatin by histone modifications. *Cell Research* 21: 381.

Bashir T., Rommelaere J. & Cziepluch C. 2001. In Vivo Accumulation of Cyclin A and Cellular Replication Factors in Autonomous Parvovirus Minute Virus of Mice-Associated Replication Bodies. *Journal of Virology* 75: 4394–4398.

Beck M., Lůí V., Förster F., Baumeister W. & Medalia O. 2007. Snapshots of nuclear pore complexes in action captured by cryo-electron tomography. *Nature* 449: 611–615.

Beeck A. op de & Caillet-Fauquet P. 1997. The NS1 protein of the autonomous parvovirus minute virus of mice blocks cellular DNA replication: a consequence of lesions to the chromatin? *Journal of Virology* 71: 5323–5329.

Bender B.J., Coen D.M. & Strang B.L. 2014. Dynamic and nucleolin-dependent localization of human cytomegalovirus UL84 to the periphery of viral replication compartments and nucleoli. *Journal of virology* 88: 11738–11747.

Bianco C. & Mohr I. 2019. Ribosome biogenesis restricts innate immune responses to virus infection and DNA. *eLife* 8.

Blackford A.N. & Jackson S.P. 2017. ATM, ATR, and DNA-PK: The Trinity at the Heart of the DNA Damage Response. *Molecular Cell* 66: 801–817.

Bobes-Bascarán J., Mosqueira-Rey E. & Alonso-Ríos D. 2021. Improving Medical Data Annotation Including Humans in the Machine Learning Loop. *Engineering Proceedings* 7: 39.

Bodendorf U., Cziepluch C., Jauniaux J.-C., Rommelaere J. & Salomé N. 1999. Nuclear export factor CRM1 interacts with nonstructural proteins NS2 from parvovirus minute virus of mice. *Journal of virology* 73: 7769–7779.

Bondarenko M.T., Maluchenko N. v., Valieva M.E., Gerasimova N.S., Kulaeva O.I., Georgiev P.G. & Studitsky V.M. 2015. [Structure and function of histone chaperone FACT]. *Molekuliarnaia biologiia* 49: 891–904.

Boulon S., Westman B.J., Hutten S., Boisvert F.M. & Lamond A.I. 2010. The nucleolus under stress. *Molecular cell* 40: 216–227.

Branco M.R. & Pombo A. 2006. Intermingling of chromosome territories in interphase suggests role in translocations and transcription-dependent associations. *PLoS biology* 4: 780–788.

Brangwynne C.P., Mitchison T.J. & Hyman A.A. 2011. Active liquid-like behavior of nucleoli determines their size and shape in Xenopus laevis oocytes. *Proceedings of the National Academy of Sciences of the United States of America* 108: 4334–4339.

Brestovitsky A., Sharf R., Mittelman K. & Kleinberger T. 2011. The adenovirus E4orf4 protein targets PP2A to the ACF chromatin-remodeling factor and induces cell death through regulation of SNF2h-containing complexes. *Nucleic acids research* 39: 6414–6427.

Brockhaus K., Plaza S., Pintel D.J., Rommelaere J. & Salomé N. 1996. Nonstructural proteins NS2 of minute virus of mice associate in vivo with 14-3-3 protein family members. *Journal of virology* 70: 7527–7534.

Brooker A.S. & Berkowitz K.M. 2014. *The roles of cohesins in mitosis, meiosis, and human health and disease*.

Bryant K.F., Colgrove R.C. & Knipe D.M. 2011. Cellular SNF2H chromatin-remodeling factor promotes herpes simplex virus 1 immediate-early gene expression and replication. *mBio* 2.

Burgess R.J. & Zhang Z. 2013. Histone chaperones in nucleosome assembly and human disease. *Nature structural & molecular biology* 20: 14.

Burke B. & Ellenberg J. 2002. Remodelling the walls of the nucleus. *Nature Reviews Molecular Cell Biology 2002 3:7* 3: 487–497.

Callaway H.M., Feng K.H., Lee D.W., Allison A.B., Pinard M., McKenna R., Agbandje-McKenna M., Hafenstein S. & Parrish C.R. 2017. Parvovirus Capsid Structures Required for Infection: Mutations Controlling Receptor Recognition and Protease Cleavages. *Journal of Virology* 91: 1–16.

Callé A., Ugrinova I., Epstein A.L., Bouvet P., Diaz J.-J. & Greco A. 2008. Nucleolin is required for an efficient herpes simplex virus type 1 infection. *Journal of virology* 82: 4762–4773.

Caragine C.M., Haley S.C. & Zidovska A. 2019. Nucleolar dynamics and interactions with nucleoplasm in living cells. *eLife* 8.

Carmichael L.E., Joubert J.C. & Pollock R. v. 1983. A modified live canine parvovirus vaccine. II. Immune response. *The Cornell veterinarian* 73: 13–29.

Carra S., Alberti S., Arrigo P.A., Benesch J.L., Benjamin I.J., Boelens W., Bartelt-Kirbach B., Brundel B.J.J.M., Buchner J., Bukau B., Carver J.A., Ecroyd H., Emanuelsson C., Finet S., Golenhofen N., Goloubinoff P., Gusev N., Haslbeck M., Hightower L.E., Kampinga H.H., Klevit R.E., Liberek K., Mchaourab H.S., McMenimen K.A., Poletti A., Quinlan R., Strelkov S. v., Toth M.E., Vierling E. & Tanguay R.M. 2017. The growing world of small heat shock proteins: from structure to functions. *Cell stress & chaperones* 22: 601–611.

Cater J.E. & Pintel D.J. 1992. The small non-structural protein NS2 of the autonomous parvovirus minute virus of mice is required for virus growth in murine cells. *The Journal of general virology* 73 (Pt 7): 1839–1843.

Chan C.M., Chu H., Zhang A.J., Leung L.H., Sze K.H., Kao R.Y.T., Chik K.K.H., To K.K.W., Chan J.F.W., Chen H., Jin D.Y., Liu L. & Yuen K.Y. 2016. Hemagglutinin of influenza A virus binds specifically to cell surface nucleolin and plays a role in virus internalization. *Virology* 494: 78–88.

Charman M. & Weitzman M.D. 2020. Replication Compartments of DNA Viruses in the Nucleus: Location, Location, Location. *Viruses* 12.

Chen A.Y., Luo Y., Cheng F., Sun Y. & Qiu J. 2010. Bocavirus Infection Induces Mitochondrion-Mediated Apoptosis and Cell Cycle Arrest at G 2 /M Phase . *Journal of Virology* 84: 5615–5626.

Chen A.Y. & Qiu J. 2010. Parvovirus infection-induced cell death and cell cycle arrest. *Future Virology* 5: 731–743.

Cheng F., Chen A.Y., Best S.M., Bloom M.E., Pintel D. & Qiu J. 2010. The Capsid Proteins of Aleutian Mink Disease Virus Activate Caspases

and Are Specifically Cleaved during Infection. *Journal of Virology* 84: 2687–2696.

Cheutin T., McNairn A.J., Jenuwein T., Gilbert D.M., Singh P.B. & Misteli T. 2003. Maintenance of stable heterochromatin domains by dynamic HP1 binding. *Science* 299: 721–725.

Choi E.-Y., Newman A.E., Burger L. & Pintel D. 2005. Replication of Minute Virus of Mice DNA Is Critically Dependent on Accumulated Levels of NS2. *Journal of Virology* 79: 12375–12381.

Christensen J., Cotmore S.F. & Tattersall P. 1995. Minute virus of mice transcriptional activator protein NS1 binds directly to the transactivation region of the viral P38 promoter in a strictly ATP-dependent manner. *Journal of virology* 69: 5422–5430.

Christensen J., Cotmore S.F. & Tattersall P. 1997. A novel cellular site-specific DNA-binding protein cooperates with the viral NS1 polypeptide to initiate parvovirus DNA replication. *Journal of virology* 71: 1405–1416.

Christensen J. & Tattersall P. 2002. Parvovirus initiator protein NS1 and RPA coordinate replication fork progression in a reconstituted DNA replication system. *Journal of virology* 76: 6518–6531.

Clemens K.E. & Pintel D.J. 1988. The two transcription units of the autonomous parvovirus minute virus of mice are transcribed in a temporal order. *Journal of virology* 62: 1448–1451.

Correll C.C., Bartek J. & Dundr M. 2019. The Nucleolus: A Multiphase Condensate Balancing Ribosome Synthesis and Translational Capacity in Health, Aging and Ribosomopathies. *Cells* 8.

Costanzi C. & Pehrson J.R. 1998. Histone macroH2A1 is concentrated in the inactive X chromosome of female mammals. *Nature 1998 393:6685* 393: 599–601.

Cotmore S.F., Agbandje-McKenna M., Canuti M., Chiorini J.A., Eis-Hubinger A.M., Hughes J., Mietzsch M., Modha S., Ogliastro M., Pénzes J.J., Pintel D.J., Qiu J., Soderlund-Venermo M., Tattersall P., Tijssen P., Lefkowitz E.J., Davison A.J., Siddell S.G., Simmonds P., Sabanadzovic S., Smith D.B., Orton R.J. & Harrach B. 2019. ICTV virus taxonomy profile: Parvoviridae. *Journal of General Virology* 100: 367–368.

Cotmore S.F., Christensen J. & Tattersall P. 2000. Two widely spaced initiator binding sites create an HMG1-dependent parvovirus rolling-hairpin replication origin. *Journal of virology* 74: 1332–1341.

Cotmore S.F., D'Abramo A.M., Carbonell L.F., Bratton J. & Tattersall P. 1997. The NS2 polypeptide of parvovirus MVM is required for capsid assembly in murine cells. *Virology* 231: 267–280.

Cotmore S.F., Gottlieb R.L. & Tattersall P. 2007. Replication initiator protein NS1 of the parvovirus minute virus of mice binds to modular divergent sites distributed throughout duplex viral DNA. *Journal of virology* 81: 13015–13027.

Cotmore S.F., Hafenstein S. & Tattersall P. 2010. Depletion of virion-associated divalent cations induces parvovirus minute virus of mice to eject its genome in a 3′-to-5′ direction from an otherwise intact viral particle. *Journal of virology* 84: 1945–1956.

Cotmore S.F. & Tattersall P. 1998. High-mobility group 1/2 proteins are essential for initiating rolling-circle-type DNA replication at a parvovirus hairpin origin. *Journal of virology* 72: 8477–8484.

Cotmore S.F. & Tattersall P. 2005. Genome packaging sense is controlled by the efficiency of the nick site in the right-end replication origin of parvoviruses minute virus of mice and LuIII. *Journal of virology* 79: 2287–2300.

Cotmore S.F. & Tattersall P. 2014. Parvoviruses: Small Does Not Mean Simple. *Annual review of virology* 1: 517–537.

Cremer T. & Cremer M. 2010. Chromosome territories. *Cold Spring Harbor perspectives in biology* 2.

Cremer T., Cremer C., Schneider T., Baumann H., Hens L. & Kirsch-Volders M. 1982. Analysis of chromosome positions in the interphase nucleus of Chinese hamster cells by laser-UV-microirradiation experiments. *Human Genetics* 62: 201–209.

Cremer T., Kreth G., Koester H., Fink R.H.A., Heintzmann R., Cremer M., Solovei I., Zink D. & Cremer C. 2000. Chromosome territories, interchromatin domain compartment, and nuclear matrix: an integrated view of the functional nuclear architecture. *Critical reviews in eukaryotic gene expression* 10: 179–212.

Crncec A. & Hochegger H. 2019. Triggering mitosis. *FEBS Letters* 593: 2868–2888.

Croft J.A., Bridger J.M., Boyle S., Perry P., Teague P. & Bickmore W.A. 1999. Differences in the localization and morphology of chromosomes in the human nucleus. *The Journal of cell biology* 145: 1119–1131.

Cronshaw J.M., Krutchinsky A.N., Zhang W., Chait B.T. & Matunis M.L.J. 2002. Proteomic analysis of the mammalian nuclear pore complex. *Journal of Cell Biology* 158: 915–927.

Cuylen S., Blaukopf C., Politi A.Z., Muller-Reichert T., Neumann B., Poser I., Ellenberg J., Hyman A.A. & Gerlich D.W. 2016. Ki-67 acts as a biological surfactant to disperse mitotic chromosomes. *Nature* 535: 308–312.

Cziepluch C., Lampel S., Grewenig A., Grund C., Lichter P. & Rommelaere J. 2000. H-1 parvovirus-associated replication bodies: a distinct virus-induced nuclear structure. *Journal of virology* 74: 4807–4815.

Dai Z., Ramesh V. & Locasale J.W. The evolving metabolic landscape of chromatin biology and epigenetics. *Nature Reviews Genetics*.

D'Angelo M.A. & Hetzer M.W. 2008. Structure, dynamics and function of nuclear pore complexes. *Trends in cell biology* 18: 456–466.

Daniely Y. & Borowiec J.A. 2000. Formation of a complex between nucleolin and replication protein A after cell stress prevents initiation of DNA replication. *The Journal of cell biology* 149: 799–809.

Deng Y.P., Liu Y.J., Yang Z.Q., Wang Y.J., He B.Y. & Liu P. 2017. Human bocavirus induces apoptosis and autophagy in human bronchial epithelial cells. *Experimental and therapeutic medicine* 14: 753–758.

Doley J., Singh L.V., Kumar G.R., Sahoo A.P., Saxena L., Chaturvedi U., Saxena S., Kumar R., Singh P.K., Rajmani R.S., Santra L., Palia S.K., Tiwari S., Harish D.R., Kumar A., Desai G.S., Gupta S., Gupta S.K. & Tiwari A.K. 2014. Canine parvovirus type 2a (CPV-2a)-induced apoptosis in MDCK involves both extrinsic and intrinsic pathways. *Applied biochemistry and biotechnology* 172: 497–508.

Dubois M.L. & Boisvert F.M. 2016. The nucleolus: Structure and function. *The Functional Nucleus*: 29–49.

Dulić V., Stein G.H., Far D.F. & Reed S.I. 1998. Nuclear Accumulation of p21 Cip1 at the Onset of Mitosis: a Role at the G 2 /M-Phase Transition . *Molecular and Cellular Biology* 18: 546–557.

Earley L.F., Powers J.M., Adachi K., Baumgart J.T., Meyer N.L., Xie Q., Chapman M.S. & Nakai H. 2017. Adeno-associated Virus (AAV) Assembly-Activating Protein Is Not an Essential Requirement for Capsid Assembly of AAV Serotypes 4, 5, and 11. *Journal of virology* 91.

Eichwald V., Daeffler L., Klein M., Rommelaere J. & Salomé N. 2002. The NS2 Proteins of Parvovirus Minute Virus of Mice Are Required for Efficient Nuclear Egress of Progeny Virions in Mouse Cells. *Journal of Virology* 76: 10307–10319.

Elmore S. 2007. Apoptosis: a review of programmed cell death. *Toxicologic pathology* 35: 495–516.

Elmore Z.C., Patrick Havlik L., Oh D.K., Anderson L., Daaboul G., Devlin G.W., Vincent H.A. & Asokan A. 2021. The membrane associated accessory protein is an adeno-associated viral egress factor. *Nature communications* 12.

Engelsma D., Valle N., Fish A., Salomé N., Almendral J.M. & Fornerod M. 2008. A supraphysiological nuclear export signal is required for parvovirus nuclear export. *Molecular biology of the cell* 19: 2544–2552.

Enoch T. & Norbury C. 1995. Cellular responses to DNA damage: cell-cycle checkpoints, apoptosis and the roles of p53 and ATM. *Trends in biochemical sciences* 20: 426–430.

Evans T., Rosenthal E.T., Youngblom J., Distel D. & Hunt T. 1983. Cyclin: a protein specified by maternal mRNA in sea urchin eggs that is destroyed at each cleavage division. *Cell* 33: 389–396.

Falahati H., Pelham-Webb B., Blythe S. & Wieschaus E. 2016. Nucleation by rRNA Dictates the Precision of Nucleolus Assembly. *Current biology : CB* 26: 277–285.

Ferrando-May E. 2005. Nucleocytoplasmic transport in apoptosis. *Cell Death and Differentiation* 12: 1263–1276.

Fuller M.S., Majumder K. & Pintel D.J. 2017. Minute Virus of Mice Inhibits Transcription of the Cyclin B1 Gene during Infection. *Journal of virology* 91.

Galibert L., Hyvönen A., Eriksson R.A.E., Mattola S., Aho V., Salminen S., Albers J.D., Peltola S.K., Weman S., Nieminen T., Ylä-Herttuala S., Lesch H.P., Vihinen-Ranta M. & Airenne K.J. 2021. Functional roles of the membrane-associated AAV protein MAAP. *Scientific reports* 11.

Gerdes J., Lemke H., Baisch H., Wacker H.H., Schwab U. & Stein H. 1984. Cell cycle analysis of a cell proliferation-associated human nuclear antigen defined by the monoclonal antibody Ki-67. *Journal of immunology (Baltimore, Md. : 1950)* 133: 1710–1715.

Gilbert N., Boyle S., Fiegler H., Woodfine K., Carter N.P. & Bickmore W.A. 2004. Chromatin architecture of the human genome: gene-rich domains are enriched in open chromatin fibers. *Cell* 118: 555–566.

Gil-Ranedo J., Hernando E., Riolobos L., Domínguez C., Kann M. & Almendral J. éM. 2015. The Mammalian Cell Cycle Regulates Parvovirus Nuclear Capsid Assembly. *PLoS pathogens* 11.

Gil-Ranedo J., Hernando E., Valle N., Riolobos L., Maroto B. & Almendral J.M. 2018. Differential phosphorylation and n-terminal configuration of capsid subunits in parvovirus assembly and viral trafficking. *Virology* 518: 184–194.

Goldman R.D., Gruenbaum Y., Moir R.D., Shumaker D.K. & Spann T.P. 2002. Nuclear lamins: building blocks of nuclear architecture. *Genes & development* 16: 533–547.

Greco A., Arata L., Soler E., Gaume X., Couté Y., Hacot S., Callé A., Monier K., Epstein A.L., Sanchez J.-C., Bouvet P. & Diaz J.-J. 2012. Nucleolin interacts with US11 protein of herpes simplex virus 1 and is involved in its trafficking. *Journal of virology* 86: 1449–1457.

Gurda B.L., Parent K.N., Bladek H., Sinkovits R.S., DiMattia M.A., Rence C., Castro A., McKenna R., Olson N., Brown K., Baker T.S. & Agbandje-McKenna M. 2010. Human bocavirus capsid structure: insights into the structural repertoire of the parvoviridae. *Journal of virology* 84: 5880–5889.

Hagting A., Jackman M., Simpson K. & Pines J. 1999. Translocation of cyclin B1 to the nucleus at prophase requires a phosphorylation-dependent nuclear import signal. *Current Biology* 9: 680–689.

Heintzman N.D., Stuart R.K., Hon G., Fu Y., Ching C.W., Hawkins R.D., Barrera L.O., Calcar S. van, Qu C., Ching K.A., Wang W., Weng Z., Green R.D., Crawford G.E. & Ren B. 2007. Distinct and predictive chromatin signatures of transcriptional promoters and enhancers in the human genome. *Nature genetics* 39: 311–318.

Henderson A.S., Warburton D. & Atwood K.C. 1972. Location of ribosomal DNA in the human chromosome complement. *Proceedings of the National Academy of Sciences of the United States of America* 69: 3394–3398.

Hendrick J.P. & Hartl F.U. 1993. Molecular chaperone functions of heat-shock proteins. *Annual review of biochemistry* 62: 349–384.

Hendzel M.J., Wei Y., Mancini M.A., Hooser A. van, Ranalli T., Brinkley B., Bazett-Jones D.P., David Allis C. & Allis C. 1997. *Mitosis-specific*

phosphorylation of histone H3 initiates primarily within pericentromeric heterochromatin during G2 and spreads in an ordered fashion coincident with mitotic chromosome condensation. Springer-Verlag.

Hengartner M.O. 2000. The biochemistry of apoptosis. *Nature* 407: 770–776.

Hernandez-Verdun D. 2011. Assembly and disassembly of the nucleolus during the cell cycle. *Nucleus (Austin, Tex.)* 2: 189–194.

Hernando E., Llamas-Saiz A.L., Foces-Foces C., McKenna R., Portman I., Agbandje-Mckenna M. & Almendral J.M. 2000. Biochemical and physical characterization of parvovirus minute virus of mice virus-like particles. *Virology* 267: 299–309.

Hetz C., Zhang K. & Kaufman R.J. 2020. Mechanisms, regulation and functions of the unfolded protein response. *Nature reviews. Molecular cell biology* 21: 421–438.

Hetzer M.W. 2010. The nuclear envelope. *Cold Spring Harbor perspectives in biology* 2: 1–16.

Hooser A. van, Goodrich D.W., David Allis C., Brinkley B.R. & Mancini M.A. 1998. Histone H3 phosphorylation is required for the initiation, but not maintenance, of mammalian chromosome condensation. *Journal of Cell Science* 111: 3497–3506.

Hristov G., Krämer M., Li J., El-Andaloussi N., Mora R., Daeffler L., Zentgraf H., Rommelaere J. & Marchini A. 2010. Through Its Nonstructural Protein NS1, Parvovirus H-1 Induces Apoptosis via Accumulation of Reactive Oxygen Species. *Journal of Virology* 84: 5909–5922.

Hsu T.-C., Wu W.-J., Chen M.-C. & Tsay G.J. 2004. Human parvovirus B19 non-structural protein (NS1) induces apoptosis through mitochondria cell death pathway in COS-7 cells. *Scandinavian journal of infectious diseases* 36: 570–577.

Hull J.A., Mietzsch M., Chipman P., Strugatsky D. & McKenna R. 2022. Structural characterization of an envelope-associated adeno-associated virus type 2 capsid. *Virology* 565: 22–28.

Iborra F.J., Pombo A., Jackson D.A. & Cook P.R. 1996. Active RNA polymerases are localized within discrete transcription "factories'' in human nuclei." *Journal of cell science* 109 (Pt 6): 1427–1436.

Ihalainen T.O., Niskanen E.A., Jylhävä J., Paloheimo O., Dross N., Smolander H., Langowski J., Timonen J. & Vihinen-Ranta M. 2009. Parvovirus induced alterations in nuclear architecture and dynamics. *PLoS ONE* 4.

Imamoto N. & Funakoshi T. 2012. Nuclear pore dynamics during the cell cycle. *Current opinion in cell biology* 24: 453–459.

Jackson P.K. 2008. The hunt for cyclin. *Cell* 134: 199–202.

Jackson S.P. & Bartek J. 2009. The DNA-damage response in human biology and disease. *Nature* 461: 1071–1078.

Jänicke R.U., Sprengart M.L., Wati M.R. & Porter A.G. 1998. Caspase-3 is required for DNA fragmentation and morphological changes

associated with apoptosis. *Journal of Biological Chemistry* 273: 9357–9360.

Jia W., Yao Z., Zhao J., Guan Q. & Gao L. 2017. New perspectives of physiological and pathological functions of nucleolin (NCL). *Life sciences* 186: 1–10.

Johnson P.R., Schnepp B.C., Connell M.J., Rohne D., Robinson S., Krivulka G.R., Lord C.I., Zinn R., Montefiori D.C., Letvin N.L. & Clark K.R. 2005. Novel Adeno-Associated Virus Vector Vaccine Restricts Replication of Simian Immunodeficiency Virus in Macaques. *Journal of Virology* 79: 955–965.

Jurvansuu J., Raj K., Stasiak A. & Beard P. 2005. Viral transport of DNA damage that mimics a stalled replication fork. *Journal of virology* 79: 569–580.

Karimian A., Ahmadi Y. & Yousefi B. 2016. Multiple functions of p21 in cell cycle, apoptosis and transcriptional regulation after DNA damage. *DNA Repair* 42: 63–71.

Kaufmann B., Simpson A.A. & Rossmann M.G. 2004. The structure of human parvovirus B19. *Proceedings of the National Academy of Sciences of the United States of America* 101: 11628–11633.

Kawamura K., Qi F., Meng Q., Hayashi I. & Kobayashi J. 2019. Nucleolar protein nucleolin functions in replication stress-induced DNA damage responses. *Journal of radiation research* 60: 281–288.

Kempfer R. & Pombo A. 2020. Methods for mapping 3D chromosome architecture. *Nature reviews. Genetics* 21: 207–226.

Kerr J.F.R., Wyllie A.H. & Currie A.R. 1972. Apoptosis: a basic biological phenomenon with wide-ranging implications in tissue kinetics. *British journal of cancer* 26: 239–257.

Kim K., Dimitrova D.D., Carta K.M., Saxena A., Daras M. & Borowiec J.A. 2005. Novel checkpoint response to genotoxic stress mediated by nucleolin-replication protein a complex formation. *Molecular and cellular biology* 25: 2463–2474.

Kim J., Sturgill D., Sebastian R., Khurana S., Tran A.D., Edwards G.B., Kruswick A., Burkett S., Hosogane E.K., William W., Weyemi U., Bonner W.M. & Luger K. 2019. Across Fragile Genomic Regions. 69: 36–47.

Kinner A., Wu W., Staudt C. & Iliakis G. 2008. Gamma-H2AX in recognition and signaling of DNA double-strand breaks in the context of chromatin. *Nucleic acids research* 36: 5678–5694.

Kobayashi J., Fujimoto H., Sato J., Hayashi I., Burma S., Matsuura S., Chen D.J. & Komatsu K. 2012. Nucleolin participates in DNA double-strand break-induced damage response through MDC1-dependent pathway. *PloS one* 7.

Kontou M., Govindasamy L., Nam H.-J., Bryant N., Llamas-Saiz A.L., Foces-Foces C., Hernando E., Rubio M.-P., McKenna R., Almendral J.M. & Agbandje-McKenna M. 2005. Structural determinants of tissue

tropism and in vivo pathogenicity for the parvovirus minute virus of mice. *Journal of virology* 79: 10931–10943.

Kudo N., Khochbin S., Nishi K., Kitano K., Yanagida M., Yoshida M. & Horinouchi S. 1997. Molecular cloning and cell cycle-dependent expression of mammalian CRM1, a protein involved in nuclear export of proteins. *The Journal of biological chemistry* 272: 29742–29751.

Kumar D., Broor S. & Rajala M.S. 2016. Interaction of Host Nucleolin with Influenza A Virus Nucleoprotein in the Early Phase of Infection Limits the Late Viral Gene Expression. *PloS one* 11.

Lafontaine D.L.J., Riback J.A., Bascetin R. & Brangwynne C.P. 2021. The nucleolus as a multiphase liquid condensate. *Nature reviews. Molecular cell biology* 22: 165–182.

Lammerding J., Hsiao J., Schulze P.C., Kozlov S., Stewart C.L. & Lee R.T. 2005. Abnormal nuclear shape and impaired mechanotransduction in emerin-deficient cells. *The Journal of cell biology* 170: 781–791.

Lange A., Mills R.E., Lange C.J., Stewart M., Devine S.E. & Corbett A.H. 2007. Classical nuclear localization signals: definition, function, and interaction with importin alpha. *The Journal of biological chemistry* 282: 5101–5105.

Larson A.G., Elnatan D., Keenen M.M., Trnka M.J., Johnston J.B., Burlingame A.L., Agard D.A., Redding S. & Narlikar G.J. 2017. Liquid droplet formation by HP1α suggests a role for phase separation in heterochromatin. *Nature* 547: 236–240.

Latonen L. 2019. Phase-to-Phase With Nucleoli - Stress Responses, Protein Aggregation and Novel Roles of RNA. *Frontiers in cellular neuroscience* 13.

Lauberth S.M., Nakayama T., Wu X., Ferris A.L., Tang Z., Hughes S.H. & Roeder R.G. 2013. H3K4me3 interactions with TAF3 regulate preinitiation complex assembly and selective gene activation. *Cell* 152: 1021–1036.

Laurell E., Beck K., Krupina K., Theerthagiri G., Bodenmiller B., Horvath P., Aebersold R., Antonin W. & Kutay U. 2011. Phosphorylation of Nup98 by multiple kinases is crucial for NPC disassembly during mitotic entry. *Cell* 144: 539–550.

Lee T.W.R., Blair G.E. & Matthews D.A. 2003. Adenovirus core protein VII contains distinct sequences that mediate targeting to the nucleus and nucleolus, and colocalization with human chromosomes. *The Journal of general virology* 84: 3423–3428.

Li L., Cotmore S.F. & Tattersall P. 2013. Parvoviral left-end hairpin ears are essential during infection for establishing a functional intranuclear transcription template and for efficient progeny genome encapsidation. *Journal of virology* 87: 10501–10514.

Lilley C.E., Schwartz R.A. & Weitzman M.D. 2007. Using or abusing: viruses and the cellular DNA damage response. *Trends in Microbiology* 15: 119–126.

Linder M.I., Köhler M., Boersema P., Weberruss M., Wandke C., Marino J., Ashiono C., Picotti P., Antonin W. & Kutay U. 2017. Mitotic Disassembly of Nuclear Pore Complexes Involves CDK1- and PLK1-Mediated Phosphorylation of Key Interconnecting Nucleoporins. *Developmental Cell* 43: 141-156.e7.

Liu X., Salokas K., Tamene F., Jiu Y., Weldatsadik R.G., Öhman T. & Varjosalo M. 2018. An AP-MS- and BioID-compatible MAC-tag enables comprehensive mapping of protein interactions and subcellular localizations. *Nature communications* 9.

Lombardo E., Ramírez J.C., Agbandje-McKenna M. & Almendral J.M. 2000. A Beta-Stranded Motif Drives Capsid Protein Oligomers of the Parvovirus Minute Virus of Mice into the Nucleus for Viral Assembly. *Journal of Virology* 74: 3804–3814.

Longo G.M.C. & Roukos V. 2021. Territories or spaghetti? Chromosome organization exposed. *Nature Reviews Molecular Cell Biology* 22: 508.

López A.J., Hecking J.K. & White A.O. 2020. The Emerging Role of ATP-Dependent Chromatin Remodeling in Memory and Substance Use Disorders. *International journal of molecular sciences* 21: 1–20.

Lou S., Luo Y., Cheng F., Huang Q., Shen W., Kleiboeker S., Tisdale J.F., Liu Z. & Qiu J. 2012. Human Parvovirus B19 DNA Replication Induces a DNA Damage Response That Is Dispensable for Cell Cycle Arrest at Phase G2/M. *Journal of Virology* 86: 10748.

Lou Z., Minter-Dykhouse K., Franco S., Gostissa M., Rivera M.A., Celeste A., Manis J.P., Deursen J. van, Nussenzweig A., Paull T.T., Alt F.W. & Chen J. 2006. MDC1 maintains genomic stability by participating in the amplification of ATM-dependent DNA damage signals. *Molecular cell* 21: 187–200.

Luger K., Mäder A.W., Richmond R.K., Sargent D.F. & Richmond T.J. 1997. Crystal structure of the nucleosome core particle at 2.8 A resolution. *Nature* 389: 251–260.

Lund E., Oldenburg A.R., Delbarre E., Freberg C.T., Duband-Goulet I., Eskeland R., Buendia B. & Collas P. Lamin A/C-promoter interactions specify chromatin state-dependent transcription outcomes.

Luo Y., Chen A.Y. & Qiu J. 2011a. Bocavirus Infection Induces a DNA Damage Response That Facilitates Viral DNA Replication and Mediates Cell Death. *Journal of Virology* 85: 133–145.

Luo Y., Lou S., Deng X., Liu Z., Li Y., Kleiboeker S. & Qiu J. 2011b. Parvovirus B19 Infection of Human Primary Erythroid Progenitor Cells Triggers ATR-Chk1 Signaling, Which Promotes B19 Virus Replication. *Journal of Virology* 85: 8046–8055.

Lymberopoulos M.H. & Pearson A. 2007. Involvement of UL24 in herpes-simplex-virus-1-induced dispersal of nucleolin. *Virology* 363: 397–409.

Maeshima K., Yahata K., Sasaki Y., Nakatomi R., Tachibana T., Hashikawa T., Imamoto F. & Imamoto N. 2006. Cell-cycle-dependent dynamics of nuclear pores: pore-free islands and lamins. *Journal of cell science* 119: 4442–4451.

Majumder K., Etingov I. & Pintel D.J. 2017. Protoparvovirus interactions with the cellular DNA damage response. *Viruses* 9.

Majumder K., Wang J., Boftsi M., Fuller M.S., Rede J.E., Joshi T. & Pintel D.J. 2018. Parvovirus minute virus of mice interacts with sites of cellular DNA damage to establish and amplify its lytic infection. *eLife* 7: 1–30.

Malumbres M. 2014. Cyclin-dependent kinases.

Mäntylä E., Aho V., Kann M. & Vihinen-Ranta M. 2020. Cytoplasmic Parvovirus Capsids Recruit Importin Beta for Nuclear Delivery. *Journal of virology* 94.

Mäntylä E., Niskanen E.A., Ihalainen T.O. & Vihinen-Ranta M. 2015. Reorganization of Nuclear Pore Complexes and the Lamina in Late-Stage Parvovirus Infection. *Journal of Virology* 89: 11706–11710.

Mäntylä E., Salokas K., Oittinen M., Aho V., Mäntysaari P., Palmujoki L., Kalliolinna O., Ihalainen T.O., Niskanen E.A., Timonen J., Viiri K. & Vihinen-Ranta M. 2016. Promoter-Targeted Histone Acetylation of Chromatinized Parvoviral Genome Is Essential for the Progress of Infection. *Journal of Virology* 90: 4059–4066.

Mao Y.S., Zhang B. & Spector D.L. 2011. Biogenesis and function of nuclear bodies. *Trends in genetics : TIG* 27: 295–306.

Marchini A., Bonifati S., Scott E.M., Angelova A.L. & Rommelaere J. 2015. Oncolytic parvoviruses: From basic virology to clinical applications. *Virology Journal* 12: 1–16.

Markaki Y., Gunkel M., Schermelleh L., Beichmanis S., Neumann J., Heidemann M., Leonhardt H., Eick D., Cremer C. & Cremer T. 2010. Functional nuclear organization of transcription and DNA replication: a topographical marriage between chromatin domains and the interchromatin compartment. *Cold Spring Harbor symposia on quantitative biology* 75: 475–492.

Maroto B., Valle N., Saffrich R. & Almendral J.M. 2004. Nuclear Export of the Nonenveloped Parvovirus Virion Is Directed by an Unordered Protein Signal Exposed on the Capsid Surface. *Journal of Virology* 78: 10685–10694.

Masui Y. & Markert C.L. 1971. Cytoplasmic control of nuclear behavior during meiotic maturation of frog oocytes. *The Journal of experimental zoology* 177: 129–145.

Matthews D.A. 2001. Adenovirus protein V induces redistribution of nucleolin and B23 from nucleolus to cytoplasm. *Journal of virology* 75: 1031–1038.

Mattola S., Hakanen S., Salminen S., Aho V., Mäntylä E., Ihalainen T.O., Kann M. & Vihinen-Ranta M. 2021. Concepts to reveal parvovirus–nucleus interactions. *Viruses* 13: 1–16.

Mattola S., Salokas K., Aho V., Mäntylä E., Salminen S., Hakanen S., Niskanen E.A., Svirskaite J., Ihalainen T.O., Airenne K.J., Kaikkonen-Määttä M., Parrish C.R., Varjosalo M. & Vihinen-Ranta M. 2022.

Parvovirus nonstructural protein 2 interacts with chromatin-regulating cellular proteins. *PLoS Pathogens* in print.
Maurer A.C., Pacouret S., Cepeda Diaz A.K., Blake J., Andres-Mateos E. & Vandenberghe L.H. 2018. The Assembly-Activating Protein Promotes Stability and Interactions between AAV's Viral Proteins to Nucleate Capsid Assembly. *Cell reports* 23: 1817–1830.
McKenna R., Olson N.H., Chipman P.R., Baker T.S., Booth T.F., Christensen J., Aasted B., Fox J.M., Bloom M.E., Wolfinbarger J.B. & Agbandje-McKenna M. 1999. Three-dimensional structure of Aleutian mink disease parvovirus: implications for disease pathogenicity. *Journal of virology* 73: 6882–6891.
McKeown P.C. & Shaw P.J. 2009. Chromatin: linking structure and function in the nucleolus. *Chromosoma* 118: 11–23.
McStay B. 2016. Nucleolar organizer regions: genomic "dark matter" requiring illumination. *Genes & development* 30: 1598–1610.
Miao B., Chen S., Zhang X., Ma P., Ma M., Chen C., Zhang X., Chang L., Du Q., Huang Y. & Tong D. 2022. T598 and T601 phosphorylation sites of canine parvovirus NS1 are crucial for viral replication and pathogenicity. *Veterinary microbiology* 264.
Millán-Zambrano G., Burton A., … A.B.-N.R. & 2022 undefined. Histone post-translational modifications—cause and consequence of genome function. *nature.com*.
Miller C.L. & Pintel D.J. 2002. Interaction between Parvovirus NS2 Protein and Nuclear Export Factor Crm1 Is Important for Viral Egress from the Nucleus of Murine Cells. *Journal of Virology* 76: 3257–3266.
Mincberg M., Gopas J. & Tal J. 2011. Minute virus of mice (MVMp) infection and NS1 expression induce p53 independent apoptosis in transformed rat fibroblast cells. *Virology* 412: 233–243.
Misteli T. 2000. Cell biology of transcription and pre-mRNA splicing: Nuclear architecture meets nuclear function. *Journal of Cell Science* 113: 1841–1849.
Miyazaki T. & Arai S. 2007. Two distinct controls of mitotic cdk1/cyclin B1 activity requisite for cell growth prior to cell division. *Cell cycle (Georgetown, Tex.)* 6: 1419–1425.
Moehler M., Blechacz B., Weiskopf N., Zeidler M., Stremmel W., Rommelaere J., Galle P.R. & Cornelis J.J. 2001. Effective infection, apoptotic cell killing and gene transfer of human hepatoma cells but not primary hepatocytes by parvovirus H1 and derived vectors. *Cancer Gene Therapy* 8: 158–167.
Moehler M., Zeidler M., Schede J., Rommelaere J., Galle P.R., Cornelis J.J. & Heike M. 2003. Oncolytic parvovirus H1 induces release of heat-shock protein HSP72 in susceptible human tumor cells but may not affect primary immune cells. *Cancer gene therapy* 10: 477–480.
Moffatt S., Yaegashi N., Tada K., Tanaka N. & Sugamura K. 1998. Human Parvovirus B19 Nonstructural (NS1) Protein Induces Apoptosis in Erythroid Lineage Cells. *Journal of Virology* 72: 3018–3028.

Morita E., Nakashima A., Asao H., Sato H. & Sugamura K. 2003. Human Parvovirus B19 Nonstructural Protein (NS1) Induces Cell Cycle Arrest at G 1 Phase . *Journal of Virology* 77: 2915–2921.

Myllys M., Ruokolainen V., Aho V., Smith E.A., Hakanen S., Peri P., Salvetti A., Timonen J., Hukkanen V., Larabell C.A. & Vihinen-Ranta M. 2016. Herpes simplex virus 1 induces egress channels through marginalized host chromatin. *Scientific Reports* 6: 1–9.

Naeger L.K., Cater J. & Pintel D.J. 1990. The small nonstructural protein (NS2) of the parvovirus minute virus of mice is required for efficient DNA replication and infectious virus production in a cell-type-specific manner. *Journal of virology* 64: 6166–6175.

Naeger L.K., Salomé N. & Pintel D.J. 1993. NS2 is required for efficient translation of viral mRNA in minute virus of mice-infected murine cells. *Journal of Virology* 67: 1034–1043.

Németh A., Strohner R., Grummt I. & Längst G. 2004. The chromatin remodeling complex NoRC and TTF-I cooperate in the regulation of the mammalian rRNA genes in vivo. *Nucleic acids research* 32: 4091–4099.

Nikolakaki E., Mylonis I. & Giannakouros T. 2017. Lamin B Receptor: Interplay between Structure, Function and Localization. *Cells* 6.

Nirmala J.G. & Lopus M. 2020. Cell death mechanisms in eukaryotes. *Cell Biology and Toxicology* 36: 145–164.

Niskanen E.A., Ihalainen T.O., Kalliolinna O., Häkkinen M.M. & Vihinen-Ranta M. 2010. Effect of ATP Binding and Hydrolysis on Dynamics of Canine Parvovirus NS1. *Journal of Virology* 84: 5391.

Niskanen E.A., Kalliolinna O., Ihalainen T.O., Häkkinen M. & Vihinen-Ranta M. 2013. Mutations in DNA Binding and Transactivation Domains Affect the Dynamics of Parvovirus NS1 Protein. *Journal of Virology* 87: 11762–11774.

Norbury C.J. & Zhivotovsky B. 2004. DNA damage-induced apoptosis. *Oncogene* 23: 2797–2808.

Nüesch J.P.F., Cotmore S.F. & Tattersall P. 1995. Sequence motifs in the replicator protein of parvovirus MVM essential for nicking and covalent attachment to the viral origin: identification of the linking tyrosine. *Virology* 209: 122–135.

Nüesch J.P.F. & Rommelaere J. 2006. NS1 interaction with CKII alpha: novel protein complex mediating parvovirus-induced cytotoxicity. *Journal of virology* 80: 4729–4739.

Nykky J., Tuusa J.E., Kirjavainen S., Vuento M. & Gilbert L. 2010. Mechanisms of cell death in canine parvovirus-infected cells provide intuitive insights to developing nanotools for medicine. *International Journal of Nanomedicine* 5: 417–428.

Ogden P.J., Kelsic E.D., Sinai S. & Church G.M. 2019. Comprehensive AAV capsid fitness landscape reveals a viral gene and enables machine-guided design. *Science (New York, N.Y.)* 366: 1139–1143.

Ohno M., Fornerod M. & Mattaj I.W. 1998. Nucleocytoplasmic transport: The last 200 nanometers. *Cell* 92: 327–336.

Ohshima T., Nakajima T., Oishi T., Imamoto N., Yoneda Y., Fukamizu A. & Yagami K.I. 1999. CRM1 mediates nuclear export of nonstructural protein 2 from parvovirus minute virus of mice. *Biochemical and biophysical research communications* 264: 144–150.

O'Keefe R.T., Henderson S.C. & Spector D.L. 1992. Dynamic organization of DNA replication in mammalian cell nuclei: spatially and temporally defined replication of chromosome-specific alpha-satellite DNA sequences. *The Journal of cell biology* 116: 1095–1110.

Orphanides G., LeRoy G., Chang C.H., Luse D.S. & Reinberg D. 1998. FACT, a factor that facilitates transcript elongation through nucleosomes. *Cell* 92: 105–116.

Osborne C.S., Chakalova L., Brown K.E., Carter D., Horton A., Debrand E., Goyenechea B., Mitchell J.A., Lopes S., Reik W. & Fraser P. 2004. Active genes dynamically colocalize to shared sites of ongoing transcription. *Nature genetics* 36: 1065–1071.

Panté N. & Kann M. 2002. Nuclear pore complex is able to transport macromolecules with diameters of ~39 nm. *Molecular Biology of the Cell* 13: 425–434.

Park Y.Y., Ahn J.H., Cho M.G. & Lee J.H. 2018. ATP depletion during mitotic arrest induces mitotic slippage and APC/CCdh1-dependent cyclin B1 degradation. *Experimental & Molecular Medicine* 50.

Parker J.S.L., Murphy W.J., Wang D., O'Brien S.J. & Parrish C.R. 2001. Canine and Feline Parvoviruses Can Use Human or Feline Transferrin Receptors To Bind, Enter, and Infect Cells. *Journal of Virology* 75: 3896–3902.

Patel B.N., Rosenberg L., Willcox G., Baltaxe D., Lyons M., Irvin J., Rajpurkar P., Amrhein T., Gupta R., Halabi S., Langlotz C., Lo E., Mammarappallil J., Mariano A.J., Riley G., Seekins J., Shen L., Zucker E. & Lungren M. 2019. Human–machine partnership with artificial intelligence for chest radiograph diagnosis. *npj Digital Medicine* 2.

Pavesi A. 2021. Origin, Evolution and Stability of Overlapping Genes in Viruses: A Systematic Review. *Genes* 12.

Pavin N. & Tolić I.M. 2021. Mechanobiology of the Mitotic Spindle. *Developmental cell* 56: 192–201.

Peña C., Hurt E. & Panse V.G. 2017. Eukaryotic ribosome assembly, transport and quality control. *Nature structural & molecular biology* 24: 689–699.

Pénzes J.J., Söderlund-Venermo M., Canuti M., Eis-Hübinger A.M., Hughes J., Cotmore S.F. & Harrach B. 2020. Reorganizing the family Parvoviridae: a revised taxonomy independent of the canonical approach based on host association. *Archives of virology* 165: 2133–2146.

Percipalle P., Fomproix N., Cavellán E., Voit R., Reimer G., Krüger T., Thyberg J., Scheer U., Grummt I. & Östlund Farrants A.K. 2006. The

chromatin remodelling complex WSTF-SNF2h interacts with nuclear myosin 1 and has a role in RNA polymerase I transcription. *EMBO reports* 7: 525–530.

Pessina F. & Lowndes N.F. 2014. The RSF1 Histone-Remodelling Factor Facilitates DNA Double-Strand Break Repair by Recruiting Centromeric and Fanconi Anaemia Proteins. *PLoS Biol* 12: 1001856.

Poole B.D., Karetnyi Y. v. & Naides S.J. 2004. Parvovirus B19-Induced Apoptosis of Hepatocytes. *Journal of Virology* 78: 7775–7783.

Pope B.D., Ryba T., Dileep V., Yue F., Wu W., Denas O., Vera D.L., Wang Y., Hansen R.S., Canfield T.K., Thurman R.E., Cheng Y., Gülsoy G., Dennis J.H., Snyder M.P., Stamatoyannopoulos J.A., Taylor J., Hardison R.C., Kahveci T., Ren B. & Gilbert D.M. 2014. Topologically associating domains are stable units of replication-timing regulation. *Nature* 515: 402–405.

Porter L.A., Cukier I.H. & Lee J.M. 2003. Nuclear localization of cyclin B1 regulates DNA damage-induced apoptosis. *Blood* 101: 1928–1933.

Porter L.A. & Donoghue D.J. 2003. Cyclin B1 and CDK1: nuclear localization and upstream regulators. *Progress in cell cycle research* 5: 335–347.

Qin W., Stengl A., Ugur E., Leidescher S., Ryan J., Cardoso M.C. & Leonhardt H. 2021. HP1β carries an acidic linker domain and requires H3K9me3 for phase separation. *Nucleus (Austin, Tex.)* 12: 44–57.

Qiu J. & Brown K.E. 1999. A 110-kDa nuclear shuttle protein, nucleolin, specifically binds to adeno-associated virus type 2 (AAV-2) capsid. *Virology* 257: 373–382.

Ran Z.H., Rayet B., Rommelaere J. & Faisst S. 1999. Parvovirus H-1-induced cell death: Influence of intracellular NAD consumption on the regulation of necrosis and apoptosis. *Virus Research* 65: 161–174.

Rao S.S.P., Huntley M.H., Durand N.C., Stamenova E.K., Bochkov I.D., Robinson J.T., Sanborn A.L., Machol I., Omer A.D., Lander E.S. & Aiden E.L. 2014. A 3D map of the human genome at kilobase resolution reveals principles of chromatin looping. *Cell* 159: 1665–1680.

Rao L., Perez D. & White E. 1996. Lamin proteolysis facilitates nuclear events during apoptosis. *The Journal of cell biology* 135: 1441–1455.

Rasim Barutcu A., Lian J.B., Stein J.L., Stein G.S. & Imbalzano A.N. 2017. The connection between BRG1, CTCF and topoisomerases at TAD boundaries. *Nucleus* 8: 150.

Raška I., Shaw P.J. & Cmarko D. 2006. Structure and function of the nucleolus in the spotlight. *Current opinion in cell biology* 18: 325–334.

Rayet B., Lopez-Guerrero J.-A., Rommelaere J. & Dinsart C. 1998. Induction of Programmed Cell Death by Parvovirus H-1 in U937 Cells: Connection with the Tumor Necrosis Factor Alpha Signalling Pathway. *Journal of Virology* 72: 8893–8903.

Reed A.P., Jones E. v & Miller T.J. 1988. Nucleotide sequence and genome organization of canine parvovirus. *Journal of virology* 62: 266–276.

Reinberg D. & Sims R.J. 2006. de FACTo nucleosome dynamics. *The Journal of biological chemistry* 281: 23297–23301.

Rhind N. & Russell P. 2012. Signaling pathways that regulate cell division. *Cold Spring Harbor Perspectives in Biology* 4: 1–15.

Riolobos L., Reguera J., Mateu M.G. & Almendral J.M. 2006. Nuclear transport of trimeric assembly intermediates exerts a morphogenetic control on the icosahedral parvovirus capsid. *Journal of molecular biology* 357: 1026–1038.

Ros C., Bayat N., Wolfisberg R. & Almendral J.M. 2017. Protoparvovirus Cell Entry. *Viruses* 9.

Ruiz Z., Mihaylov I.S., Cotmore S.F. & Tattersall P. 2011. Recruitment of DNA replication and damage response proteins to viral replication centers during infection with NS2 mutants of Minute Virus of Mice (MVM). *Virology* 410: 375–384.

Salvetti A. & Greco A. 2014. Viruses and the nucleolus: the fatal attraction. *Biochimica et biophysica acta* 1842: 840–847.

Samejima K. & Earnshaw W.C. 2005. Trashing the genome: The role of nucleases during apoptosis. *Nature Reviews Molecular Cell Biology* 6: 677–688.

Santoro R., Li J. & Grummt I. 2002. The nucleolar remodeling complex NoRC mediates heterochromatin formation and silencing of ribosomal gene transcription. *Nature Genetics* 32: 393–396.

Saraste A. & Pulkki K. 2000. Morphologic and biochemical hallmarks of apoptosis. *Cardiovascular research* 45: 528–537.

Saxena L., Kumar G.R., Saxena S., Chaturvedi U., Sahoo A.P., Singh L.V., Santra L., Palia S.K., Desai G.S. & Tiwari A.K. 2013. Apoptosis induced by NS1 gene of Canine Parvovirus-2 is caspase dependent and p53 independent. *Virus Research* 173: 426–430.

Schmidt M.H.H., Broll R., Bruch H.P., Bögler O. & Duchrow M. 2003. The proliferation marker pKi-67 organizes the nucleolus during the cell cycle depending on Ran and cyclin B. *The Journal of pathology* 199: 18–27.

Schwartz R.A., Carson C.T., Schuberth C. & Weitzman M.D. 2009. Adeno-Associated Virus Replication Induces a DNA Damage Response Coordinated by DNA-Dependent Protein Kinase. *Journal of Virology* 83: 6269–6278.

Shackelton L.A., Parrish C.R., Truyen U. & Holmes E.C. 2005. High rate of viral evolution associated with the emergence of carnivore parvovirus. *Proceedings of the National Academy of Sciences of the United States of America* 102: 379–384.

Shen Y. & Shenk T.E. 1995. Viruses and apoptosis. *Current Opinion in Genetics and Development* 5: 105–111.

Shiotani B. & Zou L. 2011. A human cell extract-based assay for the activation of ATM and ATR checkpoint kinases. *Methods in Molecular Biology* 782: 181–191.

Skibbens R. v. 2019. Condensins and cohesins – one of these things is not like the other! *Journal of Cell Science* 132.

Smith-Moore S., Neil S.J.D., Fraefel C., Michael Linden R., Bollen M., Rowe H.M. & Henckaerts E. 2018. Adeno-associated virus Rep proteins antagonize phosphatase PP1 to counteract KAP1 repression of the latent viral genome. *Proceedings of the National Academy of Sciences of the United States of America* 115: E3529–E3538.

Söderberg O., Gullberg M., Jarvius M., Ridderstråle K., Leuchowius K.J., Jarvius J., Wester K., Hydbring P., Bahram F., Larsson L.G. & Landegren U. 2006. Direct observation of individual endogenous protein complexes in situ by proximity ligation. *Nature methods* 3: 995–1000.

Stenström L., Mahdessian D., Gnann C., Cesnik A.J., Ouyang W., Leonetti M.D., Uhlén M., Cuylen-Haering S., Thul P.J. & Lundberg E. 2020. Mapping the nucleolar proteome reveals a spatiotemporal organization related to intrinsic protein disorder. *Molecular Systems Biology* 16: 1–16.

Stewart C.L., Roux K.J. & Burke B. 2007. Blurring the boundary: the nuclear envelope extends its reach. *Science (New York, N.Y.)* 318: 1408–1412.

Strohner R., Nemeth A., Jansa P., Hofmann-rohrer U., Santoro R., La G. & Grummt I. 2001. NoRC - a novel member of mammalian ISWI-containing chromatin remodeling machines, Strohner *et al*, 2001. 20.

Strohner R., Németh A., Nightingale K.P., Grummt I., Becker P.B. & Längst G. 2004. Recruitment of the Nucleolar Remodeling Complex NoRC Establishes Ribosomal DNA Silencing in Chromatin. *Molecular and Cellular Biology* 24: 1791–1798.

Strom A.R., Emelyanov A. v., Mir M., Fyodorov D. v., Darzacq X. & Karpen G.H. 2017. Phase separation drives heterochromatin domain formation. *Nature* 547: 241–245.

Suikkanen S., Aaltonen T., Nevalainen M., Välilehto O., Lindholm L., Vuento M. & Vihinen-Ranta M. 2003a. Exploitation of microtubule cytoskeleton and dynein during parvoviral traffic toward the nucleus. *Journal of virology* 77: 10270–10279.

Suikkanen S., Antila M., Jaatinen A., Vihinen-Ranta M. & Vuento M. 2003b. Release of canine parvovirus from endocytic vesicles. *Virology* 316: 267–280.

Suikkanen S., Sääjärvi K., Hirsimäki J., Välilehto O., Reunanen H., Vihinen-Ranta M. & Vuento M. 2002. Role of Recycling Endosomes and Lysosomes in Dynein-Dependent Entry of Canine Parvovirus. *Journal of Virology* 76: 4401–4411.

Suntharalingam M. & Wente S.R. 2003. Peering through the pore: Nuclear pore complex structure, assembly, and function. *Developmental Cell* 4: 775–789.

Tattersall P., Shatkin A.J. & Ward D.C. 1977. Sequence homology between the structural polypeptides of minute virus of mice. *Journal of molecular biology* 111: 375–394.

Taylor T.J. & Knipe D.M. 2004. Proteomics of herpes simplex virus replication compartments: association of cellular DNA replication, repair, recombination, and chromatin remodeling proteins with ICP8. *Journal of virology* 78: 5856–5866.

Terry L.J., Shows E.B. & Wente S.R. 2007. Crossing the nuclear envelope: hierarchical regulation of nucleocytoplasmic transport. *Science (New York, N.Y.)* 318: 1412–1416.

Trigg B.J. & Ferguson B.J. 2015. Functions of DNA damage machinery in the innate immune response to DNA virus infection. *Current opinion in virology* 15: 56–62.

Truyen U., Parrish C.R., Harder T.C. & Kaaden O.R. 1995. There is nothing permanent except change. The emergence of new virus diseases. *Veterinary microbiology* 43: 103–122.

Tsao J., Chapman M.S., Agbandje M., Keller W., Smith K., Wu H., Luo M., Smith T.J., Rossmann M.G., Compans R.W. & Parrish C.R. 1991. The three-dimensional structure of canine parvovirus and its functional implications. *Science (New York, N.Y.)* 251: 1456–1464.

Tullis G., Schoborg R. v. & Pintel D.J. 1994. Characterization of the temporal accumulation of minute virus of mice replicative intermediates. *The Journal of general virology* 75 (Pt 7): 1633–1646.

Ulianov S. v., Doronin S.A., Khrameeva E.E., Kos P.I., Luzhin A. v., Starikov S.S., Galitsyna A.A., Nenasheva V. v., Ilyin A.A., Flyamer I.M., Mikhaleva E.A., Logacheva M.D., Gelfand M.S., Chertovich A. v., Gavrilov A.A., Razin S. v. & Shevelyov Y.Y. 2019. Nuclear lamina integrity is required for proper spatial organization of chromatin in Drosophila. *Nature communications* 10.

Väisänen E., Fu Y., Hedman K. & Söderlund-Venermo M. 2017. Human Protoparvoviruses. *Viruses* 9.

Vihinen-Ranta M., Wang D., Weichert W.S. & Parrish C.R. 2002. The VP1 N-terminal sequence of canine parvovirus affects nuclear transport of capsids and efficient cell infection. *Journal of virology* 76: 1884–1891.

Vihinen-Ranta M., Yuan W. & Parrish C.R. 2000. Cytoplasmic trafficking of the canine parvovirus capsid and its role in infection and nuclear transport. *Journal of virology* 74: 4853–4859.

Visser A.E., Jaunin F., Fakan S. & Aten J.A. 2000. High resolution analysis of interphase chromosome domains. *Journal of cell science* 113 (Pt 14): 2585–2593.

Waggoner S. & Sarnow P. 1998. Viral ribonucleoprotein complex formation and nucleolar-cytoplasmic relocalization of nucleolin in poliovirus-infected cells. *Journal of virology* 72: 6699–6709.

Wang G., Jiang Q. & Zhang C. 2014. The role of mitotic kinases in coupling the centrosome cycle with the assembly of the mitotic spindle. *Journal of Cell Science* 127: 4111–4122.

Wang D., Yuan W., Davis I. & Parrish C.R. 1998. Nonstructural protein-2 and the replication of canine parvovirus. *Virology* 240: 273–281.

Wang Z., Zang C., Rosenfeld J.A., Schones D.E., Barski A., Cuddapah S., Cui K., Roh T.-Y., Peng W., Zhang M.Q. & Zhao K. 2008. Combinatorial patterns of histone acetylations and methylations in the human genome. *Nature genetics* 40: 897–903.

Wente S.R. & Rout M.P. 2010. The nuclear pore complex and nuclear transport. *Cold Spring Harbor perspectives in biology* 2.

Wilde A. & Zheng Y. 2009. *Ran out of the nucleus for apoptosis*.

Wistuba A., Kern A., Weger S., Grimm D. & Kleinschmidt J.A. 1997. Subcellular compartmentalization of adeno-associated virus type 2 assembly. *Journal of virology* 71: 1341–1352.

Wolfisberg R., Kempf C. & Ros C. 2016. Late Maturation Steps Preceding Selective Nuclear Export and Egress of Progeny Parvovirus. *Journal of Virology* 90: 5462–5474.

Wolter S., Richards R. & Armentrout R.W. 1980. Cell cycle-dependent replication of the DNA of minute virus of mice, a parvovirus. *Biochimica et Biophysica Acta (BBA) - Nucleic Acids and Protein Synthesis* 607: 420–431.

Xie Q. & Chapman M.S. 1996. Canine parvovirus capsid structure, analyzed at 2.9 A resolution. *Journal of molecular biology* 264: 497–520.

Yang J., Song H., Walsh S., Bardes E.S.G. & Kornbluth S. 2001. Combinatorial Control of Cyclin B1 Nuclear Trafficking through Phosphorylation at Multiple Sites. *Journal of Biological Chemistry* 276: 3604–3609.

Yao R.W., Xu G., Wang Y., Shan L., Luan P.F., Wang Y., Wu M., Yang L.Z., Xing Y.H., Yang L. & Chen L.L. 2019. Nascent Pre-rRNA Sorting via Phase Separation Drives the Assembly of Dense Fibrillar Components in the Human Nucleolus. *Molecular Cell* 76: 767-783.e11.

Young P.J., Jensen K.T., Burger L.R., Pintel D.J. & Lorson C.L. 2002. Minute virus of mice small nonstructural protein NS2 interacts and colocalizes with the Smn protein. *Journal of virology* 76: 6364–6369.

Yuan S. & Akey C.W. 2013. Apoptosome structure, assembly, and procaspase activation. *Structure (London, England : 1993)* 21: 501–515.

Zádori Z., Szelei J., Lacoste M.C., Li Y., Gariépy S., Raymond P., Allaire M., Nabi I.R. & Tijssen P. 2001. A viral phospholipase A2 is required for parvovirus infectivity. *Developmental cell* 1: 291–302.

ORIGINAL PAPERS

I

PARVOVIRUS NONSTRUCTURAL PROTEIN 2 INTERACTS WITH CHROMATIN-REGULATING CELLULAR PROTEINS

by

Salla Mattola*, Kari Salokas*, Vesa Aho, Elina Mäntylä, Sami Salminen, Satu Hakanen, Einari A. Niskanen, Julija Svirskaite, Teemu O Ihalainen, Kari Airenne, Minna Kaikkonen-Määttä, Coli R Parrish, Markku Varjosalo & Maija Vihinen-Ranta 2022

PLoS Pathogens 2022 Apr 8;18(4):e1010353.

PLOS PATHOGENS

RESEARCH ARTICLE

Parvovirus nonstructural protein 2 interacts with chromatin-regulating cellular proteins

Salla Mattola[1☯], Kari Salokas[2☯], Vesa Aho[1], Elina Mäntylä[3], Sami Salminen[1], Satu Hakanen[1], Einari A. Niskanen[4], Julija Svirskaite[2], Teemu O. Ihalainen[3], Kari J. Airenne[5], Minna Kaikkonen-Määttä[4], Colin R. Parrish[6], Markku Varjosalo[2], Maija Vihinen-Ranta[1]*

1 Department of Biological and Environmental Science and Nanoscience Center, University of Jyvaskyla, Jyvaskyla, Finland, **2** Institute of Biotechnology and Helsinki Institute of Life Science (HiLIFE), University of Helsinki, Helsinki, Finland, **3** BioMediTech, Faculty of Medicine and Health Technology, Tampere University, Tampere, Finland, **4** Institute of Biomedicine, University of Eastern Finland, Kuopio, Finland, **5** Kuopio Center for Gene and Cell Therapy (KCT), Kuopio, Finland, **6** Baker Institute for Animal Health, Department of Microbiology and Immunology, College of Veterinary Medicine, University of Cornell, Ithaca, New York, United States of America

☯ These authors contributed equally to this work.
* maija.vihinen-ranta@jyu.fi

OPEN ACCESS

Citation: Mattola S, Salokas K, Aho V, Mäntylä E, Salminen S, Hakanen S, et al. (2022) Parvovirus nonstructural protein 2 interacts with chromatin-regulating cellular proteins. PLoS Pathog 18(4): e1010353. https://doi.org/10.1371/journal.ppat.1010353

Editor: Matthew D. Weitzman, The Children's Hospital of Philadelphia, UNITED STATES

Received: September 7, 2021

Accepted: March 15, 2022

Published: April 8, 2022

Peer Review History: PLOS recognizes the benefits of transparency in the peer review process; therefore, we enable the publication of all of the content of peer review and author responses alongside final, published articles. The editorial history of this article is available here: https://doi.org/10.1371/journal.ppat.1010353

Data Availability Statement: All relevant data are included in the manuscript and its Supporting information files.

Abstract

Autonomous parvoviruses encode at least two nonstructural proteins, NS1 and NS2. While NS1 is linked to important nuclear processes required for viral replication, much less is known about the role of NS2. Specifically, the function of canine parvovirus (CPV) NS2 has remained undefined. Here we have used proximity-dependent biotin identification (BioID) to screen for nuclear proteins that associate with CPV NS2. Many of these associations were seen both in noninfected and infected cells, however, the major type of interacting proteins shifted from nuclear envelope proteins to chromatin-associated proteins in infected cells. BioID interactions revealed a potential role for NS2 in DNA remodeling and damage response. Studies of mutant viral genomes with truncated forms of the NS2 protein suggested a change in host chromatin accessibility. Moreover, further studies with NS2 mutants indicated that NS2 performs functions that affect the quantity and distribution of proteins linked to DNA damage response. Notably, mutation in the splice donor site of the NS2 led to a preferred formation of small viral replication center foci instead of the large coalescent centers seen in wild-type infection. Collectively, our results provide insights into potential roles of CPV NS2 in controlling chromatin remodeling and DNA damage response during parvoviral replication.

Author summary

Parvoviruses are small, nonenveloped DNA viruses, that besides being noteworthy pathogens in many animal species, including humans, are also being developed as vectors for gene and cancer therapy. Canine parvovirus is an autonomously replicating parvovirus that encodes two nonstructural proteins, NS1 and NS2. NS1 is required for viral DNA

Funding: This work was financed by the Jane and Aatos Erkko Foundation (MVR); Academy of Finland under the award number 330896 (MVR); Biocenter Finland, viral gene transfer (MVR), and the Graduate School of the University of Jyvaskyla (SM). The funders had no role in study design, data collection and analysis, decision to publish, or preparation of the manuscript.

Competing interests: The authors have declared that no competing interests exist.

replication and packaging, as well as gene expression. However, very little is known about the function of NS2. Our studies indicate that NS2 serves a previously undefined important function in chromatin modification and DNA damage responses. Therefore, it appears that although both NS1 and NS2 are needed for a productive infection they play very different roles in the process.

Introduction

Autonomous parvoviruses are small single-stranded DNA viruses that depend on host cell nuclear machinery for their replication. The nuclear events of parvovirus infection include genome replication, viral assembly, and genome packaging, which require the nuclear import of structural and nonstructural viral proteins. The nonstructural protein 1 (NS1) of canine parvovirus (CPV) is a multifunctional protein with site-specific DNA binding, ATPase, nickase, and helicase activities [1,2], and its expression induces apoptosis in host cells [3,4]. NS1 is essential for initiation and direction of viral DNA replication. However, the role of the nonstructural protein 2 (NS2) in viral replication has so far remained undefined.

Autonomous parvoviruses have an ~5-kb single-stranded DNA genome encoding two viral structural proteins, VP1 and VP2, as well as two nonstructural proteins NS1 and NS2 [5]. The CPV NS2 protein is produced from the left-hand open reading frame of the viral genome and contains 87 amino-terminal amino acids that are in common with NS1 joined by mRNA splicing to 78 amino acids from an alternative open reading frame [6,7]. Previous knowledge on NS2 protein function in parvovirus replication is mainly derived from studies of minute virus of mice (MVM). MVM NS2 is required for efficient viral replication and capsid assembly [8,9]. In infected cells MVM NS2 is known to interact with two members of the 14-3-3 family of signaling proteins [10] and the survival motor neuron protein (Smn) [11]. Mutations in MVM NS2 splice acceptor or termination sites lead to severe replication defects in murine cells, whereas in other cells lines mutant viruses replicate more efficiently [12,13], suggesting that the requirement for MVM NS2 is cell-type specific. Moreover, MVM NS2 is required for the growth and development of viral replication centers [14]. Notably, MVM NS2 also interacts with the nuclear export factor CRM1 (also known as exportin1) [15,16]. CRM1 mediates the nuclear export of nuclear export signal containing proteins [17–19]. Although the detailed mechanisms of MVM capsid nuclear egress are still not well understood, the interaction between NS2 and CRM1 seems to be essential for the progeny virus capsid export [20–23]. Studies of another parvovirus closely related to CPV, feline panleucopenia virus (FPV), have shown that FPV NS2 plays a significant role in blocking pathways that promote IFN-β production, allowing the virus to evade the host antiviral innate immune response [24]. Much less is known about the role of CPV NS2 in infection. To our knowledge, the only study assessing CPV NS2 function used various NS2 mutants containing mutations and deletions that affect NS2 mRNA splicing and protein expression, or that terminate the NS2 open reading frame without altering NS1. The impact of the mutants on viral replication depended on the site of the mutation, and infection efficiency was found to be decreased with the NS2 donor mutant [6].

During the nuclear replication parvoviruses must either confront or embrace the chromatin remodeling machinery of the host cell. To ensure a productive infection, viruses have to recruit the cellular histone modifying and nucleosome remodeling machinery for the activation of the viral genome. Many viruses are able to counteract host-mediated silencing by recruiting and redirecting cellular histone remodeling proteins to enhance viral gene expression and

replication. In herpes simplex virus 1 (HSV-1) infection the viral genome is chromatinized after its nuclear entry [25]. In a productive HSV-1 infection the modification of bound histones to an active euchromatic state is promoted by viral proteins such as ICP0 and by recruiting cellular proteins [26,27]. For example, the chromatin remodeling factor SNF2H (SMARCA5) protein from ISWI family complexes facilitates the transcription of viral immediately-early genes from the HSV-1 genome by removing or remodeling histones associated with viral promoters [28]. Viruses have also developed strategies for regulating host transcription by inactivating certain aspects of chromatin modeling while exploiting others to advance the viral life cycle. Most likely, manipulation of host cellular functions can be orchestrated and tuned by viral proteins. Consistent with this model, the HSV-1 single-stranded DNA-binding protein ICP8 has been found associated with cellular proteins involved in DNA replication, DNA repair, chromatin remodeling and RNA processing [29,30]. Similar to other DNA viruses, parvovirus replication is potentially dependent on the activation state of nucleosomes present on the nuclear viral genome [31–34]. The molecular mechanisms by which parvoviral proteins are involved in the interaction and epigenetic modification of nucleosomes associated with viral genomes remain poorly understood.

The DNA damage response (DDR) machinery plays a significant role in cells by maintaining normal chromatin functions within regions of damage [35]. DDR is initiated by sensor protein-mediated detection of DNA lesions, which is followed by the activation of major signaling kinases, ataxia telangiectasia mutated (ATM), and ATM Rad3-related (ATR) and DNA-dependent protein kinase (DNA-PK). This promotes signal-transduction through a series of downstream effector molecules from phosphoinositide 3 kinase-like kinases and lead to the phosphorylation of the histone H2A variant, H2AX. DDR plays a dual role in the regulation of viral replication. DDR is also involved in the intrinsic antiviral mechanisms that counter the nuclear replication of DNA viruses [36–39]. Conversely, DDR is also activated by many DNA viruses, and DDR factors are recruited by viruses to promote viral replication [39–42]. Autonomous parvovirus infection results in the induction of cellular DNA breaks and DDR activation by ATR and ATM signaling pathways [43–46], and it is accompanied by pre-mitotic cell cycle arrest [14,43,47,48]. In MVM infection viral replication is located at cellular DNA damage sites [34,49].

In recent years proximity-dependent biotin identification (BioID) method has been increasingly used to provide fundamental insight into the protein-protein interactions of mammalian cells. These approaches have revealed valuable details about the interactions of nuclear structures such as the nuclear pore complex (NPC) [50,51] and nuclear lamina [52–56]. Moreover, BioID also has been used to screen for proteins in cell signaling pathways [57–59], tight junctions [60] and on chromatin [61]. Finally, protein interactions between viruses and their hosts contributing to the outcomes of viral infections have been studied by BioID. For example, interacting partners have been identified for the Gag protein of human immunodeficiency virus type 1 (HIV-1) [62–64], tegument protein UL103 of cytomegalovirus [65], latent membrane protein 1 of Epstein-Barr virus [66], and Zika virus-encoded proteins [67].

Here we used BioID approaches [50–53,55] combined with interactome-based mass spectrometry (MS) microscopy analysis [68] to investigate the nuclear interactions and nuclear localization of CPV NS2 both in noninfected and infected cells. The nuclear NS2 interactome identified by BioID included several components of different chromatin remodeling and DDR complexes. Furthermore, observations from assays with NS2 mutants suggested that N-terminal NS1/2-common splice donor mutant did not produce functional viral NS2 protein, resulting in inefficient chromatin remodeling regulation and DDR response. Altogether, our studies link CPV NS2 to novel functions in the nucleus and provide a platform for further functional analyses of NS2.

Results

Production of NS2 mRNA is temporally increased in infection and NS2 is localized into nucleoli

Since the expression of both CPV nonstructural proteins is controlled by the P4 promoter, we were interested in examining the expression levels of NS1 and NS2 mRNA at different times post infection. The quantitative reverse transcription PCR (RT-qPCR) using specific primers that distinguished the different transcripts showed that both NS1 and NS2 mRNAs were detectable at 4 hours post infection (hpi) in NLFK cells (Fig 1A). At 6 hpi, the levels of both mRNAs were higher compared to the control 18s rRNA levels, and both continued to increase until 24 hpi. The Student's t-test showed no statistically significant difference between the quantities of NS1 and NS2 mRNAs ($p>0.05$) at any time point. This data shows that NS2 is expressed early and throughout the viral replication. The early expression of NS2 is consistent with previous MVM findings [69], however, in contrast to MVM studies the expression level of CPV NS2 mRNA continued to increase during infection. MVM NS2 has a short half-life, which may account for the relatively small amount of nuclear NS2 detected in MVM infection [70].

To characterize potential NS2 functions during CPV replication, we next examined the association of NS2 with specific sites in the host cell nucleus. Confocal microscope images showed that NS2-EGFP expressed in noninfected HeLa cells was mostly localized near the rim of the nuclear periphery and in distinct nucleolar foci (Figs 1B and S1). A similar pattern of intranuclear localization was observed in CPV-infected cells, but the nucleolar distribution of NS2-EGFP was more diffuse than in noninfected cells. The BirA*-tagged NS2 used in BioID assays localized diffusely in noninfected cells. In infected cells, the BirA*-tagged NS2 distribution was mostly similar to noninfected cells, however, some local accumulation close to the nucleoli and viral replication center identified by NS1 was detected (Fig 1C). The nucleoli were identified by the exclusion of chromatin and NS1 labels. The homogenous nuclear distribution of the BirA*-tagged NS2 is consistent with NS2 distribution in infected NLFK cells identified by antibody against NS2 (S2 Fig). The BirA*-tagged NS2 was also localized in the cytoplasm both in noninfected and infected cells, however, the expression of the recombinant protein was decreased in infected cells. As a verification of nucleolar NS2 localization, we also found that in many wild type (wt) virus infected NLFK cells the antibody-stained NS2 colocalized with the nucleoli identified by nucleolin staining (Fig 1D). These results suggested that NS2 is often accumulated to nucleoli, where some of the essential chromatin remodeling and DDR factors reside [71–74].

BioID links NS2 to chromatin modeling

We used BioID to identify binding partners for CPV NS2. This technique is based on the fusion of a biotin protein ligase (BirA) to the protein of interest, which leads to the biotinylation of proximal proteins of the fusion protein. BioID allows to probe both the stable, transient and proximal interactions of NS2 [52,53]. Our BioID data analysis of BirA*-tagged NS2 identified a total of 122 unique high-confidence interactions in transfected Flp-In T-REx 293 cells (Bayesian false discovery rate, BFDR, cutoff of <0.01 or <0.05), consisting of 44 interactions seen only in noninfected cells, 17 seen only in infected cells (24 hpi), and 61 seen in both (Fig 2A and S1 Table). The NS2-associated proteins in noninfected cells may represent interactions of NS2 that are independent of infection. Gene Ontology (GO) annotation analyses of biological processes, (Fig 2B and S2 Table), indicated the biotinylated proteins associated with NS2 involved in important cellular functions such as chromatin organization (GO:0006325, 34 proteins) and DDR (GO:0006974, 14 proteins) in both noninfected and infected cells.

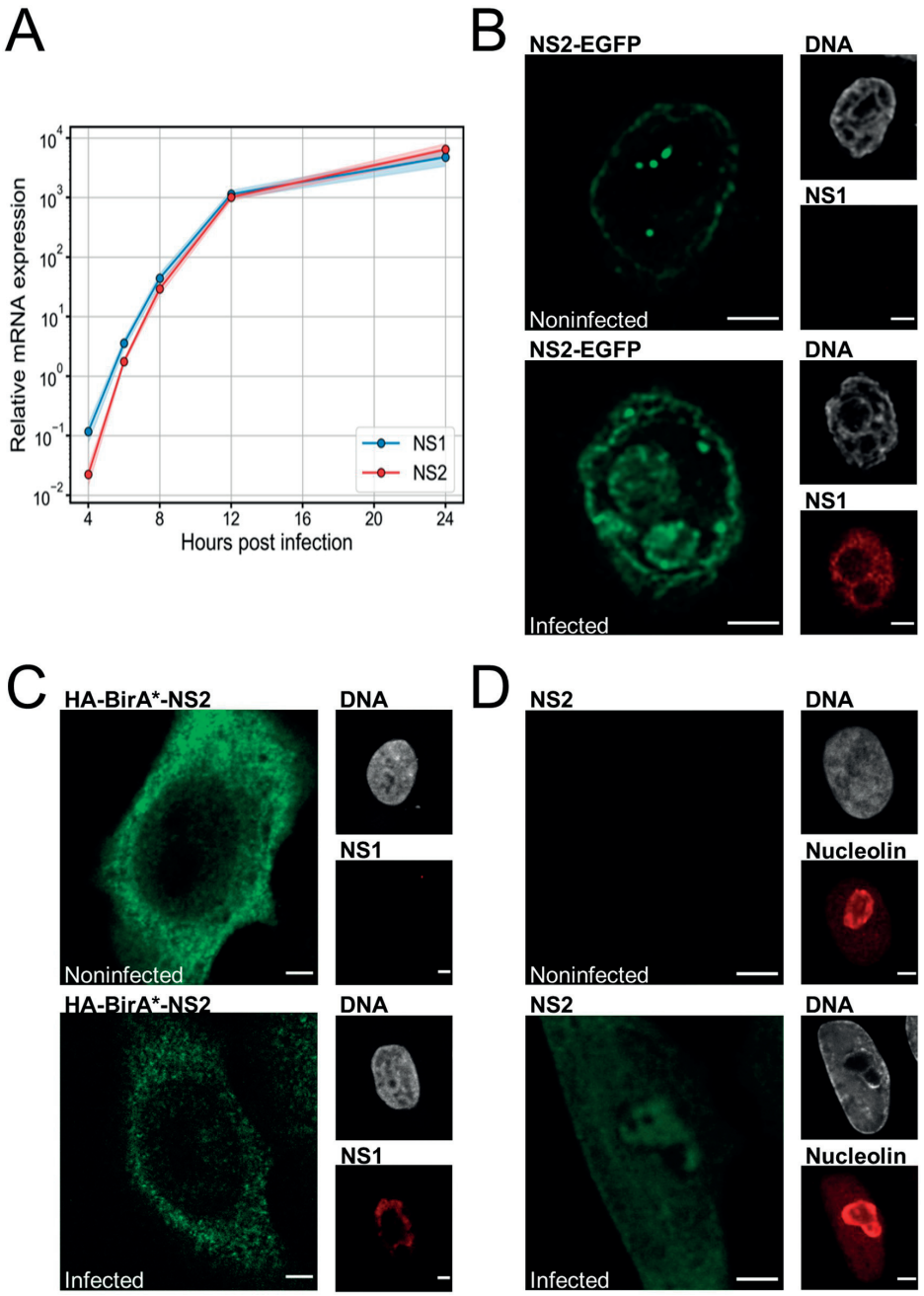

Fig 1. CPV infection leads to simultaneous expression of NS1 and NS2 genes and nucleolar accumulation of NS2. (A) Relative expression levels of NS1 (blue) and NS2 (red) measured by RT-qPCR in infected NLFK cells between 4 and 24 hours post infection (hpi). The blue and red shadings around the lines indicate the standard error of the mean (SEM, n = 3). **(B)** Representative confocal images of HeLa cells transfected with NS2-EGFP (green) and **(C)** BirA*-tagged NS2 (green) at 24 hpt in noninfected and infected cells at 24 hpi. The localization of NS1 (red) is shown in cells with DAPI-stained nucleus (gray). **(D)** Representative confocal images of noninfected and infected NLFK cells at 24 hpi stained with antibodies against NS2 (green) and nucleolin (red). Gray corresponds to DAPI staining of DNA. Scale bars, 3 μm.

https://doi.org/10.1371/journal.ppat.1010353.g001

A

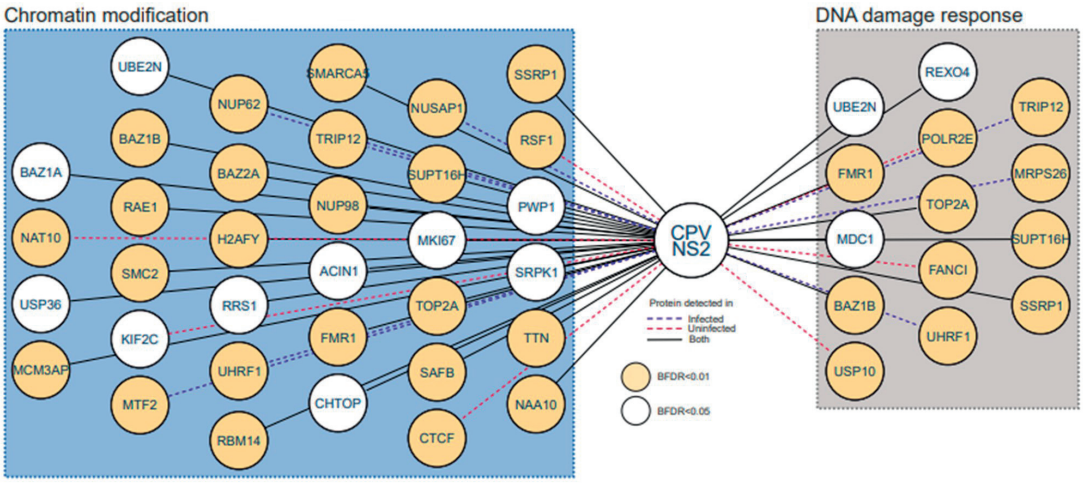

B

GO Biological process	Count in infected	Count in noninfected	Total identified
Regulation of chromosome organization	10	10	12
Chromosome condensation	5	4	5
Chromosome organization	25	24	28
Regulation of chromatin organization	8	7	9
Negative regulation of chromosome organization	5	4	6
Nucleosome positioning	1	3	3
Nucleosome organization	4	6	6
Chromatin organization	15	15	17
Chromatin assembly or disassembly	4	6	6
Histone modification	9	9	10
Covalent chromatin modification	9	9	10
Cellular response to DNA damage stimulus	11	11	14

Fig 2. Nuclear interactors of NS2. Identification of NS2 proximity interactome using BioID. (**A**) Schematic picture of 48 high-confidence BioID NS2 interactors related to chromatin modification and DNA damage response cellular processes. Interactors are presented by their gene names. Association of NS2 (HA-BirA*-NS2) is shown either in the presence (24 hpi, dark blue dashed line) or in the absence (red dashed line) of infection or in both cases (black solid line). (**B**) Table showing the GO functional annotation clusters for the NS2 BioID dataset. The functional annotation chart of NS2 high confidence interactors was created by PANTHER classification system for GO Biological process overrepresentation (http://www.pantherdb.org/) using the default BFDR < 0.01 (yellow circle) and < 0.05 (white circle) filters. The GO terms are grouped hierarchically by PANTHER to illustrate relations between functional classes and are colored based on relatedness to the two identified functional association groups: chromatin modification (blue) and DNA damage response (gray).

https://doi.org/10.1371/journal.ppat.1010353.g002

Since BioID suggested that NS2 associates with several nuclear proteins, the nuclear distribution of those NS2 interactors was further clarified using the interactome-based MS microscopy analysis. This method creates a high-precision reference molecular context proteome map generated by a combination of affinity purification mass spectroscopy and BioID. Three nuclear components–the nucleolus, chromatin and the nuclear envelope (NE)—were represented by the groups of cellular proteins proximal to rRNA 2′-O-methyltransferase fibrillarin, histone H3.1, and prelamin-A/C, respectively [68]. This proteome map analysis revealed that in noninfected cells the NS2 interactome was most similar to the NE marker, while sharing

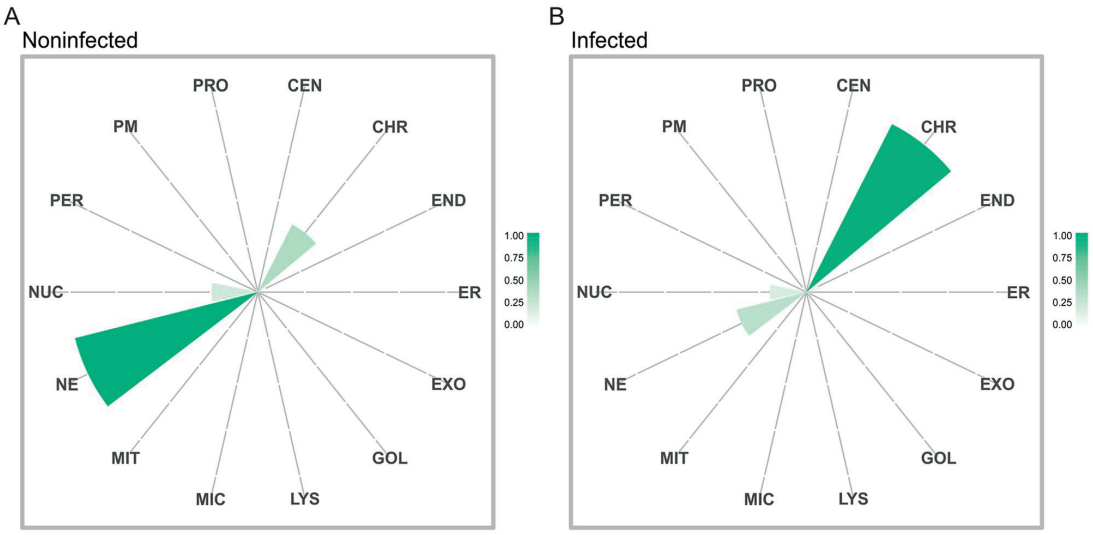

Fig 3. Molecular context of NS2 varies in noninfected and infected cells. The interactome-based localization of CPV NS2 was analyzed with mass spectrometry (MS) microscopy in (A) noninfected and (B) infected stably HA-BirA*-NS2 expressing Flp-In T-REx 293 cells. The polar plots show the location of NS2 protein associations based on cellular marker proteins. Each sector represents one subcellular location defined by our reference database. The color assigned to each of the localization is based on the annotation frequency (light green: 0–0.25; green: 0.25–0.5; dark green: 0.5–1). The markers used for nucleoli (NUC), chromatin (CHR) and nuclear envelope (NE) were rRNA 2′-O-methyltransferase fibrillarin, histone H3.1 and prelamin-A/C, respectively.

https://doi.org/10.1371/journal.ppat.1010353.g003

some interactors with nucleoli and chromatin (Fig 3A). Importantly, in infected cells the NS2 interactome shifted clearly towards chromatin (Fig 3B). This suggested that during infection NS2 is associated with proteins connected to the organization and modification of the host genomic DNA, and thereby further assessment of NS2 interactions was required.

NS2 is associated with proteins linked to chromatin organization

The NS2 BioID interactome and GO annotation analyses suggested an association between the viral NS2 protein and cellular components involved in chromatin organization. BioID based interactome linked NS2 to four different complexes which belong to the major ATP-dependent chromatin remodeling complex family ISWI (Fig 4A and S1 and S2 Tables) [75]. The mammalian ISWI complexes identified were the nucleolar chromatin remodeling complex (NoRC), WSTF-ISWI chromatin remodeling complex (WICH), the ATP-utilizing chromatin assembly and remodeling factor complex (ACF), and the remodeling and spacing factor (RSF) complex.

One of the NS2 high-confidence (BFDR <0.01) BioID hits was nucleosome-remodeling helicase matrix-associated actin-dependent regulator of chromatin A5 (gene name *SMARCA5*, also known as SNF2H) [76,77] which is associated with all four ISWI complexes. NS2-associated proteins included bromodomain adjacent to zinc finger domain 2A (BAZ2A, also known as TIP5, BFDR <0.01) [71,72], a regulator of SMARCA5 in NoRC. [71,72]. Notably, the highest average spectral counts in our BioID analysis were produced by the proliferation marker protein Ki-67 (MKI67; BFDR 0.02 in infected and 0.04 in noninfected cells). Ki-67, a nuclear protein expressed in actively dividing mammalian cells, is involved in the organization of heterochromatin and it also interacts with BAZ2A [78–80]. Moreover, NS2 was associated

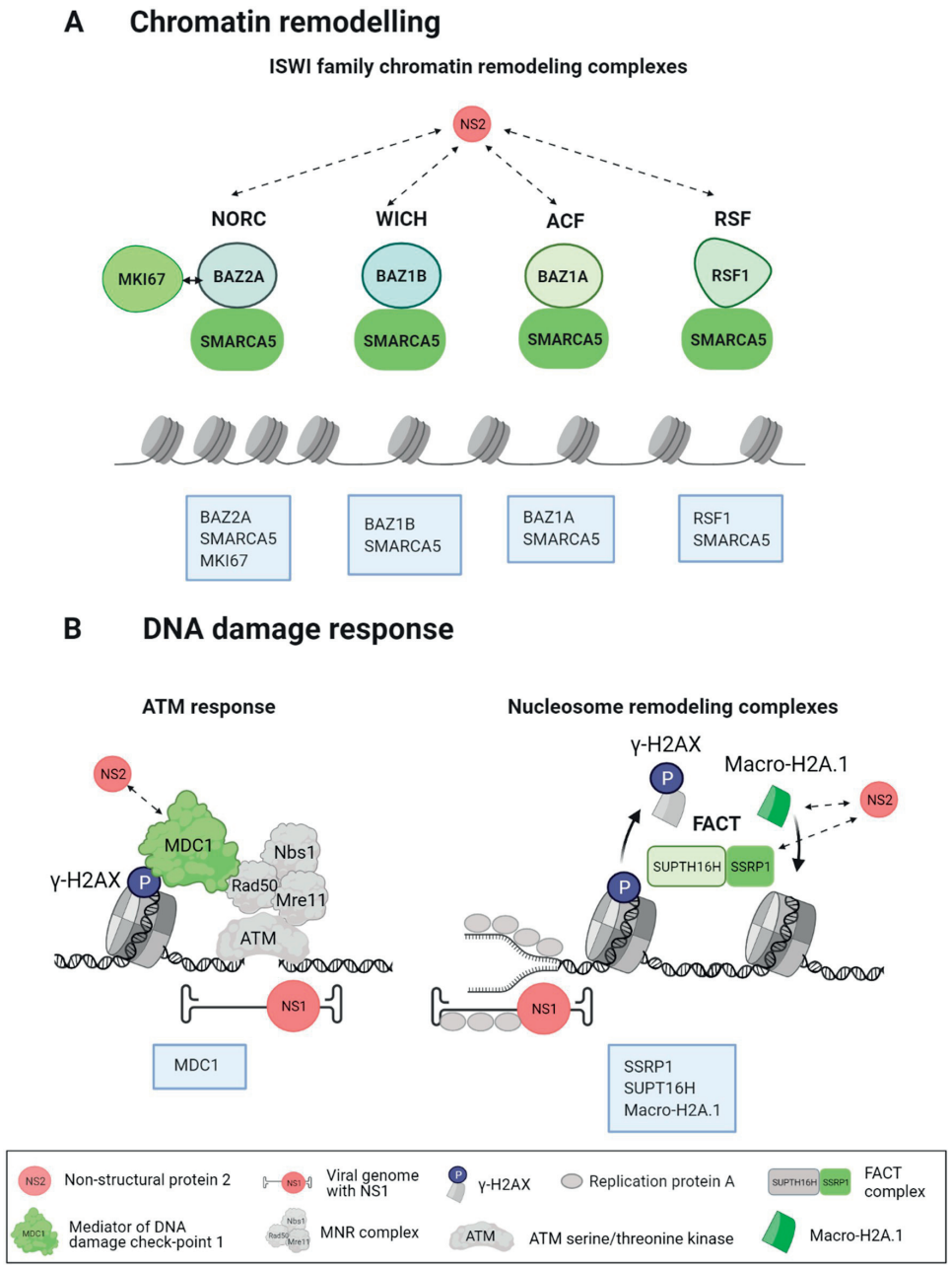

Fig 4. NS2-associated proteins play important roles in chromatin remodeling and DDR machineries. The CPV NS2 protein is linked with certain key factors that control chromatin remodeling and DDR pathways to optimize cellular conditions for viral replication. This schematic picture shows the major associations of NS2 (red) with cellular proteins (shades of green). Dashed arrows represent key factors of chromatin binding and DDR machineries interacting with NS2. (**A**) The cellular chromatin modification machinery includes chromatin remodeling complexes such as NORC, WICH, ACF and RSF. (**B**) DNA damage response (DDR) factors contain major upstream mediators of ATM response such as DNA damage checkpoint 1 (MDC1) protein and proteins

included in chromatin and nucleosome remodeling complexes. MDC1 interacts with phosphorylated γ-H2AX and mediates the recruitment of DDR response proteins to the damage site. The DDR downstream FACT complex functions as a nucleosome remodeler facilitating transcription. During replication stress, FACT orchestrates the replacement of γ-H2AX with macro-H2A.1 to the damage site. The location of parvoviral genomes and the viral replication protein NS1 (red) adjacent to DNA damage sites of the cellular chromatin are shown. Figure was created with BioRender.com.

https://doi.org/10.1371/journal.ppat.1010353.g004

with tyrosine-protein kinase BAZ1B (also known as the Williams syndrome transcription factor, WSTF, BFDR <0.01) [81] a component of WICH with SMARCA5. NS2 was associated with both BAZ1A (BAZ1A, also known as ATP-utilizing chromatin assembly and remodeling factor 1, ACF1; BFDR <0.05) and remodeling and spacing factor 1 (RSF1, BFDR <0.01). ACF [81] and RSF [82,83,84,85] are formed when SMARCA5 combines either with BAZ1A or with RSF1. The potential role of NS2 in the regulation of transcription was further supported by its interaction with a member of the histone H2A family, core histone macro-H2A.1 (H2AFY, BFDR <0.01), which has been shown to associate with transcription repression [86]. The association between NS2 and SMARCA5, BAZ1A, BAZ1B, BAZ2A, Ki-67, and macro-H2A.1 were detected both in noninfected and infected cells. Together, these data indicate that CPV NS2 associates with proteins of four chromatin-modifying complexes. Therefore, it is possible that NS2 is involved in the manipulation of chromatin modeling processes potentially inducing modifications of both cellular and viral DNA.

NS2 is linked to DDR-associated proteins

We next sought to confirm the association of NS2 with DDR factors necessary for parvoviral replication [34,87]. The progression of cell cycle is coordinated by DNA damage checkpoints, which delay or stop the cell cycle before or during DNA replication in the presence of damaged DNA [88,89]. DDR includes complex signaling cascades that require the actions of various proteins that function as DNA damage sensors, transducers, mediators, and effectors. One of the upstream mediators in DDR is DNA damage checkpoint 1 (MDC1, BFDR <0.05) protein. The BioID analysis suggested NS2 interactions with MDC1 in both noninfected and infected cells, as well as associations with DDR downstream factors, including components of the nucleolar facilitator of chromatin transcription (FACT) complex and WSTF-including nucleosome remodeling complex (WINAC) (Fig 4B and S1 and S2 Tables). FACT acts as a critical chaperon for histones in nucleosome reorganization during replication, and in the detection and response of DNA damage [90,91], stabilizing chromatin as a whole by suppressing cryptic transcription [92,93]. FACT complex subunits, structure specific recognition proteins (SSRP1, BFDR <0.01) and SUPT16H (SPT16, BFDR <0.01), were identified as high-confidence NS2 interactors both in noninfected and infected cells. SSRP1 is a histone chaperon involved in transcriptional regulation, DNA replication and damage repair [94–97]. SUPT16H also functions independently of FACT when it forms WINAC with BAZ1B (BFDR <0.01) [98,99]. WINAC is an ATP-dependent chromatin remodeling complex, which is associated with a variety of DNA processing functions. Furthermore, FACT is linked to the activation of p53, a central tumor suppressor, the stability of which is further regulated by ubiquitin carboxyl-terminal hydrolase 10 (USP10, BFDR <0.01), also identified as an NS2 interactor in BioID of noninfected cells. USP10 relocates to the nucleus in response to DDR and promotes the deubiquitination of p53 [100]. Similar function is served by E3 ubiquitin-protein ligase (TRIP12, BFDR <0.01), an NS2 interactor in infected cells, which indirectly regulates p53 activity by affecting its ubiquitination. In addition to the previously mentioned and other ubiquitination-related enzymes in the BioID results, ubiquitin-conjugating enzyme E2 N (UBE2N, BFDR <0.05) was also identified in the absence and presence of infection. It may act in non-

degradation ubiquitination targeting and DNA damage repair [101]. Taken together, these results demonstrated that NS2 is associated with the DDR signaling proteins during infection. Since DDR has a clear potential role in parvovirus replication [34,87], NS2 may recruit DDR effector proteins to regulate viral replication.

Proximity-dependent interaction analysis corroborates NS2 BioID findings

To confirm the BioID findings of NS2 association with nuclear proteins, the cellular distributions of four NS2-associated proteins from infected and noninfected cells, SMARCA5, MDC1, macro-H2A.1 and SSRP1, which represent chromatin modeling and DDR functions, were studied in noninfected HeLa cells expressing NS2-EGFP and in infected NLFK cells. As described above, NS2-EGFP was mostly localized to the NE and into nucleolar foci (Figs 1B and S1) whereas antibody-labeled NS2 showed more homogenous nuclear and nucleolar distribution (Figs 1D and S2). SMARCA5 and MDC1 and macro-H2A.1 were distributed throughout the nucleus in transfected cells, whereas macro-H2A.1 and γ-H2AX localized to the nuclear edges in infected cells. SSRP1 was mostly located into specific nucleoplasmic foci in both transfected and infected cells (S1 and S2 Figs). Confocal imaging of infected HeLa cells at 24 hpi showed that SMARCA5 and SSRP1 occupied sites that overlapped with the NS1-containing replication centers. The transcription repressor macro-H2A.1 was not found in the replication center area, but was localized close to the replication centers in regions without NS1 (S3 Fig). Together, confocal imaging therefore suggested that SMARCA5, MDC1, SSRP1, and macro-H2A.1 associated or localized adjacent to regions containing either NS2 or NS1.

To further asses NS2 interactions and to move beyond diffraction-limited observations of protein localizations, protein-protein interactions were studied with Proximity Ligation Assay (PLA) which is an immunodetection technique that generates a fluorescent signal only when two antigens of interest are within 40 nm of each other [102]. All the tested NS2 interactors, SMARCA5, SSRP1, and macro-H2A.1, gave punctate nuclear PLA signals which localized often close to the nucleoli in cells transfected with NS2-EGFP. Here, anti-GFP was used to form a PLA probe pair with antibodies against SMARCA5, SSRP1, or macro-H2A.1 (Fig 5A). The negative viral capsid antibody control in non-infected cells and technical probe controls in NS2-EGFP transfected cells (Figs 5B and S4A and S4B) indicated that the background in the nuclear area was low (approximately 0.9 ± 0.3 and 0.7 ± 0.2 PLA foci/nucleus, respectively, n = 15). A quantitative analysis of 3D data showed that within the segmented nuclei (S4C Fig), the highest number of PLA foci was detected for NS2 with macro-H2A.1 (135 ± 12 PLA foci/nucleus). A smaller number of PLA foci was detected for NS2 with SMARCA5 and SSRP1 (55 ± 11 and 7.5 ± 1.4 PLA foci/nucleus, respectively) (Fig 5C). The Poisson regression model [103] showed that NS2 with SMARCA5, macro-H2A.1 and SSRP1 had a significantly higher ($p<0.01$) number of nuclear PLA foci compared to the negative control. Moreover, NS2 interactions with SMARCA5, MDC1, macro-H2A.1, and SSRP1 were further confirmed using PLA in infected cells. Assay was performed by probing anti-NS2 antibody together with antibodies against BioID identified interactors. Similar to the NS2-EGFP transfected cells, representative examples shown in Fig 6A demonstrated proximal localization of PLA signals and the nucleoli. The highest number of PLA foci in comparison to negative control (1.9 ± 0.5 PLA foci/nucleus, Fig 6B) was detected for macro-H2A.1 (40 ± 16 PLA foci/nucleus) followed by MDC1 (22 ± 6 PLA foci/nucleus), SMARCA5 and SSRP1 foci (6.5 ± 1.5 and 3.7 ± 0.8 PLA foci/nucleus, respectively) (Fig 6C). The technical controls indicated that the background in the nuclear area was low (approximately 0.3 ± 0.3 and 1.1 ± 0.9 PLA foci/nucleus, respectively, n = 15). Together, our interaction analyses of prominent NS2 interaction partners support BioID

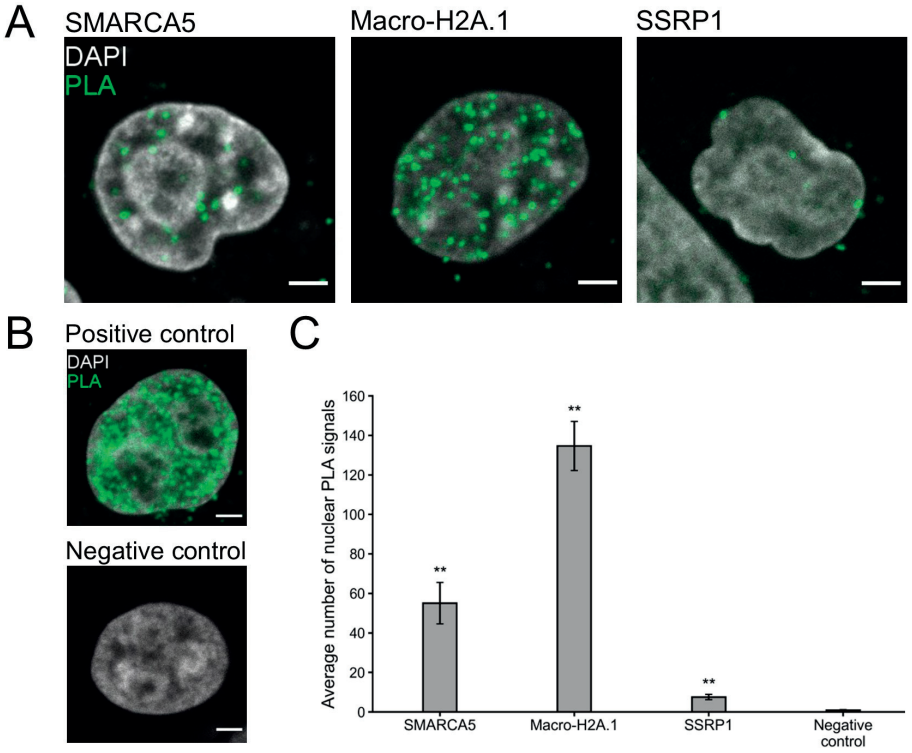

Fig 5. Close proximity analysis verifies the association of NS2 with key BioID interactors. Proximity Ligation Assay (PLA) assay was performed in HeLa cells transfected with NS2-EGFP and representative cellular proteins identified by BioID. The proteins were chromatin remodeling factor (SMARCA5), transcriptional repressor (macro-H2A.1), and histone chaperon of the FACT complex (SSRP1). (**A**) Representative single confocal cross-sections showing the localization of PLA signals (green) and the nuclei stained with DAPI (gray). (**B**) Positive and negative controls include PLA with antibodies against VP2 capsid protein and intact capsids in infected cells at 20 hpi and in noninfected cells. Scale bars, 3 μm. (**C**) The graph shows the average number of PLA signal foci per nucleus (n = 15) analyzed from 3D reconstructions of confocal images. The error bars show the standard error of the mean (SEM), and the samples having a significantly higher number of nuclear PLA foci compared to the negative control are denoted as ** ($p<0.01$). The significance was assessed using Poisson regression model.

https://doi.org/10.1371/journal.ppat.1010353.g005

results demonstrating that NS2 is likely associated with proteins of DNA modeling and DDR pathways.

Mutation of NS2 leads to changes in chromatin remodeling

Our BioID analysis showed that NS2 is associated with cellular proteins involved in chromatin organization. To further validate our findings, we compared NS2 mutant clones to the wild type (wt) infectious clone to analyze their effect on chromatin organization. In these assays, cells were transfected either with the wt infectious clone or with NS2 splice donor or splice acceptor mutants (G533A and A2003T, respectively) which were designed to disrupt the expression of NS2 but not to affect the amino acid sequence of NS1 [6]. These previously described mutants are based on the MVM mutants that have been shown to alter the expression of MVM NS2 and lead to abortive infection [12,13,104]. CPV NS2 mutants have been created by introducing termination codons into the NS2 coding sequence of the infectious clone to a site upstream of the common NS1/2 splice donor or downstream of the NS2-specific splice

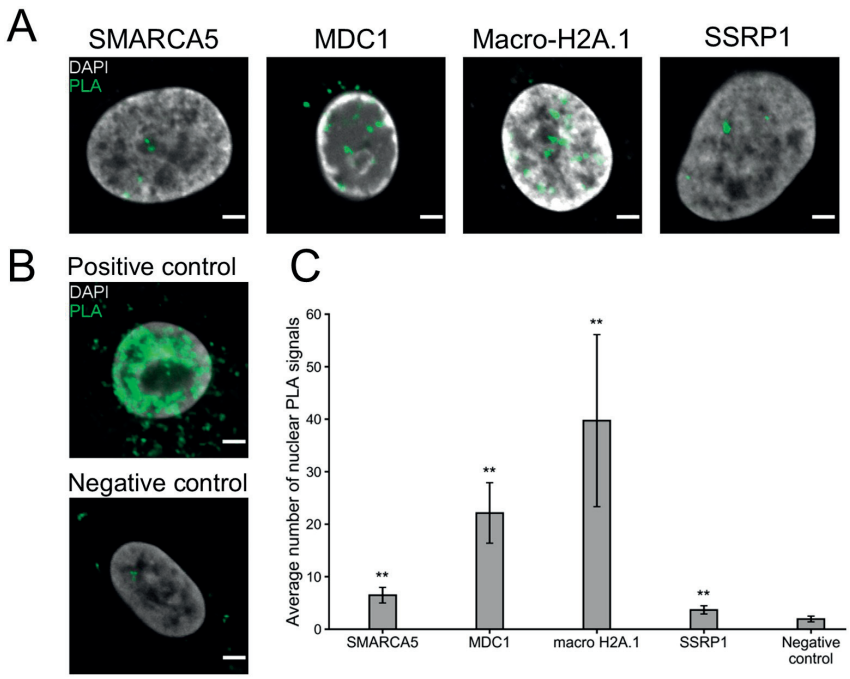

Fig 6. NS2 interacts with host proteins identified by BioID in infected cells. Analyses of NS2 interaction with SMARCA5, MDC1, macro-H2A.1, and SSRP1 in infected NLFK cells at 24 hpi. (**A**) Representative single confocal cross-sections of PLA signals (green) in the DAPI-stained nuclei (gray). (**B**) Images of positive and negative PLA controls prepared by using antibodies against VP2 and intact capsids at 24 hpi and in noninfected cells. Scale bars, 3 μm. (**C**) The analyses of 3D reconstruction of confocal PLA data showing the average number of PLA signal foci/nucleus (n = 15). The error bars show the standard error of the mean (SEM), and the samples with a significantly higher number of nuclear PLA foci compared to the negative control are denoted as ** ($p<0.01$). The significance was assessed using Poisson regression model.

https://doi.org/10.1371/journal.ppat.1010353.g006

acceptor [6]. The original publication demonstrated that the production of viral capsid proteins (VP1/VP2) and viral DNA were all significantly decreased in cells transfected with the NS2 splice donor mutant virus, while transfection with the splice acceptor mutant was comparable with wt CPV. Characterization of mutants by immunoprecipitation analyses (antibodies against the NS2 C-terminus) showed that both mutants were unable to produce intact NS2 protein [6]. However, the interpretation of mutant-induced effect on viral life cycle was complicated by RT-PCR characterization which revealed that alternative sequences used to splice the message RNA were present in both mutants [6]. It should be also noted that, that the N-terminal end of NS1, which share a common N-terminal domain with NS2, might be produced in some circumstances, and might play a role in virus-induced chromatin remodelling, although that remains to be defined.

Here, we used confocal microscopy intensity analysis to study the distribution pattern and relative amount of nuclear DNA (stained with DAPI), euchromatin (labeled for H3K27ac), and heterochromatin (labeled for H3K9me3) in HeLa cells transfected with the wt CPV clone and NS2 mutants at 24 hours post transfection (hpt). Comparison of wt and mutant viral transfection revealed that the donor NS2 mutant clone displayed a clearly higher total intensity of the euchromatin (Fig 7A and 7B). It is important to note that the increased amount of

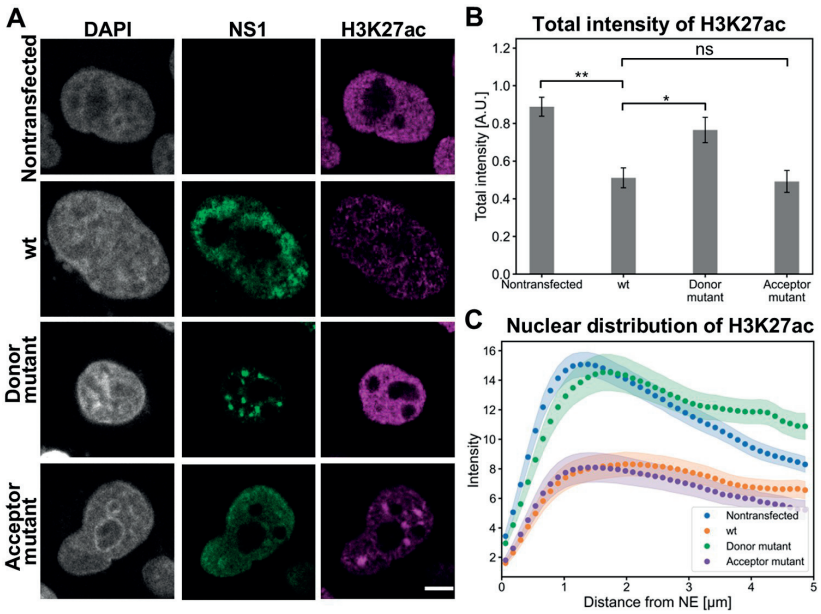

Fig 7. NS2 mutation induce changes in the amount and distribution of euchromatin. (**A**) Representative confocal images show the nuclear localization of euchromatin marker H3K27ac (magenta), NS1 (green), and DAPI staining (gray) in nontransfected HeLa cells, and cells transfected with wt, NS2 donor and acceptor mutants at 24 hpt. (**B**) Total fluorescence intensities of euchromatin. (**C**) Nuclear distribution of H3K27ac as a function of increasing distance from the NE in nontransfected, wt and NS2 mutants transfected cells (n = 29). The error bars show the standard error of the mean. Statistical significances were determined using Dunnett's multiple comparison test. The significance values shown are denoted as ** ($p<0.01$), * ($p<0.05$) or ns (not significant). Scale bars, 5 μm.

https://doi.org/10.1371/journal.ppat.1010353.g007

euchromatin in splice donor mutant transfected cells was accompanied by significantly lower total intensity of DAPI staining (S5A Fig). This indicates that infection affects the epigenetic regulation of host chromatin, and the splice donor mutation of NS2 results in a reversion towards the decondensation state seen in noninfected cells. Distribution analyses of both nuclear DNA (S5B Fig) and euchromatin (Fig 7C) as a function of the distance from the NE further demonstrated their localization both in the nuclear periphery and in the central region of the nucleus. Additionally, transfection by all clones resulted accumulation of heterochromatin at the perinuclear region and around the nucleoli (S6A Fig). Notably, NS2 mutations did not appear to affect the relative intensity of the heterochromatin label (S6B Fig). Distribution analyses of heterochromatin further confirmed its localization both close to the nuclear periphery and in the center of the nucleus (S6C Fig). Altogether, our findings demonstrated clear changes in the quantity of euchromatin in response to NS2 donor mutant transfection, suggesting that N-terminal sequence of NS2 could have a currently undefined role in chromatin remodeling during infection. This supports our BioID results demonstrating that NS2 is associated with proteins linked to chromatin organization.

The level and localization of DDR proteins change in the presence of NS2 mutant

Cellular DNA double-strand break repair sites recruit several upstream DDR proteins such as γ-H2AX [105–107] and MDC1 [108] (Fig 4B). DNA damage proteins have also been

previously observed to localize to the periphery of MVM viral replication centers [109]. As shown by our BioID data, CPV NS2 is associated with MDC1 (Fig 2 and S3 Table). To further examine the role of NS2 interactions in DNA damage, we analyzed the localization and intensity of γ-H2AX and MDC1 and their connection to replication centers in HeLa cells transfected with the wt CPV, splice donor and splice acceptor mutants at 24 hpt. Our studies demonstrated that both γ-H2AX and MDC1 localized next to the replication centers and accumulated close to the nucleoli and NE in wt or the splice acceptor mutant transfected cells, in contrast to relatively diffuse nuclear localization in nontransfected cells and in cells transfected with the splice donor mutant. NS1 accumulated in distinct nuclear foci in cells transfected with the splice donor mutant (Fig 8A and 8B). As expected, both γ-H2AX and MDC1 colocalized with DNA marker. Quantitative image analysis (Fig 8C) showed that wt and the splice acceptor mutant transfections led to relatively similar amounts of nuclear γ-H2AX, whereas it was significantly decreased in nontransfected cells and in the splice donor mutant transfected cells. The distribution analyses indicated that γ-H2AX was distributed close to the NE and in the central region of the nucleus in cells transfected with the wt and the splice acceptor mutant, whereas γ-H2AX was slightly more concentrated close to the NE in nontransfected cells and in the splice donor mutant transfected cells (Fig 8D). Intensity line profiles measured through the nucleoli verified close association between γ-H2AX and replication centers in close proximity to the nucleoli both in cells transfected with the wt and the splice acceptor mutant. The close localization between replication centers and H2AX was visible to a lesser extent in the cell transfected with the splice donor mutant (Fig 8E). Similar to γ-H2AX, the total intensity of MDC1 was clearly decreased in cells transfected with the splice donor mutant in comparison to cells transfected with wt or the splice acceptor mutant (Fig 8F), and it was localized slightly more toward the NE in the splice donor mutant transfected cells (Fig 8G). The line profiles of wt and the splice acceptor mutant transfected cells showed that replication centers and MDC1 were located close to each other and they both were located near the nucleoli (Fig 8H). The localization of MDC1 in the periphery of NS1-labeled replication center foci was indistinct. Taken together, our data reveals that transfection with the NS2 splice donor mutant resulted in significant changes in the amounts and distributions of DDR proteins. The decreasing association of H2AX and MDC1 with the viral replication centers in cells transfected with the splice donor mutant (Fig 8E and 8H) is interesting as MVM studies have demonstrated a close localization between replication centers and DDR proteins [34]. These findings show that N-terminal sequence of NS2 is required for the normal progression of DNA damage response in infection, and the mutation of splice donor site has an effect on the recruitment of H2AX and MDC1 to the replication region where they most likely associate with NS1 in wt infection.

Mutation of NS2 leads to changes in the establishment of replication centers

MVM replication centers are established at cellular DNA damage sites, which provide necessary factors for the initiation of viral replication. The progress of infection requires association with new DNA damage sites, allowing the amplification of viral replication [109]. Therefore, as our experiments demonstrated that the mutation of NS2 splice donor site leads to a decrease in DDR proteins, we assessed how NS2 mutations affect the development of viral replication centers.

As shown above both wt and the splice acceptor mutant transfections induced the development of large replication centers, which filled most of the nuclear region at 24 hpi. In contrast, multiple small replication centers were formed in cells transfected with the splice donor mutant (Figs 7A, 7B, 8A and 8B). Confocal images showed that in wt and the splice acceptor

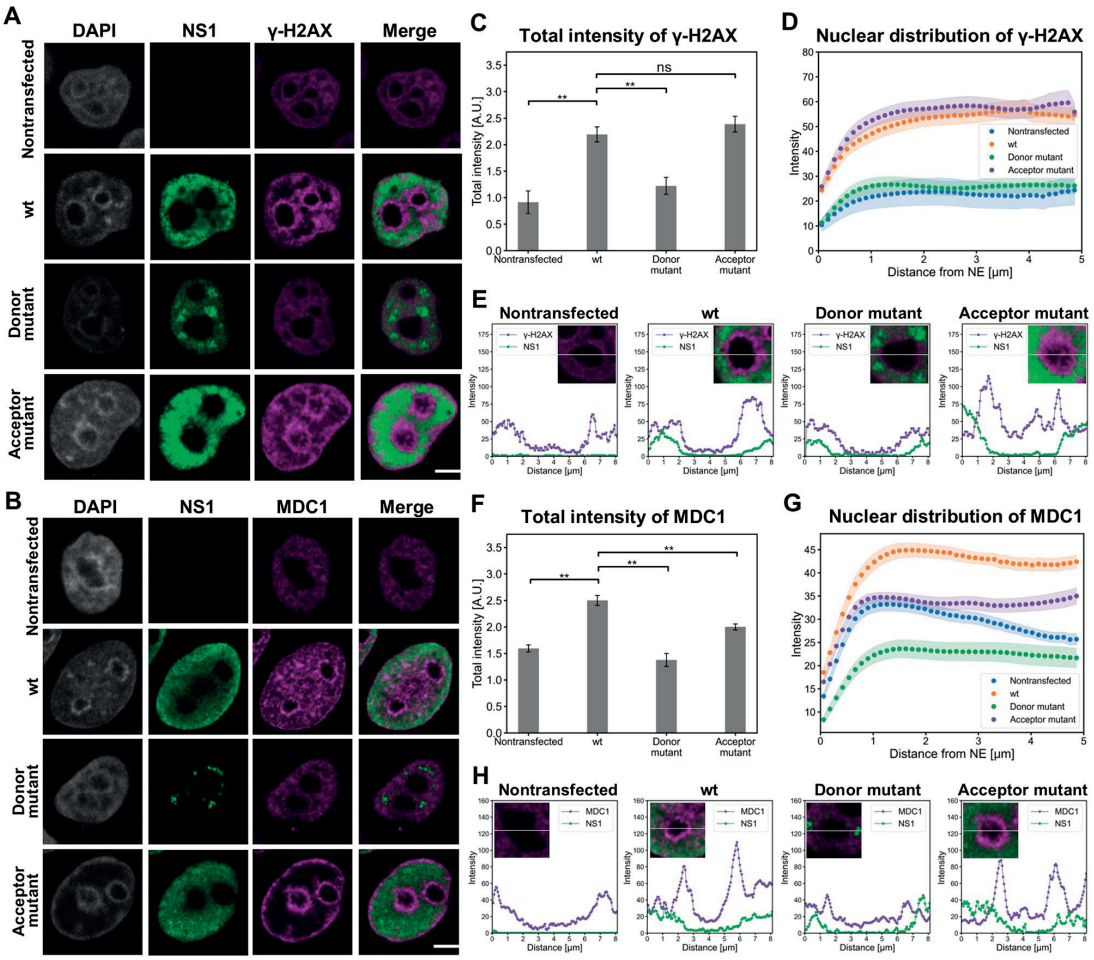

Fig 8. Mutation of NS2 induce alteration in the amount and distribution of DDR proteins. Representative confocal images show the nuclear localization of NS1 (green), (**A**) γ-H2AX (magenta), (**B**) MDC1 (magenta) and DAPI staining (gray) in HeLa cells without transfection or at 24 hpt with wt, NS2 splice donor and acceptor mutants. Scale bars, 5 μm. (**C**) Total fluorescence intensities of γ-H2AX together with (**D**) its nuclear distribution as a function of increasing distance from the NE in nontransfected, wt and NS2 mutants transfected cells (n = 29). (E) Intensity line profiles of γ-H2AX (purple) and NS1 (green) measured through the nucleoli. (**F**) Fluorescent intensities and (**G**) nuclear localization of MDC1 from the NE (n = 28). The error bars show the standard error of the mean. (H) Intensity line profiles of MDC1 (purple) and NS1 (green) measured through the nucleoli. Statistical significances were determined using Dunnett's multiple comparison test. The significance values shown are denoted as ** ($p<0.01$), * ($p<0.05$) or ns (not significant). Fluorescent intensity profiles of (**G**) γ-H2AX (magenta) with NS1 (green), and (**H**) MDC1 (magenta) with NS1 (green) in zoomed areas.

https://doi.org/10.1371/journal.ppat.1010353.g008

mutant transfections NS1 was seemingly localized to the nuclear periphery and excluded from the center of the nucleus where nucleoli are present. The NS1 foci were often localized around the nucleoli in the splice donor mutant transfected cells (Fig 9A). Comparison of NS1 intensities in transfected cells showed a significantly decreased amount of NS1 in the cells transfected with the NS2 donor mutant (Fig 9B). This data suggests that replication centers in the cells transfected with the splice donor mutant were initiated but failed to expand. This is consistent with the finding that most of NS1 in the cells transfected with the splice donor mutant was

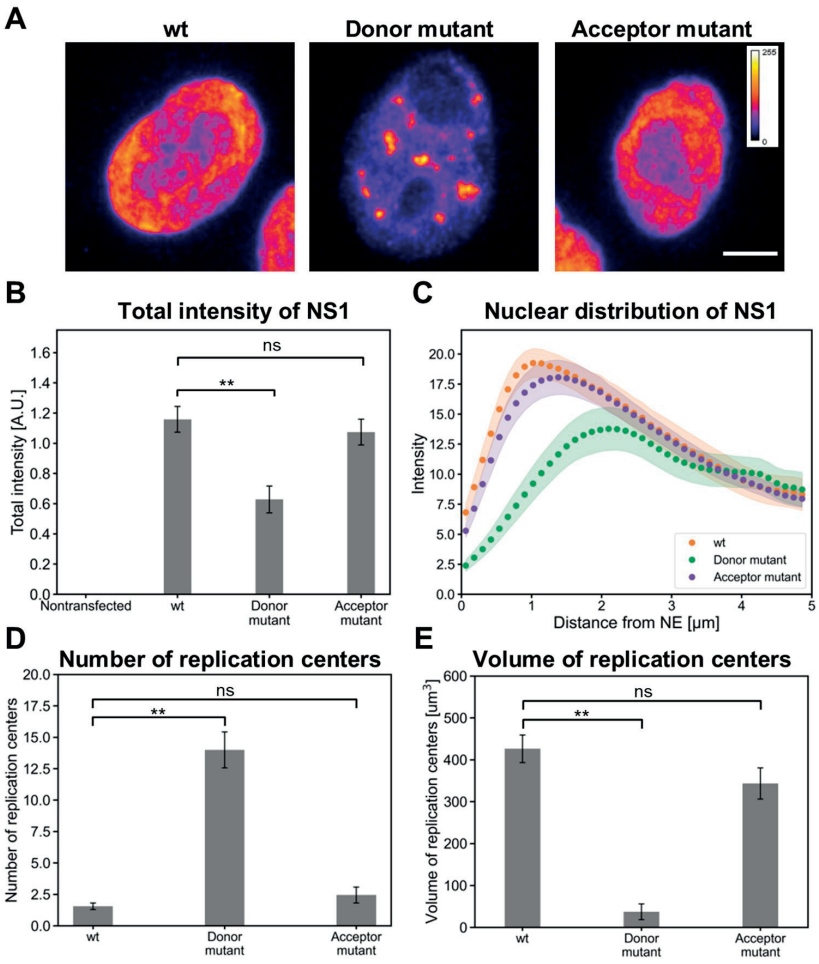

Fig 9. NS2 mutation induce changes in the number and volume of replication centers. (**A**) Representative pseudocolored sum projections of confocal image slices show the amount and distribution of nuclear NS1 in nontransfected, wt, splice donor and acceptor mutants transfected HeLa cells at 24 hpt. Calibration bar for pseudo coloring is shown. Scale bars, 5 μm. (**B**) Total fluorescence intensities of NS1. The error bars show the standard error of the mean. (**C**) Nuclear distribution of NS1 as a function of increasing distance from the NE in wt and NS2 mutants transfected cells (n = 29). (**D**) Numbers and (**E**) volumes of replication centers, identified by NS1 staining were analyzed in wt, splice donor and acceptor mutants transfected HeLa cells at 24 hpt (n = 29). The error bars show the standard error of the mean. Statistical significances were determined using Dunnett's multiple comparison test. The significance values shown are denoted as ** ($p<0.01$), * ($p<0.05$) or ns (not significant).

https://doi.org/10.1371/journal.ppat.1010353.g009

localized towards the center of the nucleus, while in the cells transfected with wt and the splice acceptor mutant NS1 was mostly found in the nuclear periphery (Fig 9C). The average number of replication center foci detected in cells transfected with the splice donor mutant was 14.0 ± 1.4 (n = 29), whereas in the cells transfected with wt and the splice acceptor mutant it was 1.6 ± 0.3 and 2.4 ± 0.6 (n = 29) (Fig 9D). This is consistent with the notion that the size of the NS2 splice donor mutant induced foci was small (40 ± 20 μm^3, n = 29) in comparison to

replication centers in the cells transfected with wt (430 ± 30 μm^3, n = 29) and the splice acceptor mutant (340 ± 40 μm^3, n = 29) (Fig 9E). As described earlier, parvoviral replication centers are associated with sites of cellular DNA damage, and progression of infection is connected to increasing DNA damage [14,34]. Our observation that mutation in N-terminal end of NS2 leads to a deficient development of viral replication centers supports a model that the role of NS2 in DDR is essential for the successful infection.

Discussion

When viruses infect cell nuclei for their own benefit, some of the host structures and functions are left unchanged while others go through dramatic remodeling processes and functional changes. Parvoviruses possess a small genome and express only a limited number of proteins, and therefore rely heavily on the nuclear machinery present in the cellular S phase for their efficient replication. As the infection proceeds, extensive changes in the nucleus occur, including altered chromatin architecture and redistribution of DDR components [43,44,110]. As with other parvoviruses, the CPV NS1 performs several functions essential for viral replication. However, the role of NS2 has remained undefined. Our BioID results demonstrate that CPV NS2 protein associates with many cellular proteins involved in essential nuclear processes such as chromatin modification and DDR, and therefore has a potentially important role in chromatin remodeling and in interactions required for viral replication.

BioID analyses linked NS2 to proteins from four chromatin remodeling complexes of the ISWI family involved in nucleosome organization during nucleosome remodeling for the regulation of gene expression [111–113] (Fig 4A). The interaction of CPV NS2 with these complexes is not unexpected as dsDNA viruses and most likely parvoviruses are challenged by cellular defense mechanisms seeking to silence viral gene expression by chromatinization of the viral genome [25,31–33]. Also, another remodeling mechanism appears to facilitate transcription from the viral genome, as the two NS1 binding promoters of CPV, P4 and P38, contain histone modifications characteristic of an accessible euchromatin state [33].

Alternatively, viruses can induce changes in host transcription by epigenetic modifications, redirecting cellular resources for viral gene expression, or interfering with the immune responses of the host cell. Our results show that CPV NS2 is linked with proteins of the nucleolar NoRC complex. This complex is involved in downregulation of ribosomal gene transcription [71,72,114]. Cellular ribosomal proteins are essential for viral translation and replication, and herpes virus studies have shown that their expression increases during infection [115,116]. For human cytomegalovirus, restricting ribosome biogenesis by NoRC-induced silencing of rRNA expression reduces the progression of infection, and ribosome biogenesis may also regulate innate immune responses of the host [117]. The connection between NS2 and NoRC proteins may benefit CPV infection by ensuring ribosome sufficiency for viral protein synthesis. The NS2 interaction with NoRC may also be associated with regulation of host innate responses—however, this requires further investigation. NS2 is also associated with WICH chromatin remodeling complex proteins involved in RNA polymerase and ribosomal RNA transcription [118]. These results suggest that NS2 might cooperate with WICH proteins to facilitate transcription on host chromatin, thereby contributing to the enhancement of RNA polymerase and ribosome production both required for viral replication. NS2 is also associated with proteins of ACF and RSF chromatin remodeling complexes. ACF is involved in nucleosome sliding, regulation of DNA replication, and DNA repair [119–121]. For adenovirus, the connection between the adenoviral protein E4orf4 and ACF complex is associated with the regulation of viral gene expression and caspase-independent cell death [122,123]. RSF complex has a role in the reorganization of compact DNA following double-stranded breaks, ensuring

the access for DDR proteins [82]. Altogether, our data demonstrate that CPV NS2 associates with factors of chromatin-modifying complexes. In this regard, NS2 has a clear potential role in chromatin remodeling. However, the mechanisms by which NS2 either directly or indirectly contributes to the reorganisation of chromatin warrant additional studies.

Our BioID data links CPV NS2 to proteins of DDR machinery (Fig 4B) such as MDC1, a transducer of DNA damage signal. MDC1 is an upstream DDR factor, which is recruited to double-strand break sites following the phosphorylation of H2AX by ATM protein kinase [40]. MDC1 has been shown to control the formation of double-strand break foci, which are characterized by the accumulation of γ-H2AX and additional DDR factors [124,125]. In MVM infection, viral replication centers are established adjacent to damage response foci containing both MDC1 and γ-H2AX [14,34]. MVM NS1 has a potential role during the localization of the viral genome to a DNA damage site [109]. For example, NS1 interacts with casein kinase 2 alpha (CK2α), which is required for the recruitment of MDC1 to the chromatin damage site [126,127]. Notably, MVM NS2 has been previously linked to DDR. Studies with NS2-deficient mutant of MVM demonstrated that NS2 is involved in the activation of ATR but not ATM-mediated signaling pathway, and it has a role in H2AX phosphorylation and formation of replication centers [14]. In contrast to MVM, CPV NS2 association with MDC1, a mediator of the interaction between H2AX and ATM [128], suggests that in CPV infection NS2 participates in the DDR signaling pathway which is orchestrated by ATM kinases. Moreover, NS2 is most likely involved in the recruitment of H2AX and MDC1 to the replication region, which is required for the normal progression of DNA damage response [14] essential for the development of the replication centers [14].

Additionally, our BioID data revealed NS2 association with certain downstream factors of DDR from the nucleosome remodeling complex FACT (Fig 4B). The nucleolar histone chaperone FACT is involved in chromatin remodeling and in maintaining chromatin integrity by nucleosome disassembly and reassembly during DNA transcription, replication, and repair [129–133]. In addition, chromatin transcription by RNA polymerases and replication by DNA polymerases are facilitated by FACT [134–136]. Beyond its role in promoting transcription and replication, FACT has also been linked to repression of transcription initiation from some specific cellular promoters, for example during perinuclear positioning and stabilization of heterochromatin [137–139]. During replication stress FACT complex is utilized to substitute γ-H2AX with macro-H2A.1 close to DNA damage regions [140]. Moreover, FACT appears to be involved in repressing transcription initiation of viral promoters during their latent life cycle. In human immunodeficiency virus type I (HIV-1) infection, interaction of FACT proteins with histones H2A/H2B lead to suppressed viral replication and facilitation of viral latency [141]. FACT also binds to an immediate early promotor of human cytomegalovirus and facilitates transcription of human cytomegalovirus immediate early genes [142]. Notably, in lytic HSV-1 infection FACT is localized to the viral replication compartment [30,143]. FACT is recruited by the HSV-1 immediate early protein ICP22 to allow efficient viral transcription at late stages of viral infection [144]. It is evident that CPV NS2 interaction with FACT may have many important functions during the infection, considering that parvoviral genes are transcribed by the FACT-associated cellular RNA polymerase II [134,145].

The complex nuclear chromatin environment presents a challenge for the replication of incoming viral genome. To ensure a successful infection cycle, viruses manipulate a range of cellular chromatin-modifying proteins to promote their own replication and to control cellular anti-viral defense mechanism. Our results demonstrate that NS2 is associated with certain key factors in chromatin remodeling, presumably either to facilitate viral replication and to inhibit cellular functions from reducing virus replication. NS2 interaction with DNA damage sensing and repair machinery is most likely required for the development of viral replication centers,

and could also be involved in the promotion of viral gene transcription, and the transcriptional silencing of host cell chromatin. Our analyses provide unique insights into the potential mechanisms and associations in nuclear processes by which parvoviral NS2 operates in infection.

Materials and methods

Cells and viruses

Norden laboratory feline kidney (NLFK) cells and human cervical carcinoma HeLa cells were grown at 37˚C in 5% CO_2 in Dulbecco´s Modified Eagle Medium supplemented with 10% fetal calf serum, 1% penicillin/streptomycin, and 1% L-glutamine (Gibco, Thermo Fischer Scientific, Waltham, MA). Flp-In T-REx 293 cell line (R78007, Invitrogen, Life Technologies, Waltham, MA) used for the generation of tetracycline-inducible stable cell lines expressing the HA-BirA*-NS2 were grown at 37˚C in 5% CO_2 in Dulbecco´s Modified Eagle Medium supplemented with 10% fetal calf serum, 1% penicillin/streptomycin and 1% L-glutamine. CPV type 2 virus was derived from an infectious plasmid clone p265 by transfection of NLFK cells. Finally, we used two NS2 mutant infectious clones with termination codons in the NS2 coding sequence which led to inactivation of splice donor (G533A) or splice acceptor (A2033T) [6].

Plasmids

N- and C-terminal fluorescent fusion mammalian expression constructs of CPV NS2 were generated. NS2 gene was PCR amplified from cells transfected with p265 plasmid [146] according to reported donor and acceptor splice sites [6]. For N-terminal fusion, NS2 gene was cloned between EcoRI and BamHI restriction enzyme sites of pEGFP-N3 vector (Clontech), and for C-terminal fusion between BglII and HindIII sites of pEGFP-C1 (Clontech). N-terminal and C-terminal NS2 clones were named NS2-EGFP and EGFP-NS2, respectively. Correctness of all clones was confirmed by sequencing. To determine the possible effect of fluorescent protein position on the cellular distribution of the fusion protein, the cellular localizations of expressed NS2-EGFP and EGFP-NS2 constructs were analyzed in HeLa ells. Both constructs showed similar nuclear distribution including accumulation to the nuclear membrane and nucleolar foci.

NS2 gene surrounded by full AttB sites for gateway cloning was generated from EGFP-NS2 by PCR. The insert was then cloned into pDENTR221 entry vector via gateway BP reaction, and into MAC-tag-C [68] via LR reaction. The resulting NS2-MAC plasmid was used for transfecting Flp-In TREX 293 cells.

RT-qPCR

The timing of NS1 and NS2 transcription in infected NLFK cells was studied with quantitative Taqman RT-PCR. Cells were plated on 3.5 cm culture dish and infected with CPV ~24 h after plating. To quantify the levels of NS1/NS2 mRNAs, cells were collected in TRIZOL (Gibco) at the selected time points at 4–24 hpi and treated with DNaseI (Promega, Madison, WI). NS1 primers were designed to amplify a 106 bp region of CPV genome that is unique to NS1 mRNA (1126 to 1231; primer sequences: RT-NS1-5, AAATGTACTTTGCGGGACTTGG 1126, RT-NS1-3 CACCTCCTGGTTGTGCCATC 1231). NS2 5'-primer contained sequence from both sides of a splice site (520–530 and 2003–2013; RT-NS2-5, CTCGCCAAAAAGTTG CAAAGAC 520–530 + 2003–2013, RT-NS2-3 TGCAAGGTCCACTACGTCCG, 2075–2094) which are joined in NS2 mRNA. NS2 3' primer was designed to yield a final product of 103 bp. Quantitative RT-PCRs were produced as triplicates. SYBR Green (Applied Biosystems, Foster City, CA) was used for detection. Single dissociation curve (Tm for NS1 = 75˚C and Tm for

NS2 = 79˚C) and AGE-gel confirmed the presence of only one product. Samples were amplified in ABI PRISM 7700 Sequence Detection System (Applied Biosystems) under the following conditions: 2 min at 50˚C and 10 min at 95˚C, followed by 40 cycles of 15 s at 95˚C and 1 min at 60˚C. As an endogenous control for the amount of template cDNA, 18S ribosomal RNA was amplified using TaqMan Ribosomal RNA Control Reagents (Applied Biosystems). Relative gene expression was calculated by comparing the expression level of the target gene to 18s rRNA expression level. Noninfected NLFK cells used as a control did not give any signal. Student's t-test was performed to compare NS1 and NS2 transcription.

BioID

BioID experiments analyzing NS2 interactome on a protein level were conducted by expressing HA- and BirA*-tagged NS2 construct (MAC tag, [68] named HA-BirA*-NS2 in Flp-In T-REx 293 cells). BioID coupled with mass spectrometry (MS) was performed in biological duplicates on NS2 bait alongside a set of negative controls. Expression of HA-BirA*-NS2 was induced with tetracycline. Cells were treated with 2 μg/ml of tetracycline (Merck KGaA, Darmstadt, Germany) and 50 mM biotin (Merck KGaA) for 20 hours prior to harvesting. Negative controls were treated only with tetracycline. For infected cells both tetracycline and biotin were added at 4 hpi in order to reach 20 h induction. Samples were purified with affinity columns, digested, desalted, and analyzed with Q-Exactive mass spectrometer as described previously [68]. Data was analyzed with SAINTexpress [147], and filtered using a protein-level Bayesian FDR of 0.05 as the cutoff. Controls included a total of 16 runs of four different GFP-BirA* constructs, including NLS-GFP, which should tag nuclear pore components encountered by most cargo [68]. Further filtering was done by integrating control experiment data from CRAPome contaminant repository [148]. Due to the comprehensive panel of control experiments used for filtering, the vast majority of identified cytoplasmic proteins in the NS2 data were filtered out. Prey proteins seen in at least 20% of CRAPome experiments were discarded, unless their average spectral value was over 3 times larger than the repository average for the prey. The resulting high-confidence interactor set was used for further analyses. Protein ANalysis THrough Evolutionary Relationships (PANTHER) classification system (http://www.pantherdb.org/) was used to create GO biological process annotation chart of NS2 interactors (S2 Table).

MS microscopy

MS-microscopy online tool [68], (www.biocenter.helsinki.fi/bi/protein/msmic/ and proteomics.fi) was used with the filtered data to obtain context-based estimates of NS2 localization. MS microscopy is a tool used to infer the localization of the bait protein based on its interactors. It assumes that the longer a bait protein is around a certain prey, the better that prey is seen in BioID results, and thus by comparing the spectral values of the identified high confidence interactome to those of cellular localization marker proteins, the functional localization of NS2 can be deduced.

Confocal microscopy

For microscopy, cells were grown on glass cover slips, fixed with 4% PFA and permeabilized with 0.1% Triton X-100 in PBS supplemented with 0.5% BSA. HeLa cells were transfected with either NS2-EGFP or with CPV wt infectious plasmid p265 or with the NS2 splice donor (G533A) or splice acceptor (A2033T) deletion mutants. Transfections were performed either with Lipofectamine 3000 transfection reagent (Thermo Fisher Scientific) or JetOptimus (Polyplus transfection). For immunolabeling studies cells were labeled with antibodies against NS1

(MAb obtained from Caroline Astell, University of British Columbia, Vancouver, CAN) (Yeung et al. 1991), NS2 (mouse Ab) (Wang et al. 1998), HA tag (rabbit polyclonal antibody, rAb; ab9110, Abcam, Cambridge, UK), SMARCA5 (rAb, ab183730, Abcam), macro-H2A.1 (mH2A.1 protein, rAb, ab183041, Abcam), SSRP1 (rAb, ab137034, Abcam), γ-H2AX (either with recombinant Alexa Fluor 647 H2A.X anti-gamma phospho S139 rabbit monoclonal antibody, ab195189 or anti-gamma H2A.X phospho S139 rabbit polyclonal antibody, ab2893, Abcam), H39me3 (rAb, ab8898, Abcam), H3K27ac (rAb, ab4729, Abcam) and MDC1 (rAb, PA5-82270, Thermo Fisher Scientific, Waltham, MA, USA). The primary antibodies were followed by goat anti-rabbit or anti-mouse Alexa 488, 546, 555 and 647-conjugated secondary antibodies (Thermo Fisher Scientific). DNA was labelled either with DAPI or with NucBlue.

The immunolabeled cells were imaged either using Olympus FV laser scanning confocal microscope with UPLSAPO 60x oil immersion objective (NA 1.35), Nikon A1R laser scanning confocal microscope (Nikon Instruments Inc., Tokyo, Japan) with CFI Plan Apo VC 60xH oil immersion objective (NA 1.4) or Leica TCS SP8 FALCON laser scanning confocal microscope (Leica microsystems, Mannheim, Germany) with HC PL APO CS2 63x/1.40 oil immersion objective (NA 1.4). For Olympus the following microscopic parameters were used. DAPI (Invitrogen) was excited with 405 diode laser and 425/50 nm band pass filter was used to detect the fluorescence. Alexa 546 and Alexa 633 were excited with 543 and 633 He-Ne lasers, and the fluorescence were collected with 555–625 nm band pass filter and 647 nm long-pass filter, respectively. Microscopic parameters for Nikon A1R were the following. NucBlue or DAPI (Invitrogen) was excited with a 405 nm diode laser and the fluorescence was detected with a 425–475 nm band-pass filter. EGFP was excited with a 488 nm argon laser and the fluorescence was collected with a 515/30 nm band-pass filter. A 561 nm sapphire laser was used to excite Alexa 546, and the fluorescence was imaged with a 595/50 nm band-pass filter. Stacks of 512 x 512 pixels were collected with a pixel size of 60 nm/pixel in the x- and y- directions, and 120–300 nm in the z-direction. Microscopy images with Leica were acquired as follows: Alexa 546 and Alexa 647 were excited with 557 nm and 653 nm wavelengths, respectively, of pulsed white light laser (80 MHz). The Emission detection range was 568–648 nm for Alexa 546 and 663–776 nm for Alexa 647. DAPI and NucBlue were excited with a 405 nm diode laser and emission between 415–495 nm was detected. Laser powers for all channels were fixed. Image stack size was 512 x 512 with a pixel size of 60 nm/pixel in the x- and y- directions, and a step size of 200 to 300 nm in the z-direction.

Fluorescence intensities in the nucleus were calculated by first segmenting the nuclei by automatically calculating an intensity threshold for the DNA label using Otsu's method [149]. The pixel intensity values within the segmented nuclei were then summed to get the total nuclear intensity. The intensity with respect to the nuclear border was calculated in 2D using the confocal layer with the largest nuclear cross-sectional area. First, the shortest Euclidean distance to the nuclear border for each pixel was calculated. The distance values were then sorted into 2-pixel wide bins, and the mean pixel intensity of each bin was calculated. The mean and standard error values were calculated over the cells.

Proximity ligation assay

For PLA, HeLa or NLFK cells were either transfected with NS2-EGFP using Lipofectamine 3000 transfection reagent (Thermo Fisher Scientific) or infected with wt CPV. Positive controls were infected with CPV whereas negative controls were noninfected. Technical probe controls were transfected with NS2-EGFP and probed either without antibodies or only with GFP antibody. The cells were fixed 20 h after transfection or 24 h after infection with 4% PFA in PBS and permeabilized with 0.1% Triton X-100 in PBS. The assay was performed with

Duolink In Situ Orange Mouse/Rabbit kit (Merck KGaA). Antibodies used for the PLA analyses were anti-GFP (9F9.F9, ab1218, Abcam) paired with each of the following antibodies SMARCA5 (ab183730, Abcam), macro-H2A.1 (ab183041, Abcam), and SSRP1 (ab137034, Abcam). PLA for infected cells was performed with anti-NS2 antibody paired with each of the following antibodies SMARCA5 (ab183730, Abcam), macro-H2A.1 (ab183041, Abcam), SSRP1 (ab137034, Abcam) and MDC1 (rAb, PA5-82270, Thermo Fisher Scientific). In the control studies the CPV VP2 capsid protein was detected with rabbit polyclonal antibody and intact capsids with a capsid-specific mouse antibody. PLA probes were incubated on cells for 1.5 h at 37˚C in a humidified chamber followed by ligation and amplification according to the manufacturer's protocol. The nuclei were stained with DAPI. PLA signals formed between NS2-EGFP and associated proteins were detected with Nikon A1R confocal microscope with CFI Plan Apo VC 60x water immersion objective (NA 1.2). Cells expressing NS2-EGFP were identified and PLA foci were imaged using excitation with a 561 nm sapphire laser, and the fluorescence was collected with a 595/50 nm band-pass filter. DAPI was excited with a 405 nm diode laser, and the fluorescence was collected with a 450/50 nm band-pass filter. The imaged stacks of single cells were of size 512 by 512 pixels with a pixel size of 60 nm and the z sampling distance of 180 nm. PLA signals in infected NLFK cells were detected with Olympus FV laser scanning confocal microscope with UPLSAPO 60x oil immersion objective (NA 1.35). Infected cells were identified by marginalized chromatin and PLA foci were imaged using 543 He-NE laser for excitation and 555–655 nm band pass filter for fluorescence collection. DAPI was excited with a 405 nm diode laser, and the fluorescence was collected with 425–475 nm band pass filter. The imaged stacks of single cells were of size 512 by 512 pixels with a pixel size of 60 nm and the z sampling distance of 180 nm.

To analyze the number of nuclear PLA signals, the nuclei were segmented from DAPI images by using automatic minimum cross entropy segmentation [150] and by filling any holes that were left inside the segmented regions. The PLA signals were segmented automatically using the maximum entropy algorithm [151]. The geometric centers of the PLA signals were calculated, and the number of signals having their geometric center inside the segmented nucleus was calculated. Because the axial resolution of confocal microscope is significantly lower than the lateral resolution, the PLA signals located near the top and bottom surfaces of the NE cannot be reliably assigned to the nucleus or cytoplasm. For this reason, only signals that had the z-component of their geometric center located within 1.75 um from the z-component of the geometric center of the nucleus were accepted into analysis. It was visually confirmed that this selection excluded signals near the top and bottom surfaces of the NE from the analysis. Poisson regression model [103] was used to evaluate the statistical significance of the number of PLA signals in comparison to the negative control.

Supporting information

S1 Fig. Nuclear distribution of NS2-EGFP and NS2 associated proteins. Representative confocal microscopy images showing the localization of NS2-EGFP (green) together with selected BioID hits SMARCA5, MDC1, macro-H2A.1, and SSRP1 (magenta) in HeLa cells at 24 hpt with NucBlue stained nuclei (blue). Merged images show the localization of NS2-EGFP with the BioID-identified interactors. Close-up images of selected regions are shown (right). Scale bars, 3 μm.
(TIF)

S2 Fig. Nuclear distribution of NS2 and NS2-associated proteins in infected cells. Representative confocal microscopy images showing the localization of NS2 (green) identified by NS2 antibody together with selected BioID hits including SMARCA5, MDC1, γ-H2AX,

macro-H2A.1, and SSRP1 (magenta) in NLFK cells at 24 hpi with DAPI-stained nuclei (blue). Merged images show the localization of NS2 with the NS2 interactors. Scale bars, 3 μm.
(TIF)

S3 Fig. Nuclear distribution of NS1 and NS2 associated proteins in CPV-infected cells. Representative confocal microscopy images showing the localization of NS1 (red) together with selected NS2 BioID hits including SMARCA5, Macro-H2A.1 and SSRP1 (green) in NucBlue-labeled nucleus (blue) of wt CPV-infected in HeLa cells at 24 hpi. Merged images show the localization of replication protein NS1 with the BioID-identified interactors of NS2. Scale bars, 5 μm.
(TIF)

S4 Fig. Technical controls and segmentation of the nucleus in PLA assay. Images of technical controls with either (**A**) both PLA probes without antibodies or (**B**) both PLA probes with only GFP antibody. Representable confocal microscopy sections show PLA signals (green) and the nuclei of HeLa cells stained with DAPI (gray). (**C**) The image shows confocal sections of nuclear DNA stained by DAPI (gray, left) and PLA signals (white, middle). The segmented nucleus is shown by xy- and yz-slices (white, right) in addition to PLA signals (black). The yz-slice is taken along the line shown in red color. Scale bars, 5 μm.
(TIF)

S5 Fig. Intensity and distribution of DNA in cells transfected with NS2 mutants. (**A**) Total fluorescence intensities of DAPI-stained DNA in nontransfected, wt and NS2 mutants transfected HeLa cells (24 hpt) (n = 27). (**B**) Localization of DNA as a function of increasing distance from the NE in transfected cells (n = 29). The error bars show the standard error of the mean. Statistical significances were determined using Dunnett's multiple comparison test. The significance values shown are denoted as ** ($p<0.01$), * ($p<0.05$) or ns (not significant).
(TIF)

S6 Fig. Nuclear intensity and distribution of heterochromatin. (**A**) Representative confocal images of heterochromatin marker H3K9me3 (magenta), NS1 (green), and DAPI (gray) distribution in nontransfected HeLa cells, and cells transfected with wt, NS2 donor and acceptor mutants at 24 hpt. (n = 25). (**B**) Fluorescent intensities and (**C**) nuclear localization of H3K9me3 in nontransfected and transfected cells. The error bars show the standard error of the mean. Statistical significances were determined using Dunnett's multiple comparison test. The significance values shown are denoted as ** ($p<0.01$), or ns (not significant). Scale bars, 5 μm.
(TIF)

S1 Table. BioID hits linking NS2 to chromatin organization and mRNA processing. The table presents 122 NS2-binding proteins that were detected as high-confidence (BFDR $\leq$0.05) interactors. Two of the inherently distinct groups of NS-associated proteins representing chromatin modification (blue) and DNA damage response (gray) are highlighted. Interactions in the presence or absence of infection are shown.
(XLSX)

S2 Table. Biological pathways of NS2 BioID hits. GO functional annotation chart of CPV NS2 high-confidence interactors created by PANTHER classification system for GO Biological process overrepresentation (default FDR < 0.05 filter). The groups are organized by the most specific subterm first, level 0 being the most specific. GO terms for chromatin modification (blue) and DNA damage response (gray) are shown.
(XLSX)

S3 Table. Unfiltered NS2 BioID data. Unfiltered SaintExpress-analyzed BioID data used in this study. For each identified prey protein, the average spectral count in infected and noninfected samples are shown, together with BFDR values that are later used for filtering the dataset. Interactors representing four distinct functional groups are colored accordingly: chromatin modification (blue) and DNA damage response (gray).
(XLSX)

S1 Data. Original data used for analyses.
(XLSX)

Acknowledgments

We thank Anssi Mähönen and Lassi Palmujoki for their assistance in constructing BirA-tagged NS2 constructs. Our special thanks go to Wendy Weichert for her help with CPV NS2 mutants.

Author Contributions

Conceptualization: Maija Vihinen-Ranta.

Data curation: Salla Mattola, Vesa Aho.

Formal analysis: Salla Mattola, Kari Salokas, Vesa Aho.

Funding acquisition: Maija Vihinen-Ranta.

Investigation: Salla Mattola, Kari Salokas, Elina Mäntylä, Sami Salminen, Satu Hakanen, Minna Kaikkonen-Määttä.

Methodology: Salla Mattola, Kari Salokas, Vesa Aho, Elina Mäntylä, Sami Salminen, Einari A. Niskanen, Julija Svirskaite, Teemu O. Ihalainen, Kari J. Airenne, Minna Kaikkonen-Määttä, Colin R. Parrish, Markku Varjosalo.

Project administration: Maija Vihinen-Ranta.

Resources: Minna Kaikkonen-Määttä, Colin R. Parrish, Markku Varjosalo, Maija Vihinen-Ranta.

Software: Vesa Aho.

Supervision: Vesa Aho, Kari J. Airenne, Maija Vihinen-Ranta.

Visualization: Salla Mattola, Sami Salminen, Einari A. Niskanen, Teemu O. Ihalainen.

Writing – original draft: Salla Mattola, Kari Salokas, Vesa Aho, Sami Salminen, Satu Hakanen, Julija Svirskaite, Colin R. Parrish, Maija Vihinen-Ranta.

Writing – review & editing: Salla Mattola, Kari Salokas, Vesa Aho, Satu Hakanen, Colin R. Parrish, Maija Vihinen-Ranta.

References

1. Niskanen EA, Ihalainen TO, Kalliolinna O, et al. Effect of ATP Binding and Hydrolysis on Dynamics of Canine Parvovirus NS1. Journal of Virology 2010; 84: 5391–5403. https://doi.org/10.1128/JVI.02221-09 PMID: 20219935
2. Niskanen EA, Kalliolinna O, Ihalainen TO, et al. Mutations in DNA Binding and Transactivation Domains Affect the Dynamics of Parvovirus NS1 Protein. J Virol 2013; 87: 11762–11774 https://doi.org/10.1128/JVI.01678-13 PMID: 23986577

3. Saxena S, Saxena L, Kumar GR, et al. Apoptosis induced by NS1 gene of Canine Parvovirus-2 is caspase dependent and p53 independent. Virus Research 2013; 173: 426–430. https://doi.org/10.1016/j.virusres.2013.01.020 PMID: 23416147
4. Gupta SK, Sahoo AP, Rosh N, et al. Canine parvovirus NS1 induced apoptosis involves mitochondria, accumulation of reactive oxygen species and activation of caspases. Virus Research 2016; 213: 46–61 https://doi.org/10.1016/j.virusres.2015.10.019 PMID: 26555166
5. Cotmore SF, Sturzenbecker LJ and Tattersall P. The autonomous parvovirus MVM encodes two nonstructural proteins in addition to its capsid polypeptides. Virology 1983; 129: 333–343. https://doi.org/10.1016/0042-6822(83)90172-1 PMID: 6623929
6. Wang D, Yuan W, Davis I, et al. Nonstructural protein-2 and the replication of canine parvovirus. Virology 1998; 240: 273–281. https://doi.org/10.1006/viro.1997.8946 PMID: 9454701
7. Cotmore SF and Tattersall P. Organization of nonstructural genes of the autonomous parvovirus minute virus of mice. Journal of Virology 1986; 58: 724–732. https://doi.org/10.1128/JVI.58.3.724-732.1986 PMID: 2939261
8. Cotmore SF, D'abramo AM, Carbonell LF, et al. The NS2 Polypeptide of Parvovirus MVM Is Required for Capsid Assembly in Murine Cells. Virology 1997; 231: 267–280. https://doi.org/10.1006/viro.1997.8545 PMID: 9168889
9. Choi E, Newman AE, Burger L, et al. Replication of Minute Virus of Mice DNA Is Critically Dependent on Accumulated Levels of NS2. Journal of Virology 2005; 79: 12375–12381. https://doi.org/10.1128/JVI.79.19.12375-12381.2005 PMID: 16160164
10. Brockhaus K, Plaza S, Pintel DJ, et al. Nonstructural proteins NS2 of minute virus of mice associate in vivo with 14-3-3 protein family members. Journal of Virology 1996; 70: 7527–7534. https://doi.org/10.1128/JVI.70.11.7527-7534.1996 PMID: 8892871
11. Young PJ, Jensen KT, Burger LR, et al. Minute virus of mice small nonstructural protein NS2 interacts and colocalizes with the Smn protein. Journal of virology 2002; 76: 6364–6369 https://doi.org/10.1128/jvi.76.12.6364-6369.2002 PMID: 12021369
12. Naeger LK, Cater J and Pintel DJ. The Small Nonstructural Protein (NS2) of the Parvovirus Minute Virus of Mice Is Required for Efficient DNA Replication and Infectious Virus Production in a Cell-Type-Specific Mannert. Journal of Virology 1990; 64: 6166–6175 https://doi.org/10.1128/JVI.64.12.6166-6175.1990 PMID: 2147041
13. Cater JE and Pintel DJ. The small non-structural protein NS2 of the autonomous parvovirus minute virus of mice is required for virus growth in murine cells. Journal of General Virology 1992; 73: 1839–1843. https://doi.org/10.1099/0022-1317-73-7-1839 PMID: 1385828
14. Ruiz Z, Mihaylov IS, Cotmore SF, et al. Recruitment of DNA replication and damage response proteins to viral replication centers during infection with NS2 mutants of Minute Virus of Mice (MVM). Virology 2010; 410: 375–384. https://doi.org/10.1016/j.virol.2010.12.009 PMID: 21193212
15. Petosa C, Schoehn G, Askjaer P, et al. Architecture of CRM1/Exportin1 Suggests How Cooperativity Is Achieved during Formation of a Nuclear Export Complex. Molecular Cell 2004; 16: 761–775 https://doi.org/10.1016/j.molcel.2004.11.018 PMID: 15574331
16. Fornerod M and Ohno M. Exportin-mediated nuclear export of proteins and ribonucleoproteins. Results Probl Cell Differ 2002; 35: 67–91. https://doi.org/10.1007/978-3-540-44603-3_4 PMID: 11791409
17. Fornerod M, Ohno M, Yoshida M, et al. CRM1 Is an Export Receptor for Leucine-Rich Nuclear Export Signals. Cell 1997; 90: 1051–1060. https://doi.org/10.1016/s0092-8674(00)80371-2 PMID: 9323133
18. Henderson BR and Eleftheriou A. A Comparison of the Activity, Sequence Specificity, and CRM1-Dependence of Different Nuclear Export Signals. Experimental Cell Research 2000; 256: 213–224. https://doi.org/10.1006/excr.2000.4825 PMID: 10739668
19. Ohshima T, Nakajima T, Oishi T, et al. CRM1 Mediates Nuclear Export of Nonstructural Protein 2 from Parvovirus Minute Virus of Mice. Biochemical and Biophysical Research Communications 1999; 264: 144–150. https://doi.org/10.1006/bbrc.1999.1478 PMID: 10527855
20. Bodendorf U, Cziepluch C, Jauniaux J, et al. Nuclear Export Factor CRM1 Interacts with Nonstructural Proteins NS2 from Parvovirus Minute Virus of Mice. Journal of Virology 1999; 73: 7769–7779 https://doi.org/10.1128/JVI.73.9.7769-7779.1999 PMID: 10438867
21. Lopez-Bueno A, Valle N, Gallego JM, et al. Enhanced Cytoplasmic Sequestration of the Nuclear Export Receptor CRM1 by NS2 Mutations Developed in the Host Regulates Parvovirus Fitness. Journal of Virology 2004; 78: 10674–10684 https://doi.org/10.1128/JVI.78.19.10674-10684.2004 PMID: 15367634
22. Miller CL and Pintel DJ. Interaction between parvovirus NS2 protein and nuclear export factor Crm1 is important for viral egress from the nucleus of murine cells. J Virol 2002; 76: 3257–3266. https://doi.org/10.1128/jvi.76.7.3257-3266.2002 PMID: 11884550

23. Maroto B, Valle N, Saffrich R, et al. Nuclear Export of the Nonenveloped Parvovirus Virion Is Directed by an Unordered Protein Signal Exposed on the Capsid Surface. Journal of Virology 2004; 78: 10685–10694 https://doi.org/10.1128/JVI.78.19.10685-10694.2004 PMID: 15367635

24. Kang H, Liu D, Tian J, et al. Feline Panleucopenia Virus NS2 Suppresses the Host IFN-β Induction by Disrupting the Interaction between TBK1 and STING. Viruses 2017; 9: 23. https://doi.org/10.3390/v9010023 PMID: 28125002

25. Oh J and Fraser NW. Temporal Association of the Herpes Simplex Virus Genome with Histone Proteins during a Lytic Infection. Journal of Virology 2008; 82: 3530–3537. https://doi.org/10.1128/JVI.00586-07 PMID: 18160436

26. Cliffe AR and Knipe DM. Herpes Simplex Virus ICP0 Promotes both Histone Removal and Acetylation on Viral DNA during Lytic Infection. Journal of Virology 2008; 82: 12030–12038. https://doi.org/10.1128/JVI.01575-08 PMID: 18842720

27. Gu H and Roizman B. Herpes Simplex Virus-Infected Cell Protein 0 Blocks the Silencing of Viral DNA by Dissociating Histone Deacetylases from the CoREST-REST Complex. Proceedings of the National Academy of Sciences—PNAS 2007; 104: 17134–17139. https://doi.org/10.1073/pnas.0707266104 PMID: 17939992

28. Bryant KF, Colgrove RC and Knipe DM. Cellular SNF2H Chromatin-Remodeling Factor Promotes Herpes Simplex Virus 1 Immediate-Early Gene Expression and Replication. mBio 2011; 2: e00330–e00310. https://doi.org/10.1128/mBio.00330-10 PMID: 21249171

29. Taylor TJ and Knipe DM. Proteomics of Herpes Simplex Virus Replication Compartments: Association of Cellular DNA Replication, Repair, Recombination, and Chromatin Remodeling Proteinswith ICP8. Journal of virology 2004; 78: 5856–5866. https://doi.org/10.1128/JVI.78.11.5856-5866.2004 PMID: 15140983

30. Dembowski JA and DeLuca NA. Selective Recruitment of Nuclear Factors to Productively Replicating Herpes Simplex Virus Genomes. PLOS Pathogens 2015; 11: e1004939 https://doi.org/10.1371/journal.ppat.1004939 PMID: 26018390

31. Ben-Asher E, Bratosin S and Aloni Y. Intracellular DNA of the parvovirus minute virus of mice is organized in a minichromosome structure. Journal of Virology 1982; 41: 1044–1054. https://doi.org/10.1128/JVI.41.3.1044-1054.1982 PMID: 7097851

32. Marcus-Sekura CJ and Carter BJ. Chromatin-like structure of adeno-associated virus DNA in infected cells. Journal of Virology 1983; 48: 79–87. https://doi.org/10.1128/JVI.48.1.79-87.1983 PMID: 6310160

33. Mäntylä E, Salokas K, Oittinen M, et al. Promoter-Targeted Histone Acetylation of Chromatinized Parvoviral Genome Is Essential for the Progress of Infection. Journal of virology 2016; 90: 4059–4066. https://doi.org/10.1128/JVI.03160-15 PMID: 26842481

34. Majumder K, Wang J, Boftsi M, et al. Parvovirus minute virus of mice interacts with sites of cellular DNA damage to establish and amplify its lytic infection. eLife 2018; 7: e37750. https://doi.org/10.7554/eLife.37750 PMID: 30028293

35. Agarwal P and Miller KM. The nucleosome: orchestrating DNA damage signaling and repair within chromatin. Biochem Cell Biol 2016; 94: 381–395. https://doi.org/10.1139/bcb-2016-0017 PMID: 27240007

36. Komatsu T, Nagata K and Wodrich H. The Role of Nuclear Antiviral Factors against Invading DNA Viruses: The Immediate Fate of Incoming Viral Genomes. Viruses 2016; 8 https://doi.org/10.3390/v8100290 PMID: 27782081

37. Ma Z, Ni G and Damania B. Innate Sensing of DNA Virus Genomes. Annual review of virology 2018; 5: 341–362. https://doi.org/10.1146/annurev-virology-092917-043244 PMID: 30265633

38. Everett RD. Interactions between DNA viruses, ND10 and the DNA damage response. Cellular microbiology 2006; 8: 365–374. https://doi.org/10.1111/j.1462-5822.2005.00677.x PMID: 16469050

39. Weitzman MD and Fradet-Turcotte A. Virus DNA Replication and the Host DNA Damage Response. Annual review of virology 2018; 5: 141–164. https://doi.org/10.1146/annurev-virology-092917-043534 PMID: 29996066

40. Polo SE and Jackson SP. Dynamics of DNA damage response proteins at DNA breaks: a focus on protein modifications. Genes & development 2011; 25: 409–433. https://doi.org/10.1101/gad.2021311 PMID: 21363960

41. Hashiguchi K, Matsumoto Y and Yasui A. Recruitment of DNA repair synthesis machinery to sites of DNA damage/repair in living human cells. Nucleic Acids Res 2007; 35: 2913–2923. https://doi.org/10.1093/nar/gkm115 PMID: 17439963

42. Luftig MA. Viruses and the DNA Damage Response: Activation and Antagonism. Annu Rev Virol 2014; 1: 605–625. https://doi.org/10.1146/annurev-virology-031413-085548 PMID: 26958736

43. Adeyemi RO, Landry S, Davis ME, et al. Parvovirus Minute Virus of Mice Induces a DNA Damage Response That Facilitates Viral Replication. PLoS pathogens 2010; 6: e1001141. https://doi.org/10.1371/journal.ppat.1001141 PMID: 20949077

44. Luo Y, Chen AY and Qiu J. Bocavirus Infection Induces a DNA Damage Response That Facilitates Viral DNA Replication and Mediates Cell Death. Journal of Virology 2011; 85: 133–145 https://doi.org/10.1128/JVI.01534-10 PMID: 21047968

45. Cotmore SF and Tattersall P. Parvovirus Diversity and DNA Damage Responses. Cold Spring Harbor perspectives in biology 2013; 5: a012989. https://doi.org/10.1101/cshperspect.a012989 PMID: 23293137

46. Cotmore SF and Tattersall P. Parvoviruses: Small Does Not Mean Simple. Annual review of virology 2014; 1: 517–537. https://doi.org/10.1146/annurev-virology-031413-085444 PMID: 26958732

47. Adeyemi RO and Pintel DJ. Replication of Minute Virus of Mice in Murine Cells Is Facilitated by Virally Induced Depletion of p21. Journal of Virology 2012; 86: 8328–8332. https://doi.org/10.1128/JVI.00820-12 PMID: 22623787

48. Adeyemi RO and Pintel DJ. The ATR Signaling Pathway Is Disabled during Infection with the Parvovirus Minute Virus of Mice. Journal of virology 2014; 88: 10189–10199. https://doi.org/10.1128/JVI.01412-14 PMID: 24965470

49. Majumder K, Etingov I and Pintel DJ. Protoparvovirus Interactions with the Cellular DNA Damage Response. Viruses 2017; 9: 323. https://doi.org/10.3390/v9110323 PMID: 29088070

50. Kim DI, Birendra KC, Zhu W, et al. Probing nuclear pore complex architecture with proximity-dependent biotinylation 2014; 111: E2453–E2461. https://doi.org/10.1073/pnas.1406459111 PMID: 24927568

51. Kim DI and Roux KJ. Filling the Void: Proximity-Based Labeling of Proteins in Living Cells. Trends in Cell Biology 2016; 26: 804–817. https://doi.org/10.1016/j.tcb.2016.09.004 PMID: 27667171

52. Roux KJ, Kim DI, Raida M, et al. A promiscuous biotin ligase fusion protein identifies proximal and interacting proteins in mammalian cells. The Journal of cell biology 2012; 196: 801–810. https://doi.org/10.1083/jcb.201112098 PMID: 22412018

53. Roux KJ, Kim DI and Burke B. BioID: A Screen for Protein-Protein Interactions. Current Protocols in Protein Science 2013; 74: 19.23.1–19.23.14. https://doi.org/10.1002/0471140864.ps1923s74 PMID: 24510646

54. Van Itallie CM, Aponte A, Tietgens AJ, et al. The N and C Termini of ZO-1 Are Surrounded by Distinct Proteins and Functional Protein Networks. The Journal of biological chemistry 2013; 288: 13775–13788. https://doi.org/10.1074/jbc.M113.466193 PMID: 23553632

55. Mehus AA, Anderson RH and Roux KJ. BioID identification of lamin-associated proteins. Methods in enzymology 2016; 569: 3–22. https://doi.org/10.1016/bs.mie.2015.08.008 PMID: 26778550

56. Chojnowski A, Ong PF, Wong ESM, et al. Progerin reduces LAP2α-telomere association in Hutchinson-Gilford progeria. eLife 2015; 4: e07759. https://doi.org/10.7554/eLife.07759 PMID: 26312502

57. Yu F, Zhao B and Guan K. Hippo Pathway in Organ Size Control, Tissue Homeostasis, and Cancer. Cell 2015; 163: 811–828. https://doi.org/10.1016/j.cell.2015.10.044 PMID: 26544935

58. Couzens AL, Knight JDR, Kean MJ, et al. Protein Interaction Network of the Mammalian Hippo Pathway Reveals Mechanisms of Kinase-Phosphatase Interactions. Sci Signal 2013; 6: rs15 https://doi.org/10.1126/scisignal.2004712 PMID: 24255178

59. Zhou Z, Rawnsley D, Goddard L, et al. The cerebral cavernous malformation pathway controls embryonic endocardial gene expression through regulation of MEKK3 signaling and KLF expression. Developmental cell 2015; 32: 168–180 https://doi.org/10.1016/j.devcel.2014.12.009 PMID: 25625206

60. Steed E, Elbediwy A, Vacca B, et al. MarvelD3 couples tight junctions to the MEKK1–JNK pathway to regulate cell behavior and survival. The Journal of cell biology 2014; 204: 821–838. https://doi.org/10.1083/jcb.201304115 PMID: 24567356

61. Lambert J, Tucholska M, Go C, et al. Proximity biotinylation and affinity purification are complementary approaches for the interactome mapping of chromatin-associated protein complexes. Journal of Proteomics 2015; 118: 81–94. https://doi.org/10.1016/j.jprot.2014.09.011 PMID: 25281560

62. Bell NM and Lever AML. HIV Gag polyprotein: processing and early viral particle assembly. Trends in Microbiology 2013; 21: 136–144 https://doi.org/10.1016/j.tim.2012.11.006 PMID: 23266279

63. Le Sage V, Cinti A, Valiente-Echeverría F, et al. Proteomic analysis of HIV-1 Gag interacting partners using proximity-dependent biotinylation. Virology journal 2015; 12: 138. https://doi.org/10.1186/s12985-015-0365-6 PMID: 26362536

64. Ritchie C, Cylinder I, Platt EJ, et al. Analysis of HIV-1 Gag Protein Interactions via Biotin Ligase Tagging. Journal of virology 2015; 89: 3988–4001. https://doi.org/10.1128/JVI.03584-14 PMID: 25631074

65. Ortiz DA, Glassbrook JE and Pellett PE. Protein-Protein Interactions Suggest Novel Activities of Human Cytomegalovirus Tegument Protein pUL103. Journal of virology 2016; 90: 7798–7810. https://doi.org/10.1128/JVI.00097-16 PMID: 27334581

66. Holthusen K, Talaty P and Everly DN. Regulation of Latent Membrane Protein 1 Signaling through Interaction with Cytoskeletal Proteins. J Virol 2015; 89: 7277–7290. https://doi.org/10.1128/JVI.00321-15 PMID: 25948738

67. Coyaud E, Ranadheera C, Cheng D, et al. Global Interactomics Uncovers Extensive Organellar Targeting by Zika Virus. Molecular & cellular proteomics: MCP 2018; 17: 2242–2255. https://doi.org/10.1074/mcp.TIR118.000800 PMID: 30037810

68. Liu X, Salokas K, Tamene F, et al. An AP-MS- and BioID-compatible MAC-tag enables comprehensive mapping of protein interactions and subcellular localizations. Nature communications 2018; 9: 1188–16. https://doi.org/10.1038/s41467-018-03523-2 PMID: 29568061

69. Clemens KE and Pintel DJ. The two transcription units of the autonomous parvovirus minute virus of mice are transcribed in a temporal order. Journal of Virology 1988; 62: 1448–1451. https://doi.org/10.1128/JVI.62.4.1448-1451.1988 PMID: 3346950

70. Cotmore SF and Tattersall P. Alternate splicing in a parvoviral nonstructural gene links a common amino-terminal sequence to downstream domains which confer radically different localization and turnover characteristics. Virology 1990; 177: 477–487. https://doi.org/10.1016/0042-6822(90)90512-p PMID: 2142555

71. Strohner R, Németh A, Nightingale KP, et al. Recruitment of the nucleolar remodeling complex NoRC establishes ribosomal DNA silencing in chromatin. Molecular and cellular biology 2004; 24: 1791–1798 https://doi.org/10.1128/MCB.24.4.1791-1798.2004 PMID: 14749393

72. Németh A, Strohner R, Grummt I, et al. The chromatin remodeling complex NoRC and TTF-I cooperate in the regulation of the mammalian rRNA genes in vivo. Nucleic acids research 2004; 32: 4091–4099. https://doi.org/10.1093/nar/gkh732 PMID: 15292447

73. Larsen DH and Stucki M. Nucleolar responses to DNA double-strand breaks. Nucleic Acids Res 2016; 44: 538–544. https://doi.org/10.1093/nar/gkv1312 PMID: 26615196

74. Korsholm LM, Gál Z, Nieto B, et al. Recent advances in the nucleolar responses to DNA double-strand breaks. Nucleic Acids Res 2020; 48: 9449–9461. https://doi.org/10.1093/nar/gkaa713 PMID: 32857853

75. Oppikofer M, Bai T, Gan Y, et al. Expansion of the ISWI chromatin remodeler family with new active complexes. EMBO Rep 2017; 18: 1697–1706. https://doi.org/10.15252/embr.201744011 PMID: 28801535

76. Wiechens N, Singh V, Gkikopoulos T, et al. The Chromatin Remodelling Enzymes SNF2H and SNF2L Position Nucleosomes adjacent to CTCF and Other Transcription Factors. PLoS genetics 2016; 12: e1005940. https://doi.org/10.1371/journal.pgen.1005940 PMID: 27019336

77. Morris SA, Baek S, Sung M, et al. Overlapping chromatin-remodeling systems collaborate genome wide at dynamic chromatin transitions. Nature structural & molecular biology 2014; 21: 73–81. https://doi.org/10.1038/nsmb.2718 PMID: 24317492

78. Cuylen S, Blaukopf C, Politi AZ, et al. Ki-67 acts as a biological surfactant to disperse mitotic chromosomes. Nature 2016; 535: 308–312. https://doi.org/10.1038/nature18610 PMID: 27362226

79. Sobecki M, Mrouj K, Camasses A, et al. The cell proliferation antigen Ki-67 organises heterochromatin. eLife 2016; 5: e13722. https://doi.org/10.7554/eLife.13722 PMID: 26949251

80. Verheijen R, Kuijpers HJ, Schlingemann RO, et al. Ki-67 detects a nuclear matrix-associated proliferation-related antigen. I. Intracellular localization during interphase. J Cell Sci 1989; 92: 123–130. https://doi.org/10.1242/jcs.92.1.123 PMID: 2674163

81. Collins N, Poot RA, Kukimoto I, et al. An ACF1–ISWI chromatin-remodeling complex is required for DNA replication through heterochromatin. Nature Genetics 2002; 32: 627–632. https://doi.org/10.1038/ng1046 PMID: 12434153

82. Pessina F and Lowndes NF. The RSF1 Histone-Remodelling Factor Facilitates DNA Double-Strand Break Repair by Recruiting Centromeric and Fanconi Anaemia Proteins. PLoS biology 2014; 12: e1001856. https://doi.org/10.1371/journal.pbio.1001856 PMID: 24800743

83. Perpelescu M, Nozaki N, Obuse C, et al. Active Establishment of Centromeric CENP-A Chromatin by RSF Complex. The Journal of Cell Biology 2009; 185: 397–407. https://doi.org/10.1083/jcb.200903088 PMID: 19398759

84. Loyola A, LeRoy G, Wang YH, et al. Reconstitution of recombinant chromatin establishes a requirement for histone-tail modifications during chromatin assembly and transcription. Genes & development 2001; 15: 2837–2851. https://doi.org/10.1101/gad.937401 PMID: 11691835

85. LeRoy G, Loyola A, Lane WS, et al. Purification and Characterization of a Human Factor That Assembles and Remodels Chromatin. Journal of Biological Chemistry 2000; 275: 14787–14790. https://doi.org/10.1074/jbc.C000093200 PMID: 10747848

86. Costanzi C and Pehrson JR. MACROH2A2, a New Member of the MACROH2A Core Histone Family. Journal of Biological Chemistry 2001; 276: 21776–21784. https://doi.org/10.1074/jbc.M010919200 PMID: 11262398

87. Majumder K and Morales AJ. Utilization of Host Cell Chromosome Conformation by Viral Pathogens: Knowing When to Hold and When to Fold. Frontiers in immunology 2021; 12: 633762. https://doi.org/10.3389/fimmu.2021.633762 PMID: 33841414

88. Harper JW and Elledge SJ. The DNA Damage Response: Ten Years After. Molecular cell 2007; 28: 739–745. https://doi.org/10.1016/j.molcel.2007.11.015 PMID: 18082599

89. Lazzaro F, Giannattasio M, Puddu F, et al. Checkpoint mechanisms at the intersection between DNA damage and repair. DNA Repair 2009; 8: 1055–1067. https://doi.org/10.1016/j.dnarep.2009.04.022 PMID: 19497792

90. Kemble D, McCullough L, Whitby F, et al. FACT Disrupts Nucleosome Structure by Binding H2A-H2B with Conserved Peptide Motifs. Molecular Cell 2015; 60: 294–306. https://doi.org/10.1016/j.molcel.2015.09.008 PMID: 26455391

91. Dion MF, Kaplan T, Kim M, et al. Dynamics of Replication-Independent Histone Turnover in Budding Yeast. Science 2007; 315: 1405–1408. https://doi.org/10.1126/science.1134053 PMID: 17347438

92. Winkler DD and Luger K. The Histone Chaperone FACT: Structural Insights and Mechanisms for Nucleosome Reorganization. The Journal of biological chemistry 2011; 286: 18369–18374. https://doi.org/10.1074/jbc.R110.180778 PMID: 21454601

93. Orphanides G, Wu WH, Lane WS, et al. The chromatin-specific transcription elongation factor FACT comprises human SPT16 and SSRP1 proteins. Nature 1999; 400: 284–288. https://doi.org/10.1038/22350 PMID: 10421373

94. Li Y, Zeng SX, Landais I, et al. Human SSRP1 Has Spt16-dependent and -independent Roles in Gene Transcription. The Journal of biological chemistry 2007; 282: 6936–6945. https://doi.org/10.1074/jbc.M603822200 PMID: 17209051

95. Falbo L, Raspelli E, Romeo F, et al. SSRP1-mediated histone H1 eviction promotes replication origin assembly and accelerated development. Nat Commun 2020; 11 https://doi.org/10.1038/s41467-020-15180-5 PMID: 32165637

96. Kumari A, Mazina OM, Shinde U, et al. A role for SSRP1 in recombination-mediated DNA damage response. Journal of cellular biochemistry 2009; 108: 508–518. https://doi.org/10.1002/jcb.22280 PMID: 19639603

97. Krohn NM, Stemmer C, Fojan P, et al. Protein Kinase CK2 Phosphorylates the High Mobility Group Domain Protein SSRP1, Inducing the Recognition of UV-damaged DNA. The Journal of biological chemistry 2003; 278: 12710–12715. https://doi.org/10.1074/jbc.M300250200 PMID: 12571244

98. Bozhenok L, Wade PA and Varga-Weisz P. WSTF-ISWI chromatin remodeling complex targets heterochromatic replication foci. The EMBO Journal 2002; 21: 2231–2241. https://doi.org/10.1093/emboj/21.9.2231 PMID: 11980720

99. Barnett C and Krebs JE. WSTF does it all: a multifunctional protein in transcription, repair, and replication. Biochemistry and cell biology = Biochimie et biologie cellulaire 2011; 89: 12–23. https://doi.org/10.1139/O10-114 PMID: 21326359

100. Yuan J, Luo K, Zhang L, et al. USP10 Regulates p53 Localization and Stability by Deubiquitinating p53. Cell 2010; 140: 384–396. https://doi.org/10.1016/j.cell.2009.12.032 PMID: 20096447

101. Hofmann RM and Pickart CM. Noncanonical MMS2-Encoded Ubiquitin-Conjugating Enzyme Functions in Assembly of Novel Polyubiquitin Chains for DNA Repair. Cell 1999; 96: 645–653. https://doi.org/10.1016/s0092-8674(00)80575-9 PMID: 10089880

102. Söderberg O, Gullberg M, Jarvius M, et al. Direct observation of individual endogenous protein complexes in situ by proximity ligation. Nature Methods 2006; 3: 995–1000. https://doi.org/10.1038/nmeth947 PMID: 17072308

103. Dunnett CW. A Multiple Comparison Procedure for Comparing Several Treatments with a Control. Journal of the American Statistical Association 1955; 50: 1096–1121. https://doi.org/10.1080/01621459.1955.10501294

104. Naeger LK, Salomé N and Pintel DJ. NS2 is required for efficient translation of viral mRNA in minute virus of mice-infected murine cells. J Virol 1993; 67: 1034–1043. https://doi.org/10.1128/JVI.67.2.1034-1043.1993 PMID: 8419637

105. Collins PL, Purman C, Porter SI, et al. DNA double-strand breaks induce H2Ax phosphorylation domains in a contact-dependent manner. Nature communications 2020; 11: 3158. https://doi.org/10.1038/s41467-020-16926-x PMID: 32572033

106. Rogakou EP, Pilch DR, Orr AH, et al. DNA Double-stranded Breaks Induce Histone H2AX Phosphorylation on Serine 139. The Journal of biological chemistry 1998; 273: 5858–5868. https://doi.org/10.1074/jbc.273.10.5858 PMID: 9488723

107. Scully R and Xie A. Double strand break repair functions of histone H2AX. Mutation research 2013; 750: 5–14. https://doi.org/10.1016/j.mrfmmm.2013.07.007 PMID: 23916969

108. Stucki M, Clapperton JA, Mohammad D, et al. MDC1 Directly Binds Phosphorylated Histone H2AX to Regulate Cellular Responses to DNA Double-Strand Breaks. Cell 2005; 123: 1213–1226. https://doi.org/10.1016/j.cell.2005.09.038 PMID: 16377563

109. Majumder K, Boftsi M, Whittle FB, et al. The NS1 protein of the parvovirus MVM Aids in the localization of the viral genome to cellular sites of DNA damage. PLOS Pathogens 2020; 16: e1009002 https://doi.org/10.1371/journal.ppat.1009002 PMID: 33064772

110. Ihalainen TO, Niskanen EA, Jylhävä J, et al. Parvovirus Induced Alterations in Nuclear Architecture and Dynamics. PloS one 2009; 4: e5948. https://doi.org/10.1371/journal.pone.0005948 PMID: 19536327

111. Gkikopoulos T, Schofield P, Singh V, et al. A Role for Snf2-Related Nucleosome-Spacing Enzymes in Genome-Wide Nucleosome Organization. Science (American Association for the Advancement of Science) 2011; 333: 1758–1760. https://doi.org/10.1126/science.1206097 PMID: 21940898

112. Smolle M, Venkatesh S, Gogol MM, et al. Chromatin remodelers Isw1 and Chd1 maintain chromatin structure during transcription by preventing histone exchange. Nature structural & molecular biology 2012; 19: 884–892. https://doi.org/10.1038/nsmb.2312 PMID: 22922743

113. Mueller-Planitz F, Klinker H, Ludwigsen J, et al. The ATPase domain of ISWI is an autonomous nucleosome remodeling machine. Nature structural & molecular biology 2013; 20: 82–89. https://doi.org/10.1038/nsmb.2457 PMID: 23202585

114. Strohner R, Nemeth A, Jansa P, et al. NoRC—a novel member of mammalian ISWI-containing chromatin remodeling machines. EMBO J 2001; 20: 4892–4900. https://doi.org/10.1093/emboj/20.17.4892 PMID: 11532953

115. Simonin D, Diaz J, Masse T, et al. Printed in Great Britain Persistence of ribosomal protein synthesis after infection of HeLa cells by herpes simplex virus type 1. Journal of General Virology 1997; 78: 435

116. Greco A, Laurent A and Madjar J. Repression of β-actin synthesis and persistence of ribosomal protein synthesis after infection of HeLa cells by herpes simplex virus type 1 infection are under translational control. Molecular and General Genetics MGG 1997; 256: 320–327. https://doi.org/10.1007/s004380050575 PMID: 9393457

117. Bianco C and Mohr I. Ribosome biogenesis restricts innate immune responses to virus infection and DNA. eLife 2019; 8 https://doi.org/10.7554/eLife.49551 PMID: 31841110

118. Percipalle P, Fomproix N, Cavellán E, et al. The chromatin remodelling complex WSTF-SNF2h interacts with nuclear myosin 1 and has a role in RNA polymerase I transcription. EMBO reports 2006; 7: 525–530. https://doi.org/10.1038/sj.embor.7400657 PMID: 16514417

119. Ito T, Bulger M, Pazin MJ, et al. ACF, an ISWI-Containing and ATP-Utilizing Chromatin Assembly and Remodeling Factor. Cell 1997; 90: 145–155. https://doi.org/10.1016/s0092-8674(00)80321-9 PMID: 9230310

120. Scacchetti A, Brueckner L, Jain D, et al. CHRAC/ACF contribute to the repressive ground state of chromatin. Life Sci Alliance 2018; 1

121. Watanabe R, Kanno S, Mohammadi Roushandeh A, et al. Nucleosome remodelling, DNA repair and transcriptional regulation build negative feedback loops in cancer and cellular ageing. Philosophical transactions. Biological sciences 2017; 372: 20160473. https://doi.org/10.1098/rstb.2016.0473 PMID: 28847829

122. Kleinberger T, Brestovitsky A and Sharf R. The adenovirus E4orf4 protein targets PP2A to the ACF chromatin remodeling factor and controls cell death through different SNF2h-containing complexes. The FASEB Journal 2011; 25: 892.1. https://doi.org/10.1096/fasebj.25.1_supplement.892.1

123. Brestovitsky A, Sharf R, Mittelman K, et al. The adenovirus E4orf4 protein targets PP2A to the ACF chromatin-remodeling factor and induces cell death through regulation of SNF2h-containing complexes. Nucleic acids research 2011; 39: 6414–6427. https://doi.org/10.1093/nar/gkr231 PMID: 21546548

124. Schultz LB, Chehab NH, Malikzay A, et al. p53 Binding Protein 1 (53BP1) Is an Early Participant in the Cellular Response to DNA Double-Strand Breaks. The Journal of cell biology 2000; 151: 1381–1390. https://doi.org/10.1083/jcb.151.7.1381 PMID: 11134068

125. Stewart GS, Wang B, Bignell CR, et al. MDC1 is a mediator of the mammalian DNA damage checkpoint. Nature 2003; 421: 961–966. https://doi.org/10.1038/nature01446 PMID: 12607005

126. Melander F, Bekker-Jensen S, Falck J, et al. Phosphorylation of SDT repeats in the MDC1 N terminus triggers retention of NBS1 at the DNA damage-modified chromatin. J Cell Biol 2008; 181: 213–226. https://doi.org/10.1083/jcb.200708210 PMID: 18411307

127. Nüesch JPF and Rommelaere J. A viral adaptor protein modulating casein kinase II activity induces cytopathic effects in permissive cells. Proc Natl Acad Sci USA 2007; 104: 12482. https://doi.org/10.1073/pnas.0705533104 PMID: 17636126

128. Lou Z, Minter-Dykhouse K, Franco S, et al. MDC1 Maintains Genomic Stability by Participating in the Amplification of ATM-Dependent DNA Damage Signals. Molecular cell 2006; 21: 187–200. https://doi.org/10.1016/j.molcel.2005.11.025 PMID: 16427009

129. Bondarenko MT, Maluchenko NV, Valieva ME, et al. Structure and function of histone chaperone FACT. Mol Biol (N Y) 2015; 49: 796–809. https://doi.org/10.7868/S0026898415060026 PMID: 26710768

130. Talbert PB and Henikoff S. Histone variants on the move: substrates for chromatin dynamics. Nature Reviews Molecular Cell Biology 2017; 18: 115–126. https://doi.org/10.1038/nrm.2016.148 PMID: 27924075

131. Hauer MH and Gasser SM. Chromatin and nucleosome dynamics in DNA damage and repair. Genes Dev 2017; 31: 2204–2221. https://doi.org/10.1101/gad.307702.117 PMID: 29284710

132. Lai WKM and Pugh BF. Understanding nucleosome dynamics and their links to gene expression and DNA replication. Nature reviews.Molecular cell biology 2017; 18: 548–562. https://doi.org/10.1038/nrm.2017.47 PMID: 28537572

133. Tsunaka Y, Fujiwara Y, Oyama T, et al. Integrated molecular mechanism directing nucleosome reorganization by human FACT. Genes Dev 2016; 30: 673–686. https://doi.org/10.1101/gad.274183.115 PMID: 26966247

134. Orphanides G, Leroy G, Chang C, et al. FACT, a Factor that Facilitates Transcript Elongation through Nucleosomes One aspect in which RNAP II transcription of chroma- tin templates in vitro differs from transcription of naked DNA is the absolute requirement for a transcriptional. Cell 1998; 92: 105 https://doi.org/10.1016/s0092-8674(00)80903-4 PMID: 9489704

135. Birch JL, Tan BC, Panov KI, et al. FACT facilitates chromatin transcription by RNA polymerases I and III. EMBO J 2009; 28: 854–865. https://doi.org/10.1038/emboj.2009.33 PMID: 19214185

136. Formosa T and Winston F. The role of FACT in managing chromatin: disruption, assembly, or repair?. Nucleic Acids Res 2020; 48: 11929–11941. https://doi.org/10.1093/nar/gkaa912 PMID: 33104782

137. Jeronimo C, Poitras C and Robert F. Histone Recycling by FACT and Spt6 during Transcription Prevents the Scrambling of Histone Modifications. Cell Reports 2019; 28: 1206–1218.e8. https://doi.org/10.1016/j.celrep.2019.06.097 PMID: 31365865

138. Duina AA. Histone Chaperones Spt6 and FACT: Similarities and Differences in Modes of Action at Transcribed Genes. Genetics research international 2011; 2011: 625210–12. https://doi.org/10.4061/2011/625210 PMID: 22567361

139. Holla S, Dhakshnamoorthy J, Folco HD, et al. Positioning Heterochromatin at the Nuclear Periphery Suppresses Histone Turnover to Promote Epigenetic Inheritance. Cell 2020; 180: 150–164.e15. https://doi.org/10.1016/j.cell.2019.12.004 PMID: 31883795

140. Kim J, Sturgill D, Sebastian R, et al. Replication Stress Shapes a Protective Chromatin Environment across Fragile Genomic Regions. Mol Cell 2018; 69: 36–47.e7. https://doi.org/10.1016/j.molcel.2017.11.021 PMID: 29249653

141. Huang H, Santoso N, Power D, et al. FACT Proteins, SUPT16H and SSRP1, Are Transcriptional Suppressors of HIV-1 and HTLV-1 That Facilitate Viral Latency. The Journal of biological chemistry 2015; 290: 27297–27310. https://doi.org/10.1074/jbc.M115.652339 PMID: 26378236

142. O'Connor CM., Nukui M, Gurova KV, et al. Inhibition of the FACT Complex Reduces Transcription from the Human Cytomegalovirus Major Immediate Early Promoter in Models of Lytic and Latent Replication. J Virol 2016; 90: 4249–4253. https://doi.org/10.1128/JVI.02501-15 PMID: 26865717

143. Dembowski JA, Dremel SE and DeLuca NA. Replication-Coupled Recruitment of Viral and Cellular Factors to Herpes Simplex Virus Type 1 Replication Forks for the Maintenance and Expression of Viral Genomes. PLOS Pathogens 2017; 13: e1006166 https://doi.org/10.1371/journal.ppat.1006166 PMID: 28095497

144. Fox HL, Dembowski JA and DeLuca NA. A Herpesviral Immediate Early Protein Promotes Transcription Elongation of Viral Transcripts. mBio 2017; 8: 745. https://doi.org/10.1128/mBio.00745-17 PMID: 28611249

145. Patton JT, Stout ER and Bates RC. Transcription of the bovine parvovirus genome in isolated nuclei. J Virol 1979; 30: 917–922. https://doi.org/10.1128/JVI.30.3.917-922.1979 PMID: 480472

146. Parrish CR. Mapping specific functions in the capsid structure of canine parvovirus and feline panleukopenia virus using infectious plasmid clones. Virology 1991; 183: 195–205 https://doi.org/10.1016/0042-6822(91)90132-u PMID: 1647068

147. Teo G, Liu G, Zhang J, et al. SAINTexpress: Improvements and additional features in Significance Analysis of INTeractome software. Journal of Proteomics 2014; 100: 37–43. https://doi.org/10.1016/j.jprot.2013.10.023 PMID: 24513533

148. Mellacheruvu D, Wright Z, Couzens AL, et al. The CRAPome: a contaminant repository for affinity purification-mass spectrometry data. Nat Methods 2013; 10: 730–736. https://doi.org/10.1038/nmeth.2557 PMID: 23921808

149. Otsu N. A Threshold Selection Method from Gray-Level Histograms. IEEE Transactions on Systems, Man, and Cybernetics 1979; 9: 62–66. https://doi.org/10.1109/TSMC.1979.4310076

150. Li CH and Lee CK. Minimum cross entropy thresholding. Pattern Recognition 1993; 26: 617–625

151. Kapur JN, Sahoo PK and Wong AKC. A new method for gray-level picture thresholding using the entropy of the histogram. Computer Vision, Graphics, and Image Processing 1985; 29: 273–285

II

PARVOVIRUS INFECTION ALTERS THE NUCLEOLAR STRUCTURE

by

Salla Mattola, Simon Leclerc, Satu Hakanen, Vesa Aho, Colin R Parrish & Maija Vihinen-Ranta 2022

Manuscript.

Request a copy from the author.

III

G2/M TRANSITION AND APOPTOSIS FACILITATE THE NUCLEAR EGRESS OF PARVOVIRAL CAPSIDS

by

Salla Mattola, Elina Mäntylä, Vesa Aho, Sami Salminen, Mikko Oittinen, Kari Salokas, Jani Järvensivu, Satu Hakanen, Teemu O Ihalainen, Keijo Viiri & Maija Vihinen-Ranta 2022

Submitted Manuscript.

Request a copy from the author.